



## Cancer Biomarker Detection: Recent Achievements and Challenges

Journal:	<i>Chemical Society Reviews</i>
Manuscript ID:	CS-REV-11-2014-000370.R2
Article Type:	Review Article
Date Submitted by the Author:	03-Nov-2014
Complete List of Authors:	Wu, L; Changchun Institute of Applied Chemistry, Chinese Academy of Sciences, Qu, Xiaogang; Changchun Institute of Applied Chemistry, Chinese Academy of Sciences, Division of Biological Inorganic Chemistry

## ARTICLE

Invited Review **Cancer Biomarker Detection: Recent Achievements and Challenges**

Cite this: DOI: 10.1039/x0xx00000x

Li Wu,<sup>a,b</sup> and Xiaogang Qu<sup>a\*</sup>Received 00th January 2012,  
Accepted 00th January 2012

DOI: 10.1039/x0xx00000x

[www.rsc.org/](http://www.rsc.org/)

Early detection of cancer can significantly reduce cancer mortality and saves lives. Thus a great deal of effort has been devoted to the exploration of new technologies to detect early signs of the disease. Cancer biomarkers cover a broad range of biochemical entities, such as nucleic acids, proteins, sugars, and small metabolites, cytogenetic and cytokinetic parameters as well as whole tumour cells found in the body fluid. They can be used for risk assessment, diagnosis, prognosis, prediction of treatment efficacy and toxicity, and recurrence. In this review, we provide an overview of recent advances in cancer biomarker detection. Several representative examples using different approach for each biomarker have been overviewed, and all these cases demonstrate that the multidisciplinary technology based cancer diagnostics are becoming an increasingly relevant alternative to traditional techniques. Besides, we also discuss the unsolved problems and future challenges in the evaluation of cancer biomarkers. Clearly, solving these hurdles requires great efforts and collaboration from different communities of chemists, physicists, biologists, clinicians, material-scientists, engineering and technical researchers. This will realize point-of-care diagnosis and individualized treatment of cancers by the non-invasive and convenient test in the future.

<sup>a</sup> Laboratory of Chemical Biology and Division of Biological Inorganic Chemistry, State Key laboratory of Rare Earth Resource Utilization, Changchun Institute of Applied Chemistry, Chinese Academy of Sciences, Changchun, Jilin 130022, P. R. China. Email: [xqu@ciac.ac.cn](mailto:xqu@ciac.ac.cn); Fax: (+86) 431-85262656.

<sup>b</sup> University of Chinese Academy of Sciences, Beijing, 100039, P. R. China

**1. Introduction**

Cancer, a complex group of diseases characterized by uncontrolled growth and spread of abnormal cells, has been the leading cause of death in many countries. Based on the GLOB-



Li Wu received her B.S. from Nanjing Normal University in 2009. She is now a PhD candidate majoring in Chemical Biology under the supervision of Prof. Xiaogang Qu in Changchun Institute of Applied Chemistry. Her PhD is focused on expanding the horizons of electrochemical biosensor construction using smart materials and exploring their applications in cancer biomarker detection.



Xiaogang Qu received his PhD from the Chinese Academy of Sciences (CAS) in 1995. He moved to the USA afterwards and worked with Professor J. B. Chaires at the Mississippi Medical Center and Nobel Laureate Professor Ahmed. H. Zewail at the California Institute of Technology. Since late 2002, he is a professor at Changchun Institute of Applied Chemistry, CAS. From 12/2006 to 05/2007, he visited the group of Nobel Laureate Professor Alan. J. Heeger at the UCSB. His current research is focused on ligand-nucleic acids or related protein interactions, and bio-functional materials for advanced medical technology.

CAN 2012 estimates<sup>1</sup>, there were 14.1 million new cancer cases, 8.2 million cancer deaths and 32.6 million people living with cancer (within 5 years of diagnosis) in 2012 worldwide. Cancer exacts a tremendous toll on society. In addition to the devastating effects on patients and their families, the economic costs of cancer are enormous, both in terms of direct medical-care resources for its treatment and in the loss of human capital due to early mortality. Cancer survival tends to be poorer most likely because of a combination of a late stage at diagnosis and limited access to timely and standard treatment. Early and accurate detection of cancer is important for clinical diagnosis, effective toxicity monitoring and ultimately successful treatment of cancers.

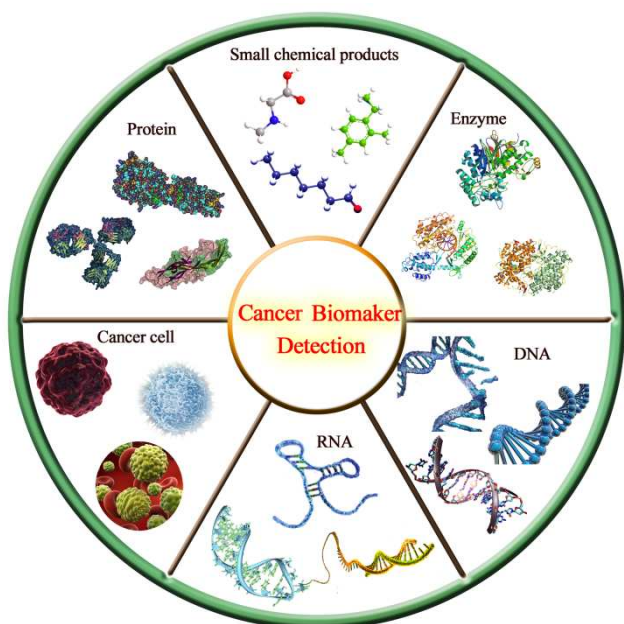


Fig. 1 Schematic illustration of various cancer biomarkers.

A biomarker is designated as “a substance or activity that can be objectively measured and evaluated as an indicator for normal biological process, pathogenic process, or pharmacological responses to a therapeutic intervention”.<sup>2</sup> Cancer biomarkers are present in tumour tissues or serum and encompass a wide variety of molecules, including DNA, mRNA, enzymes, metabolites, transcription factors, and cell surface receptors (Fig. 1).<sup>3</sup> The goal of the cancer biomarker field is to develop reliable, cost-effective, powerful detection and monitoring strategies for cancer risk indication, early cancer detection and tumour classification; so that the patient can receive the most appropriate therapy and monitor disease progression, regression and recurrence. In the past few decades, significant and substantial progress has been made in this field. Various promising detection methods based on the specific recognition of intracellular biomarkers or the biomarkers on cancer cell surface have been developed, including polymerase chain reaction (PCR),<sup>4, 5</sup> enzyme-linked immunosorbent assay (ELISA),<sup>6, 7</sup> electrophoresis,<sup>8, 9</sup> surface plasmon resonance

(SPR),<sup>10, 11</sup> surface enhanced Raman spectroscopy (SERS),<sup>12-14</sup> microcantilevers,<sup>15, 16</sup> colorimetric assay,<sup>17, 18</sup> electrochemical assay,<sup>19, 20</sup> fluorescence method,<sup>21, 22</sup> etc. Although robust and high-efficient, most of these methods still suffer from the lack of accuracy, sensitivity and specificity for clinical diagnostic applications.

The inevitable biological challenges for cancer biomarker detection encouraged researchers to continuously devote much effort in this field. Firstly, cancer is a diverse disease and a single biomarker has limited ability to detect all cancer of particular organ with high specificity and sensitivity. In addition, no biomarker has been established as an “ideal” cancer screening tool which answer meets of diagnostic, prognostic, and predictive requirements simultaneously. Thus, the validation of new cancer biomarkers for efficient cancer diagnosis-that is determination of clinical relevance and applicability- is quite necessary and challenging. And also many questions have been raised regarding how new tests will be developed, evaluated and integrated into clinical practice. Secondly, some biomarkers purport to have high sensitivity but tend to have low specificity, which faces a high risk of false-positive signals and may translate into a large number of people subjected to unnecessary costly diagnostic procedures and psychological stress. To avoid false positives in cancer diagnosis, arising from population variations in expression of a single biomarker, simultaneous evaluation of a panel of cancer biomarkers are typically important and required. The analytic techniques which possess sufficiently capacity for multi-analytes discrimination have been developed correspondingly, such as bio-barcode assay<sup>23, 24</sup> and array-based sensors.<sup>25, 26</sup> Thirdly, being considered as “liquid biopsy”, fluid sampling of biomarkers is of great interest as it is widely accepted, readily repeated, convenient, non-invasive, and low cost. Fluid biomarkers include a variety of components in blood, urine, or other fluids that reflect the presence of a tumour in the body, including circulating tumour cells (CTCs) and macromolecules such as lipids, proteins, RNA, microRNA (miRNA), and DNA that originate from tumour cells.<sup>27</sup> Although fluid-based biomarkers seem promising, their reliability has not been determined. Assay sensitivity and specificity need to be improved; techniques must be standardized and validated. Last but not the least, the sensitivity and specificity of the as-designed cancer biomarker sensing system are mainly determined by various factors, such as the binding efficiency between probe and target, the capability to convert the target-receptor binding event into measurable signals, the anti-interference ability toward non-specific biomolecules coexist in samples, etc. The means to take strategies which can achieve reliable and robust signal amplification, background signal suppression or nonspecific binding prevention is essential for improving the analytic performance. In previous work, some novel concepts have been introduced to biomarker detection field, such as molecular imprinting,<sup>28</sup> synergistic capture probe.<sup>29</sup> Furthermore, with the rapid emergence of nanotechnology, hybrid bio/nano-structures have been widely used to amplify bioassay signals, increase the sensitivity of a

biosensor and generate higher accuracy and precision.<sup>30</sup> Although the use of nanoparticles for the detection of cancer biomarkers and cancer cells has been reviewed in the literature,<sup>31</sup> the results reported and the papers cited in this review seemed to be out-of-date at present as three years passed (considering the fact that the received time of the review is May 2011). Since then, there has been rapid progress in this field, and several reviews summarized from different research point of view could be further explored.<sup>32–35</sup> Especially, from 2011 to 2014, many improved works have been carried out and some novel concepts and detection tools have been introduced to this field, which merits an updated review.

In this review, we highlight recent advances in cancer biomarker detection. We aim to provide a comprehensive review covering the existing challenges and latest development in achieving high selectivity and sensitivity for the detection of diverse cancer biomarkers. For discussion purposes, progress in cancer biomarker detection is discussed separately according to the category of cancer biomarkers, drawing on some recent examples of our own work and related studies in the literature. It is hoped that this review will inspire broader interests across various disciplines and stimulate more exciting developments in this still young yet very promising field for the benefit of human health.

## 2. The common used biomarker for cancer detection

### 2.1 Cancer protein biomarkers

Proteins are well known to be vital biomolecules in living organisms, who function as the working unit for many aspect of life, ranging from storage and metabolism of energy to regulation of cellular functions. Abnormal expression of proteins or expression of unique proteins often associates with certain disease. For cancer diagnosis, protein biomarkers include substances that are either produced by cancer cells themselves or by other cells in response to cancer.<sup>36, 37</sup> Protein biomarkers are primarily found in the blood and, sometimes, urine.<sup>38</sup> Most protein biomarkers related to cancer serve multiple clinical purposes during early or late disease progression, which are used to monitor response and/or detect recurrence or progression during follow-up after treatment.<sup>39, 40</sup> Analysing protein cancer biomarkers of low abundance faces great challenges. Firstly, proteins cannot be “amplified” as nucleic acids as they cannot replicate themselves and exponentially increase their concentration for the purpose of detection. Secondly, proteins are very sensitive to ambient environment, including temperature, ionic strength and pH, which make it more difficult to detect cancer protein biomarker with low concentration. Thirdly, the direct tracking of trace of cancer-related protein in crude or complex biological samples is limited to the high background of other proteins with high abundance, which is an immensely challenging task. Thus sensitivity, specificity, and accuracy are basic requirement when biosensors are fabricated. With these guide lines, great

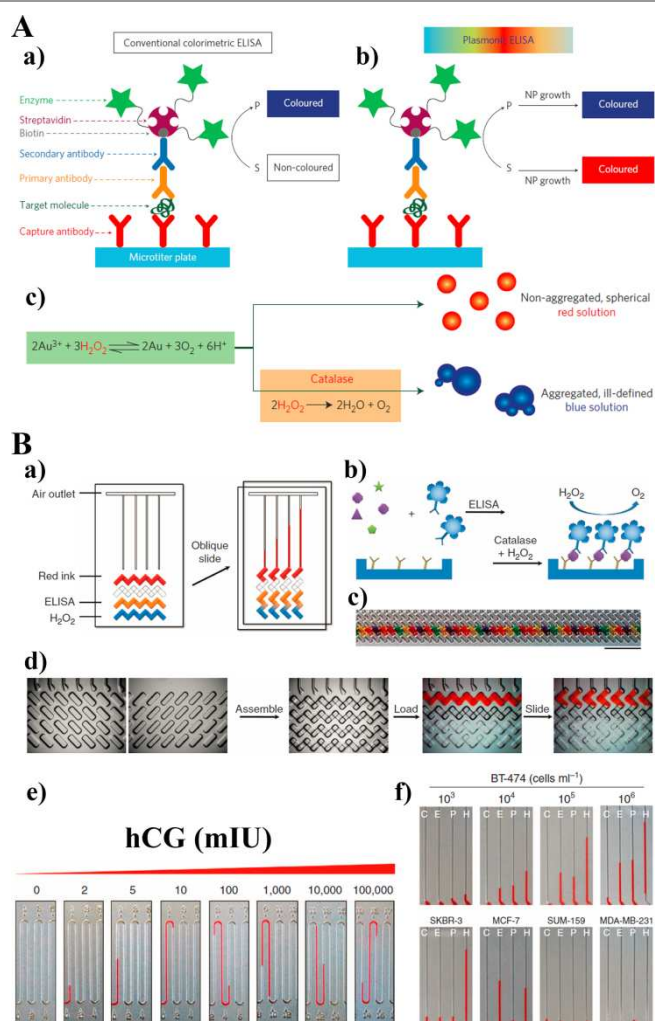


Fig. 2 (A) Schematic view of the sandwich ELISA format and two possible signal generation paths. a) Conventional colorimetric ELISA generates coloured compound by enzymatic biocatalysis. b) Plasmonic ELISA generates coloured nanoparticle solutions of characteristic tonality via the biocatalytic cycle of enzyme. c) Representation of the generation of coloured solutions for detection with the naked eye. Reprinted with permission from ref. 6. (B) Working principle of the V-chip for protein biomarker detection. a) Schematic illustration of the V-chip. b) The mechanism for oxygen generation during ELISA reaction. c) V-chip can be loaded with 50 different coloured food dyes using swab tips. d) High-magnification microscopic images of typical operation steps in a 50-plexed V-chip. e) Application of V-chip for hCG sensing in buffered solution. f) The performance of V-chip for detecting multiplexed biomarkers from cell lysates. Reprinted with permission from ref. 52.

progress has been made in designing new tools for the analysis of proteins in recent two or three years.

#### 2.1.1 ELISA-based methods

Enzyme-linked immunosorbent assay (ELISA) has been extensively used in routine clinical diagnostics, which is still suggested to be the gold standard for detection of proteins in physiological samples.<sup>41–43</sup> In traditional ELISA methods, colorimetric or fluorescent readout signals are used to visualize the binding of target protein to a specific recognition element. Despite advancements in the development of numerous new ELISA-based technologies for protein detection, many

challenges remain to their further application in point-of-care diagnostics. The ELISA principle has been frequently extended and adapted to improve its performance, such as improvements to increase sensitivity, multiplicity, quantification, portability, speed of operation, and clarity of readout, and reduce-cost.

The traditional colorimetric ELISA assay generates signal by the conversion of the enzyme substrate into a coloured molecule, and the intensity of the colour of the solution is quantified by measuring the absorbance with a plate reader (Fig. 2A-a). Although the distinguish between non-coloured and coloured solution may be realized with the naked eye, this is hardly to achieve the measurement of low concentrations of disease biomarkers with confidence, therefore making a naked-eye inspection unsuitable for ultrasensitive detection. Alternatively, Stevens *et al.* developed a new ELISA method, referred to as plasmonic ELISA, using gold nanoparticles as the probe to detect (PSA) and HIV-1 capsid antigen p24 with the naked eye.<sup>6</sup> PSA has been recognized as a valuable biomarker for cancer recurrence in patients that have undergone radical prostatectomy.<sup>44, 45</sup> As shown in Fig. 2A-b, target protein biomarker was captured with specific antibodies on a disposable substrate and subsequently labelled with enzyme catalase. The biocatalytic cycle of enzyme label was closely linked to the growth of gold nanoparticles in order to generate coloured solutions of characteristic tonality in the presence or absence of the analyte. In the absence of the analyte, the reduction of gold ions with hydrogen peroxide occurred at a fast rate, obtaining quasi-spherical, non-aggregated gold nanoparticles (Fig. 2A-c). Under this condition, the solution appeared to be red coloured. While in the presence of the analyte, the enzyme catalase consumed hydrogen peroxide and slowed down the kinetics of gold crystal growth, which resulted in the growth of nanocrystals showing an ill-defined morphology comprising aggregated nanoparticles (Fig. 2A-c). In this case, the solution turned blue. The blue and red colours are easily discriminable at a glance, thus facilitating the sensitive detection of PSA. The methodology presented here is a general tool for the detection of any clinically relevant analyte at a glance as long as antibodies directed against it are available. Tang's group also developed an enzyme-cascade-amplification strategy to enhance the performance of colorimetric ELISA for PSA detection.<sup>46</sup> In the presence of target PSA, the labelled alkaline phosphatase on secondary antibody catalyses the formation of palladium nanostructures, serving as the catalyst of 3, 3', 5, 5'-tetramethylbenzidine-H<sub>2</sub>O<sub>2</sub> system to produce the coloured products, thus resulting in the signal cascade amplification. As a promising candidate for artificial enzymes, catalytically active nanomaterials (nanozymes) show several advantages over natural enzymes in ELISA application,<sup>47, 48</sup> such as controlled synthesis in low cost, tunability in catalytic activities, as well as high stability against stringent conditions. A highly sensitive and compatible gold nanoparticle (AuNP)-based fluorescence-activatable ELISA method for sensing ultralow levels of PSA in patient serum samples was presented by Chen and coworkers.<sup>49</sup> The detection limit of the newly developed assay for PSA was

pushed down to 0.032 pg/mL, which was more than 2 orders of magnitude lower than that of the conventional fluorescence probe. The ability to detect single enzyme molecules provides another means to quantitate low abundance cancer markers which is hardly to be realized by traditional ELISA assay. Shim *et al.* reported a microfluidic droplet-based highly flexible and sensitive diagnostic platform for the counting of individual analyte molecules and detecting a biomarker for prostate cancer in buffer with the detection limit down to a concentration of 46 fM.<sup>50</sup> Other efficient methods for highly sensitive detection are based on reducing the background signal. Specifically, since biological samples have a negligible magnetic background, magnetic signal-based ELISA platforms can avoid detectable magnetic background signals, produce low noise signal and enable the detection of nanomolar cell suspension receptor concentrations or attomolar concentrations of proteins in serum.<sup>7, 51</sup> However, these technologies are time consuming to manipulate and require sophisticated instruments to read the results.

Clinical research has demonstrated that multi-protein measurements provide more accurate diagnostic results. Qin *et al.* created a new volumetric bar-chart chip (V-chip) that allows quantitative, multiplexed and instrumental-free protein measurement.<sup>52</sup> The multiplexed volumetric V-chip integrates ELISA reactions with volumetric measurements of oxygen generated on a microfluidic chip (Fig. 2B), allowing instant and visual quantification of biomarkers without the need for optical instruments or any data processing or plotting steps. After a simple oblique sliding of the upper plate over the lower, the advance of ink in each individual channel indicated the amount of catalase reacted in that well, which was proportional to the concentration of the corresponding ELISA target protein. Using this strategy, they demonstrated the rapid quantification of chronic gonadotropin (hcG) protein (Fig. 2B-e), which was a pregnancy indicator and widely accepted biomarker for some types of cancer, including breast and ovarian.<sup>53</sup> Furthermore, the V-chip approach also enabled multiplex measurement of target protein biomarkers from cell lysates (Fig. 2B-f). The sensitivity could be further amplified by introducing PtNPs to the V-Chip platform as a nanoparticle substitute for catalase.<sup>54</sup>

### 2.1.2 Electrochemical and electrical detection methods

A principle challenge for many label free assays of protein biomarkers is both that a relatively less significant change in properties occurs upon target binding and that those responses acquired must be retained as highly specific. Thus a sensitive readout method is required. Electrochemical/electrical detection strategies commonly have an innate high sensitivity and simplicity that can be effectively married to miniaturized hardware.<sup>55-57</sup> As such, they constitute, arguably, the most practical, quantifiable and saleable of all low cost diagnostic assessments of protein presence.<sup>20, 34</sup> A number of promising electrochemical/electrical strategies have been explored in the development of protein biosensors for biomedical applications, including voltammetric techniques<sup>58-62</sup> (such as cyclic voltammetry, linear sweep voltammetry, differential pulse

voltammetry and square wave voltammetry, stripping voltammetry), amperometry,<sup>63</sup> impedimetric methods,<sup>64</sup> electrochemiluminescent (ECL)<sup>65</sup> assays, field-effect transistors,<sup>66, 67</sup> nanochannel/nanopore-based electrical technique,<sup>68, 69</sup> etc.

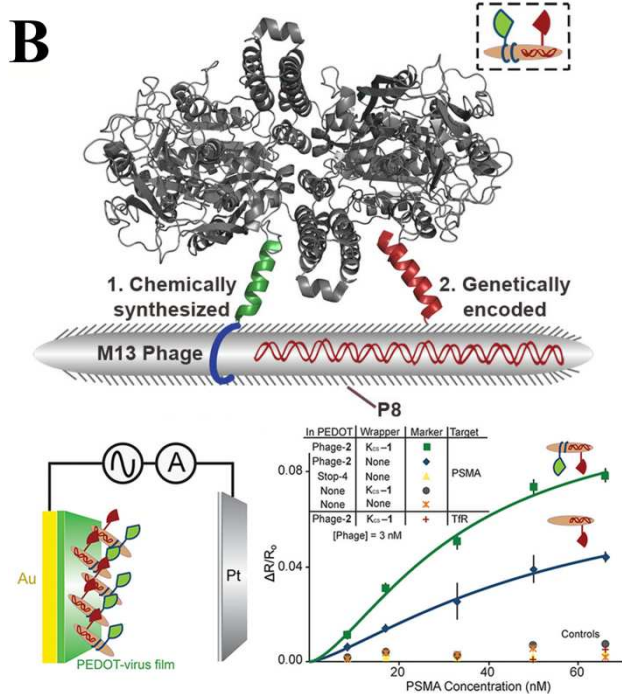
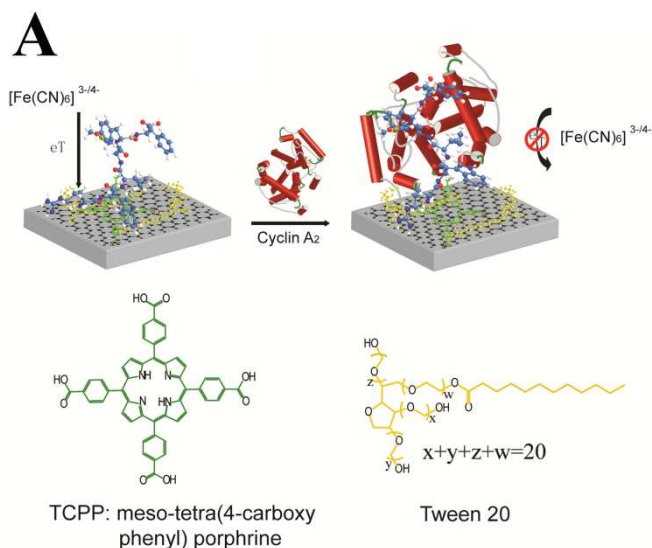


Fig.3 (A) Schematic diagram of the porphyrin-noncovalently functionalized graphene-based peptide sensor for cyclin A<sub>2</sub> detection. Reprinted with permission from ref. 74. (B) Schematic indication of bidentate binding to PSMA by chemically synthesized (KCS-1, green) and genetically encoded (peptide 2, red) ligands to PSMA and the biosensing experiment. Reprinted with permission from ref. 29.

Among these electrochemical methods, electrochemical impedance spectroscopy (EIS) is highly sensitive for measuring electrode surface changes; it allows complex bio-recognition

events to be probed with a simple, label-free and mediator-free strategy.<sup>70-72</sup> However, the application of impedance biosensors has been limited by their sensitivity to nonspecific adsorption, which often limits the selectivity of biosensors applied to complex matrices and controls the background response, directly regulating the device's sensing performance.<sup>73</sup> Using Tween 20 for preventing nonspecific binding, our group realized sensitive detection of cyclin A<sub>2</sub> by using meso-tetra (4-carboxyphenyl) porphyrin (TCPP) noncovalently functionalized graphene modified electrode and one specific hexapeptide P<sub>0</sub> (RWIMYF) as detection probe (Fig. 3 A).<sup>74</sup> Cyclin A<sub>2</sub> is a prognostic indicator in early-stage cancers and has been reported overexpressed in many types of cancers including breast cancer, liver cancer, lung cancer, soft tissue sarcoma, leukemia, and lymphoma.<sup>75-80</sup> P<sub>0</sub>, screened from synthetic combinatorial libraries, is a hexapeptide that binds to a surface pocket in cyclin A<sub>2</sub> with high affinity and inhibits the kinase activity of CDK<sub>2</sub>-cyclin A complex.<sup>81, 82</sup> The attachment of cyclin A<sub>2</sub> hampered the redox probe [Fe(CN)<sub>6</sub>]<sup>3-/4-</sup> close to the electrode surface which changed electrochemical impedance signal. The detection limit of the electrochemical impedance sensor reached 1.02 pM in cell extracts; and it could also differentiate cancer cells from normal ones. Furthermore, by comparing anticancer drug doxorubicin (DOX)-treated cancer cells with none-treated cells, this platform provided the potential of using simple electrochemical technique to estimate the efficiency of anticancer drugs in cancer therapy. Weiss and coworkers described a bio-affinity matrix of viruses integrated into electronically conductive polymer films for electrochemical sensing of prostate-specific membrane antigen (PSMA), a prostate biomarker (Fig. 3B).<sup>29</sup> Viruses that infect only bacteria, the M13 bacteriophage have a readily customized protein coat, which can be tailored to bind to cancer biomarkers.<sup>83, 84</sup> Thus the whole virus particles can be used as a bio-affinity matrix for biosensors. The phages have a high density of peptides displayed on their surface, offering higher density ligands for PSMA binding. Furthermore, the chemically synthesized secondary recognition ligand was used to wrap around the phage to form bidentate binder with genetically encoded ligand. High sensitivity to PSMA resulted from synergistic action by two different ligands to PSMA on the same phage particle. This strategy could sensitively measure PSMA in synthetic urine with a detection limit of 100 pM without requiring enzymatic or other amplification.

Electrochemiluminescence (ECL), the smart combination of chemiluminescence and electrochemistry, has become a powerful analytical tool in the detection of biomolecules, clinical diagnostics, environmental and food monitoring, and biowarfare agent detection due to its simplified setup, label-free, low background signal, and high sensitivity.<sup>85, 86</sup> A label-free, ultra-sensitive and selective electrochemiluminescence assay was developed for detection of cyclin A<sub>2</sub> by using highly efficient ECL graphene-upconversion hybrid (Fig. 4A).<sup>87</sup> Since the expression level of cyclin A<sub>2</sub> is quite low, direct detection of cyclin A<sub>2</sub> in crude cancer cell extracts is challenging and important for both clinical diagnosis of cancer in the early stage

and the treatment. By chemically grafting cyclin A<sub>2</sub> detection specific probe, a PEGylated hexapeptide, to graphene-upconversion hybrid, the constructed ECL biosensor displays a superior performance for cyclin A<sub>2</sub>, which can not only detect cyclin A<sub>2</sub> directly in cancer cell extracts, but also discriminate between normal cells and cancer cells. The inherent luminescent property of ECL also makes it an attractive imaging tool to investigate biological recognition events of interest directly by naked eye (Fig. 4B).<sup>88</sup>

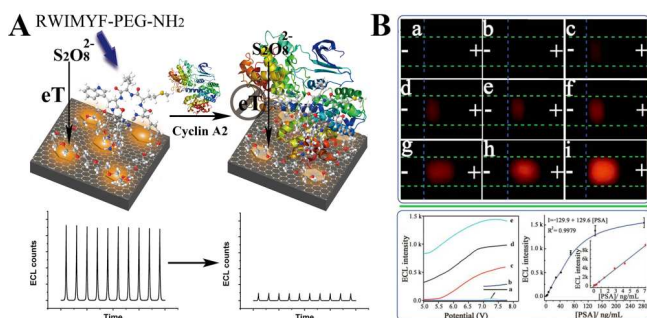


Fig. 4 (A) Graphene-upconversion nanocomposite-based peptide sensor for cyclin A<sub>2</sub> detection. Reprinted with permission from ref. 87. (B) ECL images of the bipolar electrodes (BPEs) after treated with different concentration of PSA and the corresponding ECL intensity analysis. Reprinted with permission from ref. 88.

Biosensors made from field effect transistors (FET) are kind of a big deal in the biosensors world—they're incredibly sensitive, allow label-free and real-time detection, and support nondestructive sampling.<sup>89, 90</sup> Recently, a number of nanoscale FET devices utilising functionalized nanomaterials, such as graphene,<sup>66</sup> carbon nanotubes,<sup>91</sup> and MoS<sub>2</sub> nanosheet,<sup>67</sup> have been reported to have high capability for assaying protein cancer biomarker. Under appropriate conditions, the charge depletion-accumulation associated with selective binding events can be sufficiently sensitive to achieve protein detection down to fM or even lower levels.<sup>67</sup> Although promising, most of these sensors have a lack of specificity to perform biomarker detection directly from physical fluids mainly because of challenges caused by the complexity of media. Passivating devices with blocking agent offers a promising strategy to decrease the false-positive signals induced by nonspecific binding of proteins and other biomaterials in serum and improves the sensitivity of constructed biosensor. With this in mind, Zhou *et al.* developed an In<sub>2</sub>O<sub>3</sub> nanowire-based FET biosensing system that is capable of detection of multiple cancer biomarkers with high reliability at clinically meaningful concentrations from whole blood collected by a finger prick.<sup>92</sup>

Microfluidic-based point-of-care platforms, possessing the high degree of integration of fluidic handling, specimen processing and consumption of reagents, can perform quantitative, rapid and affordable high-throughput measurements, and therefore have the potential to revolutionize clinical genomic and proteomic analyses and personalized diagnostics.<sup>93-96</sup> Further, microfluidics is easily integrated within standard electronic micro-fabrication formats, making it possible for the facile multiplexed detection of a range of

proteins in a small analytical volume using a cost-effective and portable device. A microfluidic purification chip (MPC) was

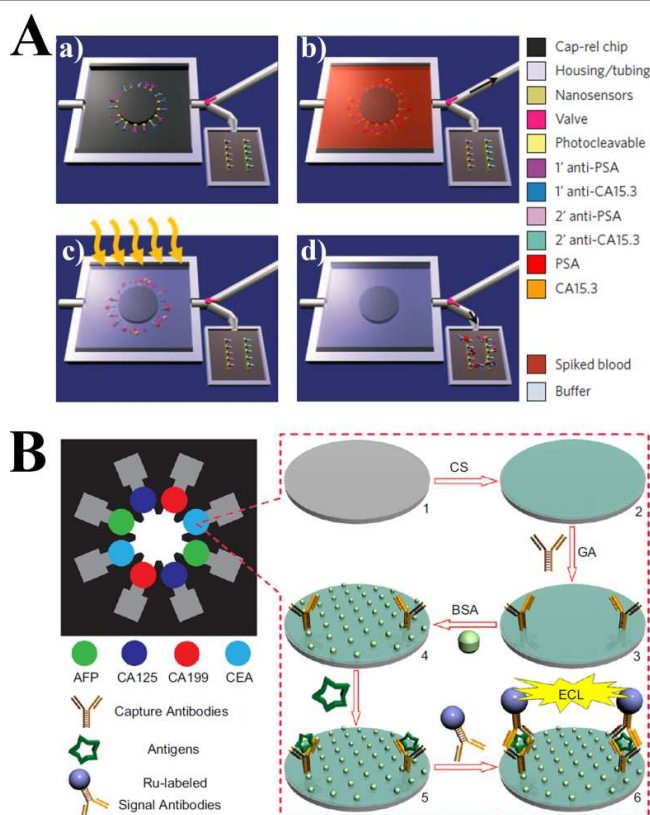


Fig. 5 (A) Schematic of microfluidic purification chip (MPC) operation. a) Primary antibodies to multiple biomarkers are bound with a photocleavable crosslinker to the MPC. b) Whole blood is injected into the chip with the valve set to the waste compartment, biomarkers presented in the sample bind to their cognate antibodies. c) After washing, the photocleavable crosslinker was cleaved by UV irradiation, releasing the antibody-antigen complexes into solution. d) The valve is set to nanosensor reservoir, enabling label-free sensing to be carried out to determine the presence of specific biomarkers. Reprinted with permission from ref. 97. (B) Schematic representation of biomarker detection using 3D paper-based ECL device. Reprinted with permission from ref. 103.

developed for multiplexed cancer biomarker sensing by using distinct components within the sensor to perform purification and detection.<sup>97</sup> As shown in Fig. 5 A, this new in-line MPC captured cancer biomarkers from physiological solutions, after washing, released them into a pure buffer for sensing, which overcame the limitations for detecting cancer biomarkers in physiological fluid samples, such as biofouling and non-specific binding. This technique enabled specific and quantitative detection of two model cancer antigens from a 10  $\mu$ L sample of whole blood in less than 20 min without the challenges associated with tailoring sensor operation for the medium of interest or engineering nanosensors that can withstand complex fluid media. Another microfluidic-based sensing system, named digital microfluidic assay was constructed by Javanmard's group for both cancer-related protein abundance and activity detection by integrating microfluidic technology with electrical impedance sensing and embodying a unique two-chamber architecture in which the

capture/reaction and detection steps were physically separated from one another.<sup>98</sup> Although promising, there remains several practical barriers that limit the application of microfluidic chips in clinics and in patients' homes. For example, traditional reliance on the fluid-introducing accessories and syringe pump control systems in microfluidics platforms result in significant additional cost and operational space. Additionally, the collection of analysis results still requires traditional instruments, such as fluorescence, absorption, mass spectrometers, or glucose meters, and others. Furthermore, complicated fluidic networks also limit the number of measurements per chip and thereby throughput of the device.<sup>99</sup> <sup>100</sup> The integration of small strip or electrochemical sensor in a paper-based device improves the quantification of the analytes in a user-friendly way.<sup>101, 102</sup> These microfluidic paper-based electrochemical techniques are affordable, easy-to-use and deliverable to end-users. A three-dimensional (3D) paper-based ECL device based on wax-patterned technology and screen-printed paper-electrodes was presented by Yu and coworkers for the diagnosis of four tumour markers in real clinical serum samples (Fig. 5B).<sup>103</sup> This proposed 3D paper-based ECL immuno-device combined the simplicity and low-cost of microfluidic paper-based analytical device and the sensitivity and specificity of ECL immunoassay, demonstrating high-throughput, rapid, sensitive, stable and reusable ECL response to trace amount of analyte in real biological samples.

### 2.1.3 Optical methods

Optical techniques, including colorimetric assays caused by light adsorption or light scattering,<sup>18</sup> fluorescent methods,<sup>104, 105</sup> and SPR strategies,<sup>106</sup> show promise for use in POC early cancer diagnostics because the signal is often detectable by naked eye and these assays are rapid without the requirement of any washing steps. Song and coworkers designed a multifunctionalized multiwalled carbon nanotube (MWCNT)-based rolling circle amplification colorimetric and chemiluminescent system for cancer protein biomarkers detection by integrating the binding ability of proteins, hybridization and replication ability of DNA, and the catalytic ability of enzymes.<sup>107</sup> The in situ rolling circle replication of DNA primer on the surface of MWCNTs created long single-strand DNA where a large number of nanoparticles or proteins could be loaded, forming a nano-hybridized 3D structure with a powerful amplification ability. The translation of antigen-antibody recognition process into DNA detection events that can be greatly amplified via isothermal rolling circle amplification (RCA) or PCR provides another new approach for signal amplified detection of protein.<sup>5, 108</sup> For example, using a genetically encoded unnatural amino acid with orthogonal chemical activity to conjugate oligonucleotides to antibodies, Schultz *et al.* developed an immuno-PCR method to detect HER<sup>+</sup> cells.<sup>5</sup> Proximity ligation assay (PLA) is an assay mechanism for sensitive high-capacity protein measurements by converting the detection of specific proteins, in which target molecules must be recognized by antibodies, to the analysis of DNA sequences. Proximity probes containing oligonucleotide

extensions are designed to bind pairwise to target proteins and to form amplifiable tag sequences by ligation when brought in proximity.<sup>109</sup> This reporter DNA molecule could be quantified by real-time quantitative PCR (qPCR) as a measure of detected target complexes, offering high specificity and sensitivity. Taking this method, Kamali-Moghaddam and coworkers developed a modified PLA to evaluate the suitability of prostasomes as biomarkers for prostate cancer.<sup>108</sup> These immune-PCR assay combined the specificity of antibodies with the amplification power of PCR allowing increased sensitivity for cancer biomarker evaluation. Further combination of these promising approaches in a microfluidic format could extend the utility of existing methods by reducing sample and reagent consumption and enhancing sensitivities and specificities for cancer diagnostics.<sup>110, 111</sup>

DNA-barcoding is an attractive technology and emerging diagnostic tool, used for the ultrasensitive and multiplexed detection of various targets.<sup>112-114</sup> In the case of proteins, the barcode assay can be between one and six orders of magnitude more sensitive than conventional ELISA-based assays, which offer the opportunity to monitor existing biomarkers a levels not possible with conventional assays.<sup>112</sup> Although promising, the application of DNA barcoding assay for cellular protein measuring remains challenging as barcode amplification and readout techniques are often incompatible with the cellular microenvironment. A photocleavable DNA barcode-antibody conjugate method, named "light-mediated cellular barcoding" (LMCB), was developed by Weissleder's group to overcome these shortcomings for rapid, quantitative, and multiplexed detection of proteins in single live cells.<sup>24</sup> The generic concept of the LMCB method is illustrated in Fig. 6A. DNA encoded antibodies firstly recognized the specific protein biomarkers on cell surface. Then the barcodes could be released into the solution for easy isolation by irradiating the labelled cells with light (~365 nm). Barcode amplification by PCR and subsequent gel electrophoresis analysis of the amplified barcodes allowed simultaneous detection and quantification of multiple proteins from single cells. In order to achieve the challenging requirement of detecting extremely low concentrated samples in real-life multiplexed biosensing, Hildebrandt and coworkers developed an optically multiplexed six-colour Förster resonance energy transfer (FRET) biosensor for simultaneous monitoring of five different individual binding events at very low concentrations (Fig. 6B).<sup>115</sup> They combined simultaneous FRET from one Tb complex donor to five different organic dye acceptors measured in a filter-based time-resolved detection format with a sophisticated spectral crosstalk correction, which resulted in very efficient background suppression. Low picomolar (ng/mL) detection limits for five different lung cancer tumour markers were obtained in this very challenging immunoassay involving 10 different antibodies and five different tumour markers in a single 50  $\mu$ L human serum sample, thus providing an effective early screening tool for lung cancer with the possibility of distinguishing small-cell from non-small-cell lung carcinoma.

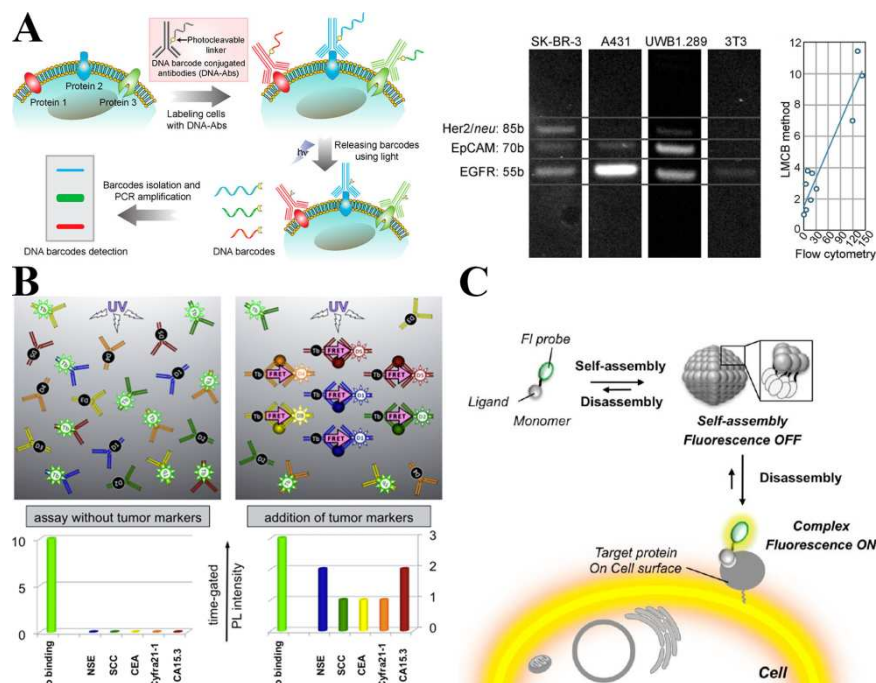


Fig. 6 (A) Schematic representation of the light-mediated cellular barcoding strategy and their sensing performance for multiplexed protein detection. Reprinted with permission from ref. 24. (B) 15-component multiplexed FRET lung cancer immunoassay for the simultaneous detection of five different tumour markers. Reprinted with permission from ref. 115. (C) Cell surface protein imaging using a disassembly-driven turn-on fluorescent probe. Reprinted with permission from ref. 22.

Visualization of tumour-specific protein biomarkers on cell membranes has the potential to contribute greatly to basic biological research and therapeutic applications. In most cases, antibodies appended with fluorescent molecules or nanomaterials are used to visualize these endogenous biomarkers on living cell surface.<sup>116-119</sup> However, the intrinsic fluorescent property of these components inevitably requires additional washing operations for accurate molecular imaging on cells. Target-responsive fluorescence switching mechanism is particularly promising to solve this problem. Using newly synthesized self-assembling turn-on fluorescent nanoprobe, Hamachi and coworkers successfully imaged cancer-specific biomarkers such as the folate receptor (FR) and transmembrane-type carbonic anhydrases (CA) under a live cell setting without needing any washing operations (Fig. 6C).<sup>22</sup> Moreover, the extended nanoprobe could also be successfully used in a cell-based inhibitor assay for CA on the surface of live cells. Taking the opposite point of the above mechanism, Liu and coworkers developed a novel bioprobe with aggregation-induced emission (AIE) characteristic by integrating tetraphenylsilole fluorogenic unit with a targeting ligand cyclic arginine-glycine-aspartic acid tripeptide (cRGD) to quantitate the integrin  $\alpha_v\beta_3$  (a unique molecular target for

early detection and treatment of rapidly growing solid tumours) in solution and implement the real-time imaging of the binding process between cRGD and integrin  $\alpha_v\beta_3$  on cell membrane.<sup>120</sup>

SPR is an optical technique which is the resonant oscillation of conduction electrons at the interface between a negative and positive permittivity material stimulated by incident light.<sup>121, 122</sup> It is the basis of many standard tools for measuring adsorption of material onto planar noble metal (typically gold and silver) surface or onto the surface of metal nanoparticles, and is also the fundamental principle behind many colour-based biosensor applications and different lab-on-chip sensors. SPR has become a prominent sensing technique for cancer diagnostic applications because of the capability of real-time monitoring analyte-analyte interactions with high sensitivity.<sup>10, 11, 14, 123-125</sup> Dai's group prepared a nanostructured plasmonic gold film with uniform solution-phase growth onto whole glass slides, which afforded near-infrared fluorescence enhancement of up to 100-fold.<sup>126</sup> They further fabricated protein microarrays on plasmonic gold substrates, enabling multiplexed protein analysis and affording detection limits as low as a few fM of a model cancer biomarker, carcinoembryonic antigen (CEA), with six orders of magnitude dynamic range (Fig. 7A). The high sensitivity, broad dynamic

## ARTICLE

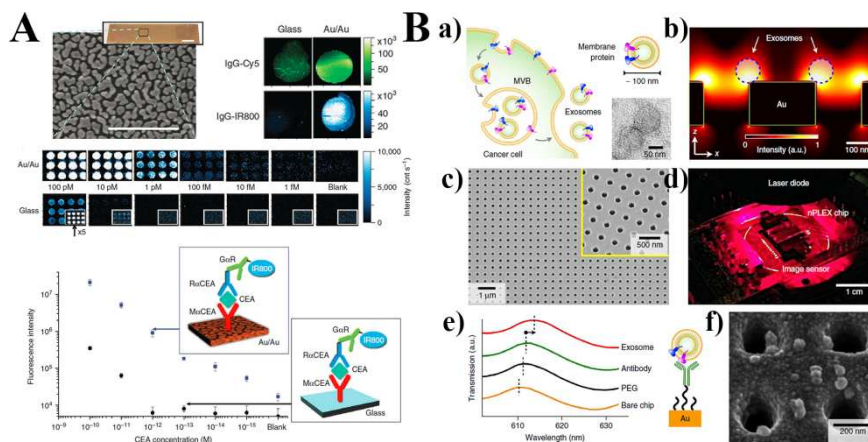


Fig. 7 (A) Near-infrared fluorescence enhanced protein microarrays on plasmonic gold-on-gold nano-island films probed by IR800. Reprinted with permission from ref. 126. (B) Label-free detection of exosomes with nano-plasmonic exosome (nPLEX) sensor. a) Cancer cells secrete an abundance of exosomes through fusion of a multivesicular body (MVB) with the cellular plasma membrane. b) Finite-difference time-domain simulation shows the enhanced electromagnetic fields tightly confined near a periodic nanohole surface. The field distribution overlaps with the size of exosomes captured onto sensing surface, maximizing exosome detection sensitivity. c) Scanning electron microscope image of the periodic nanoholes in the nPLEX sensor. d) A prototype miniaturized nPLEX imaging system developed for multiplexed and high-throughput analyses of exosomes. e) Schematic illustration of changes in transmission spectra showing exosome detection with nPLEX. f) Scanning electron micrograph demonstrates exosome capture by functionalized nPLEX. Reprinted with permission from ref. 130.

range and easy adaptability of this plasmonic chip presented new opportunities in proteomic research and diagnostic applications.

Exosomes are membrane-bound phospholipid nanovesicles (50–100 nm in diameter) actively secreted by mammalian cells.<sup>127</sup> Exosomes illustrate potential for cancer diagnostics as they carry molecular information about the parent tumour.<sup>128</sup> Evaluation of cancer cell secreted exosomes and capturing clinical information without biopsying the tumour could be a useful clinical and research tool.<sup>129</sup> Lee *et al.* developed a nano-plasmonic exosome (nPLEX) assay based on transmission surface plasmon resonance through periodic nanohole arrays for label-free and high throughput quantification of exosomes (Fig. 7 B).<sup>130</sup> Each array was functionalized with affinity ligands to enable profiling of exosome surface proteins and proteins present in exosome lysates. With target-specific exosome binding, the nPLEX sensor displayed spectral shifts or intensity changes proportional to target marker protein levels. The probing depth of plasmonic nanoholes was readily matched to exosome size, which improved the detection sensitivity. Combining the nanohole chip with a miniaturized imaging setup, they further developed an nPLEX imaging system, which was readily scalable for massively parallel and real-time monitoring of molecular binding.

#### 2.1.4 Other techniques

Kotov *et al.* found that plasmonic effects observed in chiral assemblies of nanoparticles could be used for versatile biosensing platforms construction.<sup>131</sup> Plasmonic enhancement of the chirality of the biomolecular bridges between the nanoparticles, the bisignate nature of the CD bands, and an unusual dependence of the intensity of CD bands on the distance between the nanoparticles enabled exceptionally low limits of detection for both small and peptides/proteins, even in complex media with multiple biological components. Mass spectrometry (MS) has been established as a key technique of choice in metabolomics studies due to its high sensitivity and resolution, wide dynamic range, reproducible quantitative analysis, and the ability to analyze biofluids with extreme molecular complexity.<sup>132</sup> Motivated by the success of MS in metabolomics, the analytical community has initiated efforts towards MS-based metabolomics to investigate metabolic cancer biomarkers.<sup>133</sup> For example, capillary electrophoresis–mass spectrometry (CE-MS) has been used for the metabolome analysis of human HT29 colon cancer cells.<sup>134</sup> Metabolites are first separated by CE based on charge and size, and then selectively detected using MS by monitoring ions over a large range of *m/z* values. CE-MS has a short analysis time with less than 20 min per sample and allowed the simultaneous and reproducible analysis of more than 80 metabolites in a single run with a minimum consumption of sample and reagents. Furthermore, large-scale metabolomic technologies based on liquid chromatography–mass spectrometry (LC-MS) are also increasingly gaining tremendous attention for their use in the

diagnosis of cancer. Li and coworkers developed a universal metabolome-standard (UMS) method in conjugation with chemical isotope labeling LC–MS for a urine metabolomics study of bladder cancer.<sup>135</sup> In this method, UMS of a specific type of sample was firstly labeled by an isotope reagent and then spiked into any individual samples labeled by another form of the isotope reagent in a metabolomics study. The resultant mixture was analyzed by LC–MS to provide relative quantification of the individual sample metabolome to UMS. Taking selected reaction monitoring (SRM) technique, which had emerged as a promising technology for high-throughput mass spectrometry-based quantification of target proteins in biological and clinical specimens, Qian and coworkers presented an antibody-free strategy for sensitive prostate cancer related protein quantification.<sup>136</sup> Another mass spectrometric sensor was fabricated by Wu's group using nanoporous silicon microparticles to capture, enrich, protect, and detect low-molecular-weight peptides sieved from a pool of highly abundant plasma proteins in colorectal cancer patient's serum.<sup>137</sup> Some magnetic and mechanical assays had also been used for cancer protein biomarker evaluation.<sup>138-141</sup> However these techniques all requires expensive equipment, sophisticated instrumentation, and specially trained technical personnel, which goes against the basic requirements of point-of-care testing that needs compact, robust, and inexpensive instruments.

## 2.2 Cancer related enzyme dysregulation

### 2.2.1 Telomerase

Human telomerase is a specialized ribonucleoprotein polymerase that contains an integral RNA with a short template element that directs the synthesis of telomeric repeats at chromosome ends and protects chromosomes from fusion, recombination and degradation.<sup>142</sup> Most germ-line and stem cells, and about 85% of human tumours contain telomerase.<sup>143</sup> The differential expression of telomerase between normal somatic cells and tumour cells makes telomerase an attractive diagnostic and prognostic tumour marker and a potential therapeutic target for chemotherapy.<sup>144-146</sup> However, the goal of using telomerase as a common clinical cancer marker has not yet been achieved currently. Achieving this goal will encourage scientists to develop more robust bioanalytical methods for the rapid, sensitive, and reliable detection of telomerase activity in a particular cell or clinical tissue and body fluids to provide more reliable biomedical information. Recently, a comprehensive review had been organized by Xing's group, offering unique insights in this field.<sup>147</sup> They highlighted some of the latest methods for identifying telomerase activity and inhibition, discussed some of the challenges for designing innovative telomerase assays and also summarized the current technologies and speculate future directions for telomerase testing. The research field of telomerase measurement is extremely active and highly important. Especially, the lack of available assays to measure telomerase in a sufficiently reliable, quantitative, and sensitive way continues to be a strong driving

force in telomerase research. Recently, the highly interdisciplinary collaborations enable more rapidly advances in this field, obtaining significant new progress in biomedical telomerase research. Here, we just share the latest development in telomerase activity detection, which is not covered by Xing's review.

One of the most important criteria for evaluating an assay for telomerase activity analysis is the sensitivity. The traditional telomeric repeat amplification protocol (TRAP) has been developed as a gold-standard assay to measure telomerase activity in small samples of cell or tissue extracts due to its ultra-high sensitivity.<sup>143</sup> Although quite powerful, this gel electrophoresis-based assay is time-consuming, not easily quantitated, and subject to PCR-related artefacts and it is also inappropriate for the evaluation of quadruplex ligand telomerase inhibitors.<sup>148, 149</sup> Therefore, alternative PCR-free methods have been actively developed to address these problems, including colorimetric methods,<sup>150</sup> electrochemical and electrochemiluminescent technique,<sup>151-153</sup> fluorescent sensor,<sup>154-158</sup> silicon-based microring resonator biosensor,<sup>159</sup> glucose meter,<sup>160</sup> and single-molecule real-time detection assay,<sup>161</sup> etc. The introduction of signal amplification mechanism is critical for ameliorating PCR-free methods to achieve the sensitivity comparable to TRAP assay. A novel exponential isothermal amplification of telomere repeat (EXPIATR) assay was developed by Weizmann and coworkers as a sensitive, simple, and reliable in vitro method for measuring telomerase activity in cell extracts.<sup>162</sup> EXPIATR was based upon a strategically designed path of nucleic acid isothermal amplifications using the ability of a restriction enzyme to nick a recognition site and a polymerase to replicate and displace the target repeatedly. This fantastic protocol not only shared the superiorities of TRAP but also made several improvements. For example, it abandoned the expensive thermal cycling protocol and achieved ultrafast detection: telomerase activity equivalent to a single HeLa cancer cell could be detected in ~25 min. Although EXPIATR method for telomerase activity detection can reach the excellent sensitivity of a single cancer cell, one potential problem is the risk of generating false-negative results due to the presence of inhibitors of the amplification reactions in the analysis of total protein cell extracts. To meet this case, they further improved the above EXPIATR method with AuNPs to improve the specificity of isothermal strand-displacement amplification and resolve the issues of the EXPIATR assay when performed on complex, protein rich samples.<sup>163</sup> In the presence of AuNPs, the sensitivity of the detection of telomerase activity in complex samples was improved five-fold with the traditional assay, providing an efficient way to enhance the reliability of the EXPIATR assay to a new level. AuNPs could be used not only to enhance the structural stability and maintain the bioactivity of enzymes, but also as signal reporter for the indication of telomerase extension reaction. The colour change of AuNPs provides an elegant platform for absorption-based colorimetric detection with AuNPs as signal reporters. Using telomerase reaction products to regulate the aggregation behaviour of gold

nanoparticles and generate a concomitant change in colour, our group developed novel visual methods for measuring telomerase activity with naked eye.<sup>17, 164</sup> Taking the similar sensing mechanism as our previous work,<sup>17</sup> Cui *et al.* further presented a telomeric elongation controlled surface enhanced Raman scattering (TEC-SERS) based protocol for the ultrasensitive telomerase detection.<sup>165</sup> In their method, thiolated telomerase substrate oligonucleotide (TS primer) and Raman reporter molecules were attached to gold nanoparticles to form SERS active Au-Tag nanoparticles. Telomerase extension reaction generated long G-rich single strand which could fold into G-quadruplex structures as the block layer to prevent the salt induced aggregation of Au-Tag nanoparticles. While in the absence of telomerase, TS primer was not elongated, Au-Tag NPs illustrated the positive tendency to aggregate after the salt addition. As the aggregation behaviour of Au-Tag NPs was closely related to SERS intensity, telomerase activity can be measured using SERS signals as the indicator. The authors reported an impressive sensitivity (the LOD was 1 tumour cell/mL or 1 tumour cell in  $1 \times 10^6$  normal cells) for telomerase activity detection.

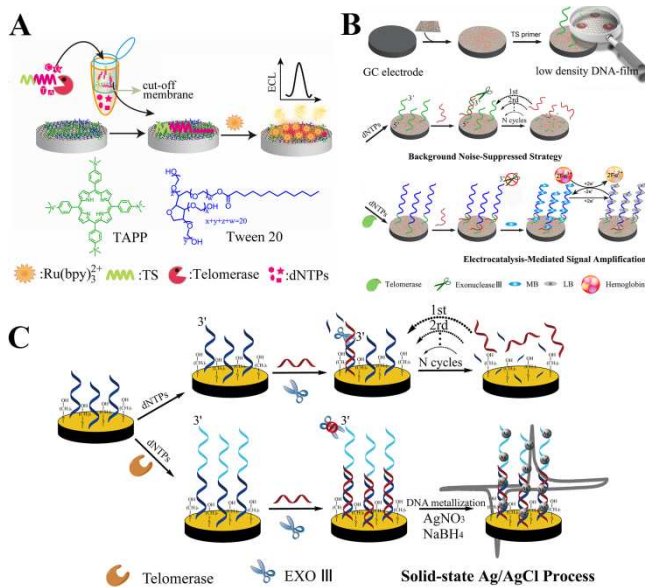


Fig. 8 Schematic representations of electrochemical biosensors for telomerase activity detection. (A) Label-free electrochemiluminescence assay for telomerase activity detection based on Porphyrin-Graphene Nanocomposite modified electrode. Reprinted with permission from ref. 167. (B) Label-free electrocatalysis assay for human telomerase activity detection based on GSPHS-modified electrode. Reprinted with permission from ref. 168. (C) DNA-metallization based signal amplification assay for human telomerase activity detection using enzyme-assisted background current-suppression and highly characteristic solid-state electrochemical process. Reprinted with permission from ref. 169.

Nanotechnology offers unique opportunities for creating highly sensitive innovative biosensing devices and ultrasensitive bioassays.<sup>30, 35</sup> To obtain successful and reproducible detection of biological targets using nanomaterials, the as-synthesized nanomaterials must be well dispersed in aqueous solution with minimal to no aggregation and nonspecific binding to biomolecules or substrates. The

enormous signal enhancement associated with the use of nanoparticle amplifying labels and with the formation of nanoparticle-biomolecule assemblies provides the basis for ultrasensitive optical and electrical detection with PCR-like sensitivity.<sup>166</sup> Using functional nanomaterials as the nanostructured electrode materials or electrochemical signal reporters, our group constructed a series of electrochemical biosensors for the telomerase activity measurement and telomerase inhibitor screening.<sup>167-170</sup> Electrochemistry provides powerful analytical techniques encompassing the advantages of instrumental simplicity, moderate cost and portability, which is often used for sensitive, selective, rapid and facile sensor fabrication in biomedical fields.<sup>171, 172</sup> As a one-atom-thick planar sheet of sp<sup>2</sup>-bonded carbon atoms, graphene owns unusual electronic properties, such as ballistic electron transport along with highly electrical conductivity.<sup>173, 174</sup> It has been widely used in electrochemical biosensor constructions.<sup>175</sup> Using a cation porphyrin, meso-tetra(4-N,N,N-trimethylanilinium) porphyrin (TAPP) functionalized chemically converted graphene (TAPP/CCG) as electrode materials and Tween 20 as blocking agent for preventing of nonspecific binding, we fabricated a label-free electrochemiluminescent (ECL) sensor for telomerase detection.<sup>167</sup> As shown in Fig. 8A, the products of telomerase reaction was pretreated by dialysis tube with the cut-off membrane of Mw=2000 to remove the unreacted dNTPs, and then conjugated on positively charged graphene modified electrode surface through electrostatic attraction and  $\pi$ - $\pi$  stacking. The negatively charged DNA skeleton fixed on electrode surface provided sufficient binding site for signal reporter Ru(bpy)<sub>3</sub><sup>2+</sup>, which consequently produced the ECL signal with tripropylamine (TPA) as the coreactant. The binding site of ECL probe was correlated to the extended degree of telomerase substrate by telomerase as elongated telomere repeat units could attract more Ru(bpy)<sub>3</sub><sup>2+</sup> to electrode surface. Our ECL sensor can detect telomerase activity as low as in 10 HeLa cells/mL. Despite the intrinsic specificity of the above method, the background ECL signal generated by telomerase substrate crippled the sensing performance. Additionally, most reported electrochemical sensors currently lack the required sensitivity to detect biologically levels of cancer biomarkers. Thus, a means to reliably and robustly amplify the electrochemical signal for biomedical application is the key point in this field. Electrocatalysis provides electronic amplification, or gain, and thus facilitates high sensitivity readout: hundreds of electrons can result from each bimolecular complexation event.<sup>176</sup> In electrocatalysis, the redox reporter is coupled with a freely diffusing electron sink, which could return the reporter back to its oxidized form through electron transfer, and allowing the signal amplification. With this in mind, using hemoglobin as the electron sink, combined with enzyme-assisted background noise-suppressed strategy and functional graphene, we developed a novel activity-based PCR-free, electrocatalysis platform for less than single-cell level detection of telomerase activity, as shown in Fig. 8B.<sup>168</sup> In this work, graphene-mesoporous silica-palladium nanoparticles (Pd

NPs) hybrids (GSPHs) was synthesized as the electrode material for the immobilization of low-density telomerase primer DNA film and promoting efficient telomerase binding events. The hybridization of TS primer with its complementary DNA produced the cleavage sites for exonuclease III (Exo III), the nuclease which specifically cleaved duplex DNA from blunt or recessed 3'-termini and removed unreacted telomerase substrates from electrode surface.<sup>177</sup> Telomerase reaction disturbed the recognition site of Exo III, kept the products on electrode surface and offered abundant binding site for electroactive molecules methylene blue. Once electrocatalyzed by hemoglobin, the electrochemical response of conjugated methylene blue was dramatically increased, realizing the signal amplified detection of telomerase activity.

The newly developed methods for cancer biomarker detection prefer using some minimally-invasive or non-invasive sampling methods, such as biopsy specimens and body-fluidic samples for early cancer diagnosis,<sup>27</sup> which requires the assay to be applied to samples with minute amount of cancer cells in an environment with hundreds or even thousands of normal cells. Taking into account these factors, we attempted to measure telomerase activity in CTCs using PCR-free method for the first time.<sup>169</sup> CTCs are cells that disseminate from a primary tumour throughout the circulatory system and that can ultimately form secondary tumours at distant sites.<sup>178</sup> "Liquid biopsy" using CTCs is potentially a minimally invasive alternative to traditional tissue biopsy to determine cancer therapy.<sup>179</sup> The principle of this method was similar to the previous electrocatalysis assay instead of using DNA-templated deposition of silver nanoparticles (NPs) as electro-active labels through a highly characteristic solid-state Ag/AgCl reaction to generate measurable electrochemical signal, as shown in Fig. 8C. Since CTCs circulates in the blood flow among thousands of other human cells, the TRAP assay is hard to indicate the telomerase activity in CTCs under the interference of abundant genomic DNA and protein impurities in cell mixtures. Our DNA-metallization based signal amplification strategy showed a high performance for telomerase activity evaluation in artificial CTCs. It is at the preliminary stage for telomerase activity sensing in CTCs and using them to provide diagnostic information in clinical cancer treatment. Our design of measuring telomerase activity in CTCs with PCR-free method paves a new way in this field, hoping to realize point-of-care diagnosis and individualized treatment of cancers by non-invasive routine blood test in the future.

The development of PCR-free methods presently mainly focuses on using cell extract for telomerase activity analysis, thus failing to in situ detect and provide telomerase information at single-cell levels. Ju's group concentrated on developing in situ detection protocol for monitoring intracellular telomerase activity.<sup>180-182</sup> They designed telomerase-responsive mesoporous silica nanoparticles (MSNs) with black hole fluorescence quencher covalently immobilized on their inner walls, serving as nanocontainers for fluorescein.<sup>181</sup> The wrapping of telomerase substrate DNA (O1) sealed MSNs probe and prevented the escape of loaded fluorescein from

inner mesopores. The in situ synthesis of telomeric repeats at the 3'-end of O1 by telomerase reaction induced the formation of rigid-hairpin like DNA structure and led to the detachment of O1 from MSNs surface (Fig. 9A). The detachment of "biogate" triggered the release of fluorescein, realizing "off-on" switchable fluorescent imaging of intracellular telomerase activity. The proposed strategy realized in situ tracking of intracellular telomerase activity with good performance and could evaluate the level of telomerase activity in various cells. Additionally, this probe could be further employed for monitoring the change of intracellular telomerase activity in response to drugs (Fig. 9B). Encouraged by the above successful results, they further designed a nicked molecular beacon (MB) functionalized probe for in situ imaging and detection of intracellular telomerase activity through a one-step incubation procedure. MBs are hairpin shaped molecules with an internally quenched fluorophore whose fluorescence is restored when they bind to a target nucleic acid sequence.<sup>183</sup> As shown in Fig. 9C, telomerase reaction triggered the opening of MB and led to the separation of Cy5 from gold nanoparticles, generating "turn-on" fluorescent signal for telomerase activity indication.<sup>182</sup>

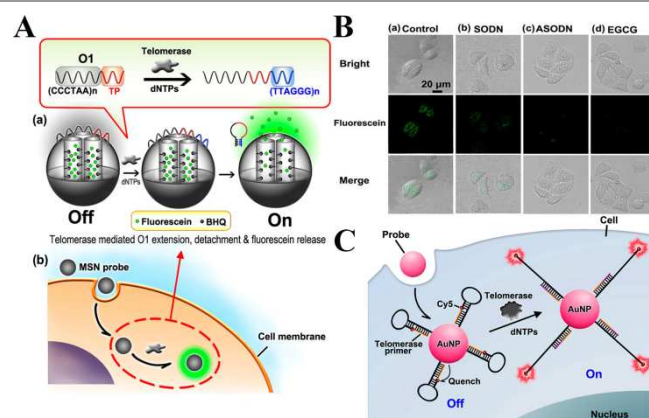


Fig. 9 Schematic illustration of intracellular analysis of telomerase using MSN probe (A) (Reprinted with permission from ref. 181.) and the nicked molecular beacon-functionalized gold nanoparticle (C) (Reprinted with permission from ref. 182). (B) Confocal images of (a) control HeLa cells and HeLa cells pretreated with (b) SODN, (c) ASODN; and (d) EGCG after incubation with 15  $\mu\text{L}$  MSN probe (1  $\text{mg mL}^{-1}$ ) for 1.5 h. Reprinted with permission from ref. 181.

Taken together, there is still a lack of available assays to measure telomerase activity in a sufficiently reliable, quantitative, and sensitive way, which continues to be a strong driving force for scientists to improve or develop more robust telomerase assays for fundamental biomedical research and clinical investigation. Future telomerase evaluation tends to measure telomerase activity in complex pathological sample matrix, such as cells collected from tissues or body fluid, to collect more accurate diagnostic information for potential clinical applications.

### 2.2.2 Protease and other enzymes

Changes of enzyme activity in tissues, body fluids, and serum as well as changes of isoenzymes and enzyme variants in

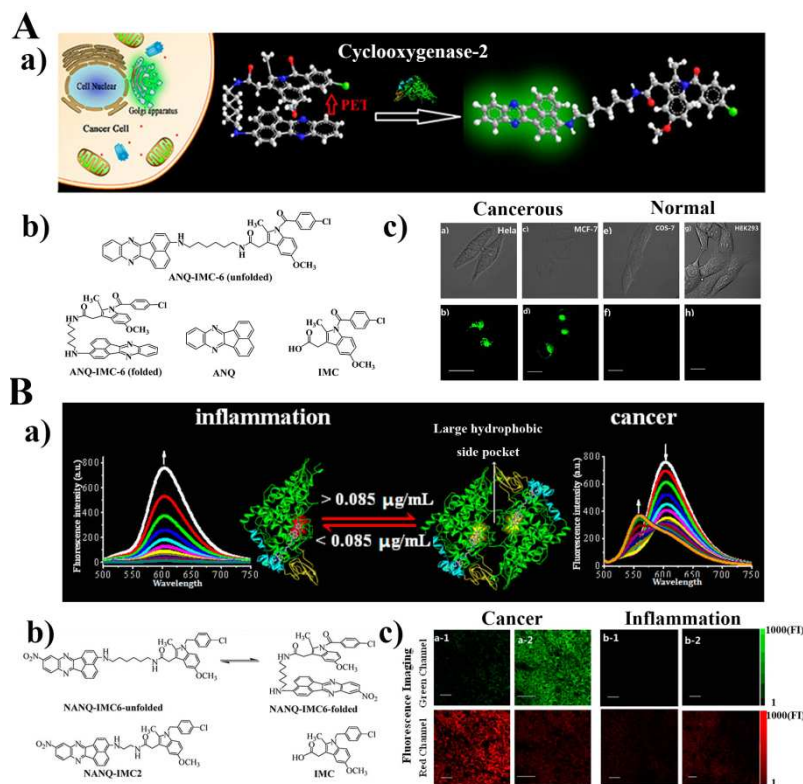


Fig. 10 Smart “off-on” cyclooxygenase-2 (COX-2)-specific fluorescence probe for the identification of cancer cells or tissues. (A) a) Schematic illustration of using COX-2-specific fluorescent probe, ANQ-IMC-6 for rapid identification of cancer cells by imaging. b) Chemical Structures of ANQ, IMC, and ANQ-IMC-6 (Folded and Unfolded). c) Living cells stained with ANQ-IMC-6 (5.0 μM). White light images (a, c, e, g) and fluorescence images (b, d, f, h). Reprinted with permission from ref. 186. (B) a) Representation of using COX-2-specific fluorescent probe NANQ-IMC6 for identification of cancer from inflammation. b) Chemical structures of NANQ-IMC6-unfolded, NANQ-IMC6-folded, NANQ-IMC2, and IMC. c) Quantitative labelling tumour (a) or inflammation (b) tissues at various stages of development by a ratio imaging method. (a-1) Sample was the 5 day sarcoma of nude mice. (a-2) Sample was the 15 day sarcoma of nude mice. Reprinted with permission from ref. 190.

patients with malignancy suggest that these parameters may be used as efficient biomarkers in the diagnosis of some types of cancer.<sup>184, 185</sup> Design of fluorescent turn-on probes for the targeting of endogenous, intracellular, cancer-associated enzymic biomarkers provides a well-established tool for identification and enumeration of living cancer cells and their type differentiation. The fluorescent reporter signal of molecular probes is generated by enzyme activation through the enzyme-induced conformational change of probe or enzymatically stimulated removal of fluorescence quencher from the probe. Peng *et al.* designed a smart “off-on” cyclooxygenase-2-specific fluorescence probe, named ANQ-IMC-6, and evaluated their performance for reporting the presence of cancer cells and imaging Golgi-related events.<sup>186</sup> As shown in Fig. 10A-a, the fluorescence of ANQ-IMC-6 is quenched through photoinduced electron transfer (PET) between the acenaphtho [1,2-b] quinoxaline (ANQ, a

fluorophore) and indomethacin (IMC, an inhibitor of COX-2) (Fig. 10A-b) in its folded conformation in aqueous buffered solution. Binding of ANQ-IMC-6 to COX-2 in the Golgi apparatus restrained PET and generated increased fluorescence signal, allowing for the rapid, selective and sensitive identification of cancer cells from normal cells (Fig. 10A-c). Additionally, the push-pull charge-transfer structure of ANQ-IMC-6 provided significant two-photon properties, permitting the visualization of dynamic morphological changes of the Golgi apparatus during cancer cell apoptosis. Although COX-2 is a promising candidate of cancer imaging target, which is highly expressed in various tumours but barely in normal cells, their expression at different levels in inflammatory lesions is a considerable clinical limitation for the discrimination of tumours from inflammation.<sup>187-189</sup> Accordingly, using the similar sensing mechanism, they further reported a novel COX-2-specific fluorogenic probe NANQ-IMC6, which could not

only distinguish normal cells/tissues from cancer cells/tissues but also discriminate the cancer from sites of inflammation (Fig. 10B).<sup>190</sup> The “off-on” fluorescent behaviour of NANQ-IMC6 probe was observed in both inflammatory lesions and tumours with quite different fluorescent emission. In inflammation sites, the fluorescence emission was at 615 nm and increased gradually with increasing COX-2, while in cancer sites, the fluorescence emission at 615nm decreased gradually and a new emission at 555 nm appeared and increased with the increasing COX-2. Thus, the cancerous tissues revealed a strong fluorescence signal in the green channel, while inflammatory tissues showed an image in the red channel, with negligible emission in the green channel (Fig. 10B-c). This assay could accurately discriminate cancerous, inflamed and normal tissues

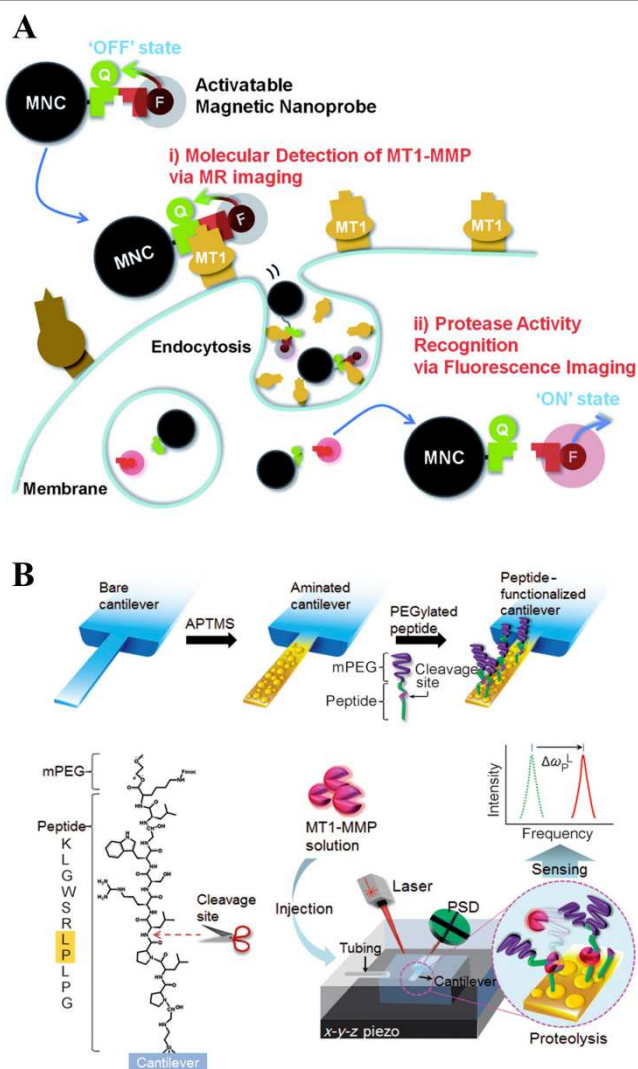


Fig. 11 (A) Schematic illustration of the dual imaging process of activatable magnetic nanoprobes for i) molecular detection of MT1-MMP anchored on invasive cancer cells by MR imaging, and ii) sensitive recognition of the proteolytic activity of MT1-MMP by fluorescence imaging. Reprinted with permission from ref. 197. (B) Representation of cantilever assay to decipher the kinetics of MT1-MMP activity for various invasive cancer cells. Reprinted with permission from ref. 201.

in vivo by the unaided eye using a hand-held ultraviolet lamp emitting at 365 nm, having potential application varying from cancer inflammation diagnosis to guiding tumour resection during surgery.

Compared to the above mentioned enzyme-induced conformational change method, enzymatically stimulated removal of fluorescence quencher from the probe is the most widely used strategy for cancer-associated enzyme sensing, such as human NAD(P)H: quinone oxidoreductase isozyme 1 (hNQO1),<sup>191</sup> glutathione transferases,<sup>192</sup> legumain,<sup>193-195</sup> urokinase-type plasminogen activator (uPA),<sup>196</sup> human epidermal growth factor receptor 2 (HER2)<sup>196</sup> and matrix metalloproteinase (MMP)<sup>197-200</sup>. In particular, this route often employs probes whose reporter fluorescence is quenched by photoinduced electron transfer from a covalently attached enzyme substrate. Fluorescence regenerates from the reporter upon removal of the quencher substrate by an endogenous, cytosolic, disease associated enzyme. For example, Haam's group designed and synthesized a peptide probe ActFP (Cy5.5-GPLPLRSWGLK(BHQ-3)) and developed a membrane type-1 matrix metalloproteinase (MT1-MMP)-targetable fluorogenic magnetic nanoprobe (MNC-ActFP) for the simultaneous assessment of the expression and proteolytic activity of MT1-MMP anchored on invasive cancer cells by magnetic resonance (MR) and NIR fluorescence imaging (Fig. 11A).<sup>197</sup> The molecular detection of MT1-MMP expressed on cancer cell surface was confirmed by  $T_2$ -weighted MR imaging of MNC-ActFP, which was specifically attached to MT1-MMP. Furthermore, the monitoring of MT1-MMP's protease activity was realized from the proteolytic activation of cellular NIR fluorescence. Although promising, the fluorogenic bioassay is not effective in deciphering the kinetics of MT1-MMP-driven proteolysis due to the photobleaching (or photoquenching) and/or light interference, which is inappropriate for the quantification of proteolytic activities of MT1-MMP on invasive cancer cells. Alternatively, Kwon and coworkers successfully fabricated a label-free, real-time cantilever bioassay for specific measurements of the proteolytic activity of MT1-MMP by functionalizing a cantilever surface with a specific peptide sequence.<sup>201</sup> As shown in Fig. 11B, the peptide chains attached on cantilever surface could be specifically snipped by MT1-MMP, leading to a decrease in the effective mass of cantilever and generating a measurable shift in the resonant frequency of the cantilever. The mechanical signal transduction-based cantilever bioassay enabled not only highly sensitive detection but also quantitative detection of biomolecular interactions, exhibiting detection sensitivity below 1 nM for sensing MT1-MMP-driven proteolysis. Taking the analogical detection principle, a nanoplasmonic resonator (NPR) sensor was constructed by Zhang and coworkers for the measurement of protease activity.<sup>202</sup> The proteolytically active prostate-specific antigen (paPSA) cleaves the peptide substrate, leading to the release of the SERS molecule Rhodamine 19 and a subsequent decrease in the Raman scattering intensity in a dose- and time-dependent manner. The protease activity could

## ARTICLE

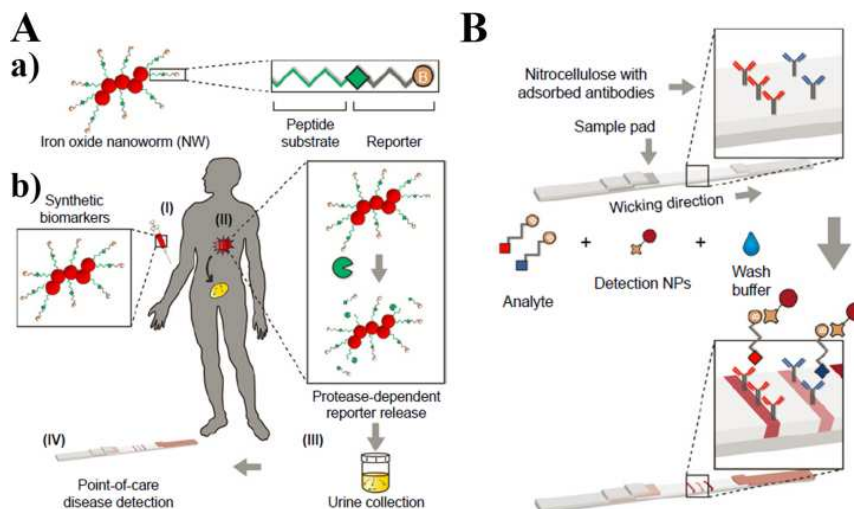


Fig. 12 Protease-sensitive nanoparticles for point-of-care (POC) urinary monitoring of disease. (A) a) Substrate-reporter tandem peptides were conjugated to carrier iron oxide nanoworms (NWs) to form synthetic biomarkers. Proteolytic cleavage of the linking peptide substrate liberates ligand-encoded reporters that filter into urine. b) (i) A patient suspected of harboring a disease receives a disease-tuned diagnostic NWs mixture. (ii) NWs infiltrate the disease site and release reporters upon proteolytic cleavage of peptide substrates. (iii) The liberated reporters passively filter through the kidney and can be collected in patient's urine sample. (iv) Application of unprocessed urine to low-cost POC paper lateral flow assay (LFA) enables diagnosis. (B) The development of paper assay and their application for the detection of protease activity. Reprinted with permission from ref. 204.

be accurately quantified with a sensitivity level of 6 pM (0.2 ng/mL) and a dynamic range of 3 orders of magnitude.

Since the naturally occurring biomarkers are frequently found in low concentrations in the circulation, are difficult to resolve in complex biological fluids and can be degraded rapidly both *in vivo* and *in vitro*, their applications to indicate disease is limited by fundamental technical and biological challenges. Bhatia's group worked on designing new strategy to bypass these limitations by exploiting "synthetic biomarkers" nanoparticle agents to sample disease-associated protease and produce a urinary signal.<sup>203-205</sup> The basic principles of this promising method were as follows: Firstly, the protease-sensitive peptide substrates were encoded with specific reporters and conjugated to nanoparticles to form synthetic biomarkers, as shown in Fig. 12A-a. Subsequently, upon intravenous injection, these synthetic biomarkers passively targeted disease sites, such as solid tumour cells or blood clots, where up-regulated protease cleaved the peptide substrates and released into the urine as reporters to indicate disease state (Fig. 12A-b). The reporters could be engineered for detection both by mass spectroscopy with mass-encoded peptide substrates<sup>205</sup> and by sandwich immunoassays with reporter-specific capture antibody<sup>204</sup>. Taking the sandwich immunoassay as example, they adopted a paper lateral flow assay (LFA) for the quantification of reporters directly from unmodified urine. As illustrated in Fig. 12B, the captured antibodies were adsorbed

onto a highly porous test strip, which served to wick fluids and transport analytes from the sample pad to the capture regions. The recognition of analytes could be visualized by a detection agent coupled to gold nanoparticles that created a coloured line detectable by eye without enzymatic amplification. Using mouse models of thrombosis or colorectal cancer, they showed that this paper diagnostic assay could noninvasively monitor various diseases without the need for invasive core biopsies, expensive equipment, or trained medical personnel, which substantially improved early detection of cancer compared with current clinically used blood biomarkers.

## 2.3 Nucleic acids-based biomarkers

### 2.3.1 Measurement of DNA

Tumour cells may release DNA into the circulation so that increased quantities of DNA are found in the plasma of cancer patients compared with healthy controls.<sup>206</sup> Circulating tumour DNA (ctDNA) is a promising biomarker, which has the potential to revolutionize detection and monitoring of tumours in a non-invasive way.<sup>207-209</sup> However, the existing ctDNA analysis methods have insufficient sensitivity or patient coverage for broad clinical applicability. An economical and ultrasensitive method, cancer personalized profiling by deep sequencing (CAPP-Seq) for quantifying ctDNA was developed by Diehn and coworkers.<sup>210</sup> They implemented CAPP-Seq for

non-small-cell lung cancer (NSCLC) with a design covering multiple classes of somatic alternations that identified mutations in >95% of tumours. They realized the detection of ctDNA in 100% of patients with stage II-IV NSCLC and in 50% of patients with stage I, with 96% specificity for mutant allele fractions down to ~0.02%. Finally, they evaluated biopsy-free tumour screening and genotyping with CAPP-Seq. Due to their high sensitivity and specificity, lack of a need for patient-specific optimization and coverage of nearly all patients with NSCLC, CAPP-Seq could therefore be routinely applied clinically and has potential for accelerating the personalized detection, therapy and monitoring of cancer.

Identification of DNA mutation is another important aspect of cancer therapy, because mutations can modulate the effectiveness of biological reagents on target-specific pathways and plays important role in carcinogenesis, metastasis, and therapeutic resistance.<sup>13, 211, 212</sup> Since initial mutagenesis occurs inherently at the single-cell level, the detection and characterization of carcinogenesis will be dramatically facilitated by analytical techniques with single-cell resolution. An agarose-droplet-based platform that leveraged emulsion-generator-array technology was fabricated for high-throughput single-cell analysis.<sup>213</sup> Single cells were microfluidically encapsulated together with primer-functionalized beads in agarose-gel droplets for subsequent SDS lysis and proteinase K digestion to release genomic DNA. Subsequently, the agarose droplets were equilibrated in PCR buffer containing fluorescent forward primers, emulsified with oil by mechanical agitation, and thermally cycled. Following multiplex PCR amplification, primer beads were released by breaking the emulsion and melting the agarose and quantified by flow cytometry or further subjected to PCR amplification for the sequencing of target genes. The coupling of robust and high-throughput single-cell DNA-purification method with the sequencing of multiple gene targets within single-cells would enable detailed studies of mutation co-occurrence and synergy during carcinogenesis.

DNA methylation is an important component of epigenetic regulation and cancer-linked DNA hypermethylation leads to functional silencing of some tumour suppressor genes due to chromatin compaction, which is responsible for tumour formation and progression.<sup>214-217</sup> Thus, the detection of DNA methylation could provide a powerful tool for early cancer diagnosis and cancer type identification.<sup>218-220</sup> Recently, a fluorescence resonance energy transfer assay based on cationic conjugated polymer was used for quantitatively analysing of DNA methylation levels of colon cancer-related genes in a Chinese population.<sup>221</sup> This method demonstrated high accuracy and sensitivity in discriminant analysis and cumulative detection, which might be useful for the screening and differential diagnosis of patients with colon cancer and performing clinical correlation analyses. As an emerging single-molecule technique, nanopore sequencing has shown promise for simultaneous DNA sequencing and methylation detection.<sup>222-224</sup> Gundlach *et al.* developed a single-molecule tool based on the engineered biological protein pore *Mycobacterium smegmatis* porin A (MspA) to detect and map 5-

methylcytosine and 5-hydroxymethylcytosine within single strands of DNA.<sup>224</sup> Hydroxymethylation, which differs from methylation by only one oxygen atom, could also be distinctly discriminated. In future, this technique may be developed into a research tool and may ultimately lead to clinical tests.

In many cases, the harmful methylation states are linked to the abnormal expression and activity of DNA methyltransferases.<sup>214</sup> Strategies to detect human DNA methyltransferases are urgently needed, given that abnormalities in methyltransferase activity usually occur far before other signs of malignancy and could be used as efficient biomarker for early cancer detection. Barton and coworkers described a nonradioactive, antibody-free, electrochemical assay and implemented this assay with a multiplexed chip platform for measuring both bacterial (SssI) and human (Dnmt1) methyltransferase activity.<sup>225</sup> The advantages of electrochemistry over radioactivity and fluorescence make this assay an accessible and promising new strategy for the sensitive, label-free detection of human methyltransferase activity.

### 2.3.2 Measurement of RNA

Altered mRNA metabolism is a feature of many cancers. Indeed, loss of function of many tumour suppressors regulating cell proliferation, survival, and differentiation results from aberrant mRNA processing, nuclear export, and/or translation.<sup>226, 227</sup> Tumour-related mRNA has been widely used as a specific marker to assess the migration of tumour cells locally or in the bloodstream.<sup>228-230</sup> Changes in the level of tumour-related mRNA expression are correlated with tumour burden and malignant progression. The detection of tumour-related mRNA markers in intact cancer cells provides new tools for identifying cancer cells in clinical samples.

miRNAs are short noncoding RNAs that post-transcriptionally regulate gene expression. miRNAs' ability to inhibit translation of oncogenes and tumour suppressor genes implies they have an involvement in carcinogenesis.<sup>231</sup> Many studies have shown that miRNA dysregulation is involved in cancer initiation, invasion, metastasis, and so forth.<sup>232, 233</sup> Notably, recent studies have revealed secretory miRNA levels in blood and other body fluids to correlate significantly with cancer progression, therapeutic response and patient survival.<sup>234, 235</sup> The distorted and unique expression profile of miRNAs in different types and subsets of tumour coupled with their presence in biological fluids make of miRNAs an attractive source of sensitive biomarkers.<sup>236, 237</sup> However, the sequence homology, low abundance, and common secondary structures of miRNAs have complicated efforts to develop accurate, unbiased quantification techniques with both high sensitivity and specificity.

#### 2.3.2.1 Electrophoresis-based methods

Santiago *et al.* developed a reagentless two-stage hybridization assay based on isotachopheresis (ITP) for the measuring of let-7a miRNA, which played important role in

cell development,<sup>238</sup> with single-nucleotide specificity (Fig. 13A).<sup>8</sup> ITP is an electrokinetic technique that uses a

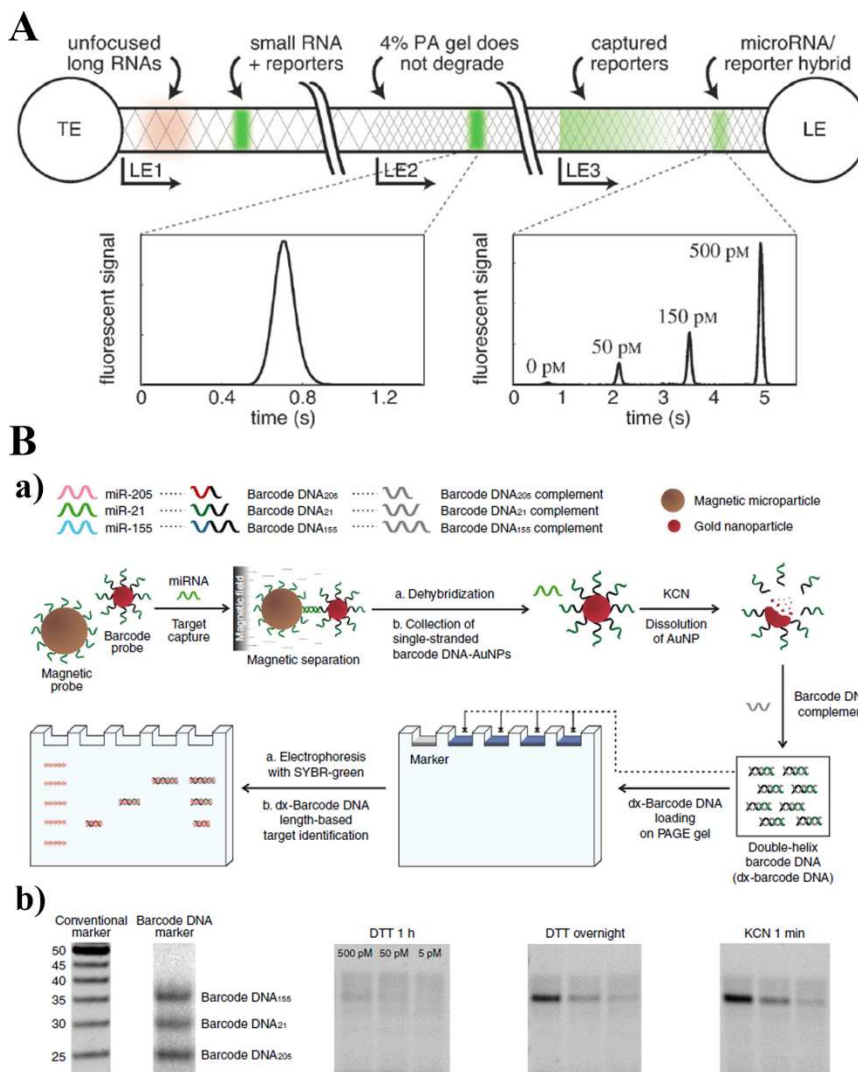


Fig. 13 (A) Schematic diagram of the two-stage ITP assay for specific miRNA detection. Reprinted with permission from ref. 8. (B) Bio-barcode gel assay and KCN-based barcode DNA release. a) The schematic illustration of the bio-barcode gel assay for miRNA analysis. b) Electrophoretic analysis of released barcode DNA after 20 mM DTT or 50 mM KCN treatment. Reprinted with permission from ref. 9.

heterogeneous buffer system, composed of leading and trailing electrolytes, to perform more than 10000-fold focusing.<sup>239</sup> The combination of ITP technique that sped up hybridization kinetics between target molecules and fluorescent reporters, with an in-line affinity purification photopatterned functionalized hydrogel enabled sufficiently rapid, specific, and sensitive evaluating of miRNA in real total RNA samples. Although this method addressed a currently unmet need for miRNA analysis, the lack of capability for multiplexed detection of various combinations of miRNA sequences impeded its progress for further clinical applications. Multiple different miRNAs collaboratively regulate important cellular events at the same time, especially in cancer progression.<sup>240</sup> Thus, it is important to simultaneously monitor different miRNAs in cells. Crucially, though, the inherent property of miRNAs that have a similar length makes it impossible or very difficult to differentiate them in gel image. To this end Krylov

*et al.* reported the first direct quantitative analysis of multiple miRNAs by using a capillary-electrophoresis-based hybridization assay with an ideologically simple combination of two well-known separation-enhancement approaches: drag tags on the DNA probes and single strand DNA binding protein in the buffer.<sup>241</sup> Nam and coworkers developed a bio-barcode gel (bio-BaGel) assay for multiplexed detection of an ultra-low amount of miRNA with a conventional gel electrophoresis platform without enzymatic amplification.<sup>9</sup> Instead of directly detecting miRNA, the final measuring signal of bio-BaGel assay was obtained from the amount of barcode DNA; an artificially designed DNA represented each miRNA target sequence in a way that a specific barcode label represented a specific product (Fig. 13B). Briefly, a barcode DNA possessed two regions; one region that could capture target miRNA and the other region with a varying length of the encoding sequence. miRNA induced the conjugation of magnetic probe

and barcode probe (barcode DNA modified gold nanoparticles), which could be readily separated by a magnetic field. Barcode DNA could be released in a very short time by dissolving the AuNPs and further amplified the detection signal intensity during the gel electrophoresis of double-helix barcode DNA. The bio-BaGel assay offers a straightforward detection signal amplification strategy on a conventional gel electrophoresis platform, allowing multiplexed detection of several artificially different miRNA targets in one sample and evaluation of varying miRNA levels from breast and lung cancer cells with high sensitivity and selectivity.

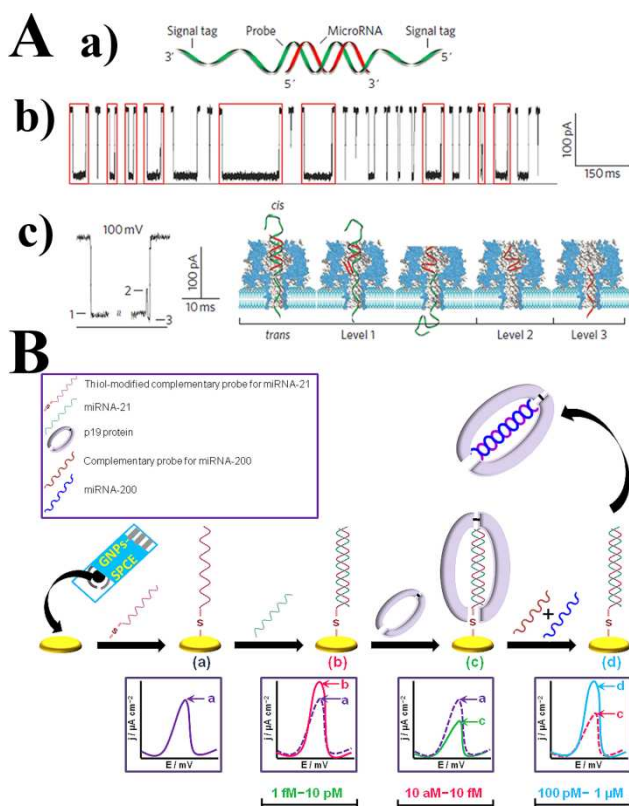


Fig. 14 (A) Nanopore-based detector for miRNA analysis. a) Schematic illustration of miRNA and probe used in nanopore sensor. b) Electrical signal in the presence of 100 nM miR-155 and 100 nM P155. c) A typical multi-level long block (from b) at 100 mV generated by the miR-155-P155 hybrid (left) and the corresponding molecular mechanism (right). Reprinted with permission from ref. 245. (B) Schematic diagram of the three-mode electrochemical sensor designed for the determination of miRNAs. Reprinted with permission from ref. 19.

### 2.3.2.2 Electrochemical and electrical detection methods

The development of nanopore-based miRNA detectors is a novel effort in this rapidly evolving field.<sup>242</sup> The nanopore is a molecular-scale pore structure that is able to detect the position and conformation of a single molecule that is present within the pore lumen with high sensitivity.<sup>243</sup> From the characteristic change in nanopore conductance, one can electrically elucidate

single-molecule kinetic pathways and quantify the target. Drndić *et al.* reported the use of a 3nm synthetic pore to quantify the translocation of enriched miRNAs that were hybridized to a probe.<sup>244</sup> In addition, a nanopore sensor based on  $\alpha$ -hemolysin protein-nanopore was also developed for the quantification of cancer-associated miRNAs in samples of blood from lung cancer patients (Fig. 14A).<sup>245</sup> This nanopore-based miRNA sensor could directly detect miRNA in a fluctuating background, such as plasma RNA extracts from clinical samples, as well as distinguish single-nucleotide differences. Further introduction of a polycationic peptide-PNA probe as the carrier enabled the selective miRNA detection in a complex nucleic acid mixture.<sup>246</sup>

Electrochemistry-based sensors offer sensitivity, selectivity and low cost for the detection of nucleic acid sequences or mutated genes associated with human disease. DNA-based electrochemical sensing methods combine nucleic acid layers with electrochemical transducers to produce a biosensor and promise to provide a simple, accurate and inexpensive platform for cancer diagnostics.<sup>57</sup> Recently, a three-mode electrochemical sensor with low detection limit and wide dynamic range was developed by Berezovski and coworkers for quantitative detection of miRNA (Fig. 14B).<sup>19</sup> The sensor facilitated three detection modalities based on hybridization, p19 viral protein binding, and protein displacement. The binding between p19 and dsRNAs occurs via electrostatic and hydrogen-binding interactions between the  $\beta$ -sheet formed by the p19 homodimer and the sugar-phosphate backbone of dsRNA, making its binding sequence-independent of the RNA substrate while not binding to ssRNA, rRNA, mRNA, ssDNA, or dsDNA.<sup>247</sup> The fabricated sensor could identify as low as 5 aM or 90 molecules of miRNA per 30  $\mu$ L of sample and could be operated within the dynamic range from 10 aM to 1  $\mu$ M. In addition, the sensor also enabled the recognition of miRNAs with different A/U and G/C content, the discriminant of single base mutation, and the direct profiling of three endogenous miRNAs in human serum. Using RNA binding viral protein as a selective biorecognition element Pingarrón *et al.* developed another amperometric magnetobiosensor for miRNA quantification.<sup>248</sup> The p19 protein-based magneto-sensors were able to detect 0.4 fmol of a synthetic target and endogenous miR-21 in total RNA extracted from cancer cells and human breast-tumour specimens in only 2h without sample processing and PCR amplification. Nanotechnology<sup>249</sup> and DNA nanostructures<sup>250</sup> can further improve the sensitivity of electrochemical mRNA/miRNA sensor, which is able to detect mRNA/miRNA with PCR-like sensitivity.

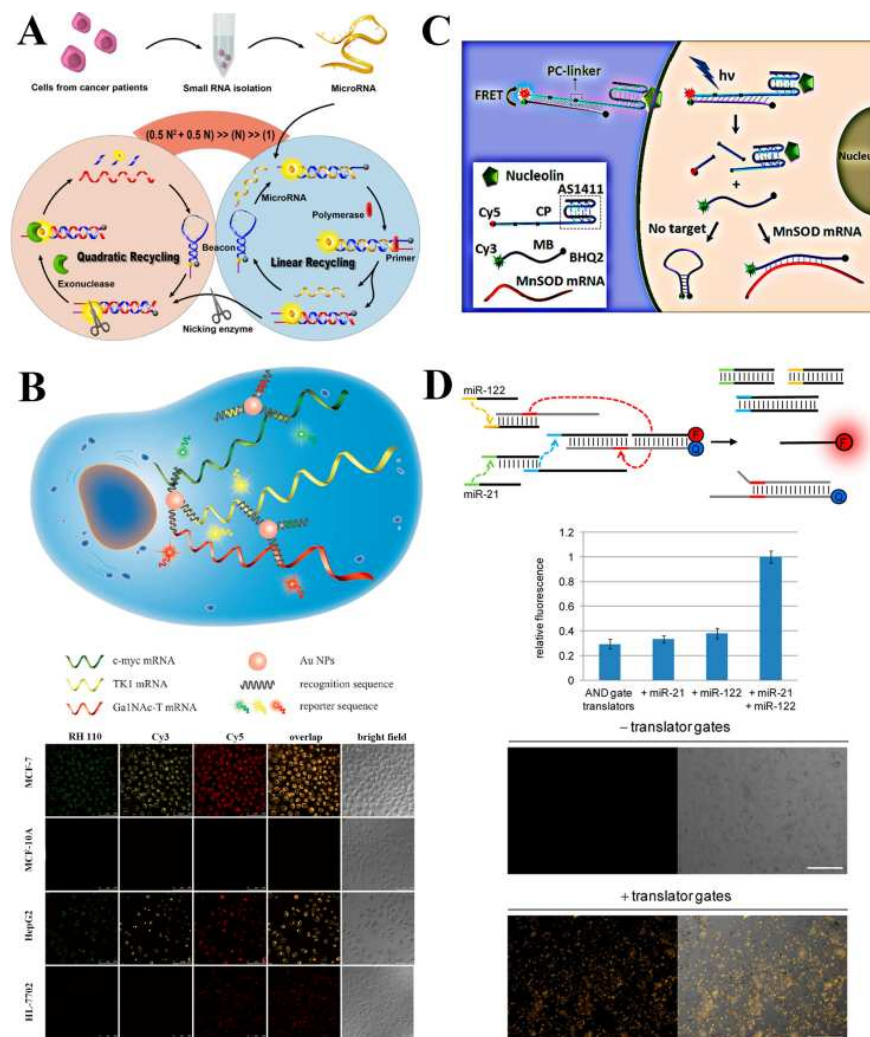


Fig. 15 (A) Schematic representation of the hairpin-mediated quadratic enzymatic amplification strategy based on a Bst polymerase-induced strand-displacement reaction and a lambda exonuclease-aided recycling reaction. Reprinted with permission from ref. 255. (B) Illustration of the multicolour nanoprobe and their application for the detection of intracellular tumour-related mRNAs. Reprinted with permission from ref. 257. (C) Schematic diagram of the carrier probe/molecular beacons for spatiotemporal MnSOD mRNA detection in living cells. Reprinted with permission from ref. 259. (D) Engineered miR-21/122 translator-coupled AND gate for dual detection of endogenous miRNA expression patterns. Reprinted with permission from ref. 270.

### 2.3.2.3 Fluorescent methods

Among the miRNA detection methods, RT-PCR has attracted much attention because of its high sensitivity and practicality.<sup>251, 252</sup> Nevertheless, RT-PCR requires precise control of the temperature cycling to achieve amplification, which imposes instrumentation constraints on its wider and more versatile applications. In addition, the short length of miRNAs makes the PCR design very sophisticated and decreases the assay reliability due to cross contamination, especially in some complex clinical samples with PCR

inhibitors and interferents. Alternatively, nucleic acid sequence-based amplification is a one-step isothermal process for amplifying miRNA, which does not get false positives caused by genomic dsDNA, as in the case of RT-PCR. In this sense, Ye's group created a new signal-amplifying mechanism, duplex-specific nuclease (DSN) signal amplification, to increase the detection sensitivity of miRNAs.<sup>253</sup> DSN enzyme displays a strong preference for cleaving double-stranded DNA or DNA in DNA: RNA heteroduplexes, and is practically inactive toward single-stranded DNA, or single- or double-stranded RNA.<sup>254</sup> In this work, DSN was employed to recycle

the process of target-assisted digestion of Taqman probes through which one target molecule cleaved thousands of probe molecules, thus resulting in significant fluorescence signal amplification. This amplification strategy demonstrated a high sensitivity for quantitating miRNAs in the femtomolar range and a high selectivity for discriminating differences between miRNA family members. To further improve the sensitivity, Xia's group reported a hairpin-mediated quadratic enzymatic amplification strategy based on polymerase-aided strand-displacement polymerization and exonuclease-assisted template recycling for miRNA analysis (Fig. 15A).<sup>255</sup> The assay required only one-step to realize quadratic amplification, achieving rapid, isothermal, and highly sensitive detection of miRNAs extracted from cancer cell lines and even clinical patient tissues.

Fluorescence imaging analysis offers an appealing approach for the detection of cancer at the cellular level, which may be of prognostic significance. Combining with the remarkable affinity and specificity of locked nucleic acid (LNA) to miRNA, a delivery system using the nanocarrier of polyethyleneimine-grafted graphene nanoribbon was proposed for effectively transferring LNA molecular beacon into the cells to analyse the intracellular level of miRNA.<sup>256</sup> Intracellular imaging techniques for simultaneous detection of multiple targets, such as tumour-related mRNAs or miRNAs, bring new opportunities for improving the accuracy and promoting the progress of early cancer detection over the single-marker assay. A multicolour fluorescence nanoprobe based on nanoflares was designed by Tang and coworkers for simultaneous detection of three intracellular tumour-related mRNAs.<sup>257</sup> As illustrated in Fig. 15B, the recognition sequences hybridized to three short different dye-terminated reporter sequences were linked to gold nanoparticles by gold-thiol bond to form the nanoprobe for intracellular imaging. The fluorescence of the three dyes was quenched by gold nanoparticles. The recognition of mRNA targets formed longer and more stable duplexes, and triggered the release of the reporter sequences from AuNPs surface, producing fluorescence signals correlated with the amount of the specific mRNA targets. The nanoprobe exhibited high specificity, nuclease stability and good biocompatibility, enabled the imaging of three tumour related mRNA in live cells, discriminant of cancer cells from normal cells, and identification of changes in the expression levels of tumour-related mRNAs in living cells. The nanoprobe designed in this work provided new opportunities for detection and imaging of multiple markers in living cells, which could be potentially used in evaluating the stage of tumour progression and in making treatment decisions. A similar sensing mechanism was taken for multiplexed quantification of miRNA expression levels in living cells by using nanosized graphene oxide and peptide nucleic acid probes.<sup>258</sup>

To visualize and track disease related targets in specific living cells with high spatiotemporal resolution, the probe used for intracellular imaging must initially meet two important requirements: specific and automatic delivery into target cell's cytoplasm, and optical signal response to the specific targeting

event. DNA-based probe used in previous intracellular sensing methods are usually negatively charged and hydrophilic, which cannot freely permeate the lipophilic cell membrane. Delivery strategies with the advantages of high throughput, cell type specificity, low cost, and facile preparation are being sought and introduced to this field. For example, a targeted, self-delivered, and photocontrolled aptamer-based molecular beacon was designed by Tan and coworkers for intracellular mRNA analysis.<sup>259</sup> An internalizing aptamer AS1411 with an extended cDNA sequence functionalized as a carrier probe for cell-specific delivery of the MB designed to signal target mRNA (Fig. 15C). AS1411 is an aptamer that can specifically bind to nucleolin overexpressed on the membranes of tumour cells.<sup>260</sup> Additionally, two photocleavable linkers were inserted into the carrier probe sequence to exert spatiotemporal control over the detection function of MB in living cells. After entering the cytoplasm under the guidance of aptamer, MB could be released and activated to target mRNA by irradiation with a pulse of UV light. Aside from its extraordinary self-assembly properties, DNA has also proven to be a unique template for the synthesis of fluorescent nanoparticles for biosensing applications.<sup>261</sup> With this in mind, Ma *et al.* designed a new type of DNA-templated hetero-bivalent quantum dots nanoprobe with dual extracellular and intracellular targeting and imaging capabilities of intracellular mRNA cancer biomarkers.<sup>262</sup> Fluorescent SnO<sub>2</sub> nanoparticles<sup>263</sup> and liposome<sup>264</sup> could also be used as the vectors to help the miRNA probe entering into live cells.

DNA computation can utilize logic gates as modules to create molecular computers by integrating multi-input sensing with biological inputs.<sup>265, 266</sup> In this process, modular circuits recognize nucleic acid inputs through strand hybridization and activate computation cascades to produce controlled outputs. This allows for the construction of synthetic circuits that can be interfaced with cellular environments for variety applications. For example, under the control of an aptamer-encoded logic gate, an autonomous DNA nanorobot could transport molecular payloads to specific cells in response to cell surface inputs through the conditionally triggered activation and reconfiguration of structure for payload delivery.<sup>267</sup> In addition, DNA circuits also showed unique advantages in the discrimination of different cell types by using their surface markers as inputs.<sup>268</sup> Apart from extracellular logic gate operations, DNA computation in live cells allows for Boolean logic gate operations with miRNA inputs, and the generated outputs enable applications beyond miRNA pattern detection. For example, anticancer therapies could be engineered to detect and respond to complex cellular conditions in individual cells with high specificity. A cell-type "classifier" based on scalable transcriptional/posttranscriptional synthetic regulatory circuit was developed for the sensing of expression levels of a customizable set of endogenous miRNAs and triggering a cellular response under specific cellular environments.<sup>269</sup> This HeLa cancer cell classifier could selectively identify HeLa cells and triggered apoptosis without affecting non-HeLa cell types. However, this miRNA detection method by logic operations in

live cells required plasmid constructs for the expression of protein gate components. Alternatively, synthetic circuits were constructed for engineering oligonucleotide AND gate to respond to specific miRNA inputs in live mammalian cells without the requirement of the transfer of genetic information, allowing the circuits to be orders of magnitude smaller in size based on DNA sequence (Fig. 15D).<sup>270</sup> Overall, nucleic acid logic gates that are functional in a cellular environment and recognize endogenous inputs significantly expand the potential of DNA computation to monitor, image, and respond to cancer cell-specific biomarkers and shed light on the development of biomarker-triggered logical drug release system for cancer therapy.

#### 2.4 Small chemical products of cellular metabolism

Early cancer detection mainly focuses on the specific recognition of large sized molecules such as proteins or DNAs, even though small chemicals can also be extremely effective cancer biomarkers. Recently, a new non-invasive and potentially inexpensive frontier for cancer diagnosis has been explored, which relies on the detection of volatile organic compounds (VOCs) in exhaled breath samples. Haick *et al.* has organized comprehensive reviews in this field, they shed light on the pathophysiology causing metabolic changes in the VOC levels and compositions in cancer.<sup>271</sup> Additionally, according to their previous experiences of using exhaled breath for cancer diagnosis, they also give deep insights toward the development of breath testing systems.<sup>272</sup> For example, using gold nanoparticles they constructed an array of sensors which can rapidly distinguish the breath of lung cancer patients from the breath of healthy individuals in an atmosphere of high humidity without pre-concentration or dehumidification of the breath sample. (Fig. 16A).<sup>273</sup> They collected exhaled alveolar breath of lung cancer patients and healthy subjects, and then used GC-MS in combination with solid-phase microextraction (SPME) to identify the VOCs that can serve as biomarkers for lung cancer in the breath samples. Subsequently, the detection of lung cancer by means of breath testing was carried out by using an array of nine cross-reactive chemiresistors, which were constructed of different organic functionalized gold nanoparticles. Using principal component analysis, the response of the nine-sensor array to both healthy and lung cancer breath samples was analysed. The obtained simulated clusters were well defined, with no overlaps occurring between the simulated healthy breath and lung cancer breath mixtures (Fig. 16A-c). Additionally, the simulated clusters were fully contained in the clusters resulting from actual breath testing, indicating the simulation approach was robust and served the purpose of “training” the array of sensors. Using the similar array sensing method, they further realized the detection and discrimination between different VOC biomarkers of cancer by covering 30%-90% of the surface of random networks of carbon nanotubes (RN-CNTs) based chemiresistors with self-assembled hexa-*peri*-hexabenzocoronene derivative HBC-C<sub>12</sub> caplayers.<sup>274</sup> These results presented by Haick and coworkers could lead to the development of cost-effective, low-power, lightweight, and

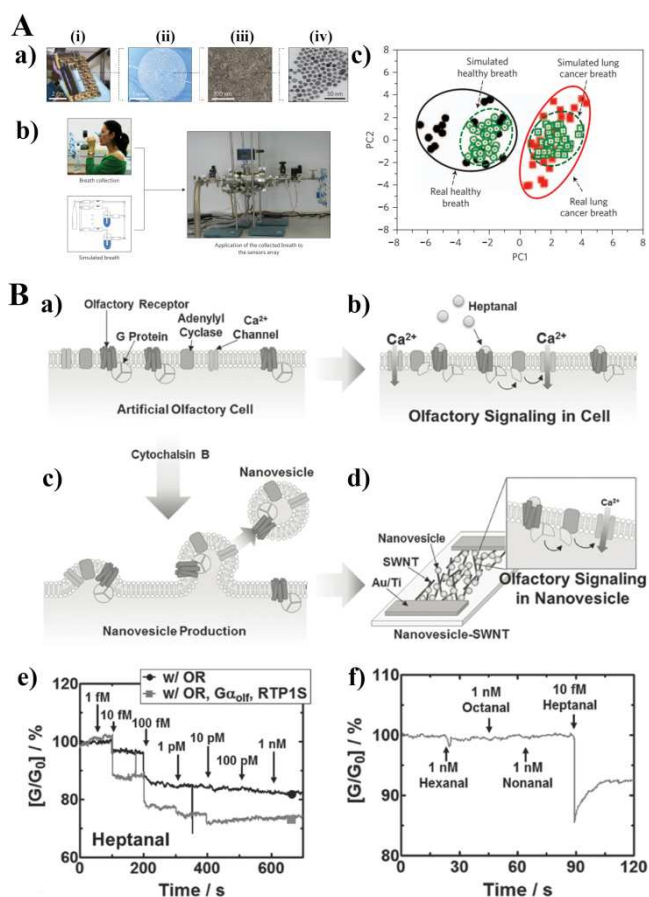


Fig. 16 (A) Representation of the diagnosis of lung cancer using breath testing. a) A photograph of the array of chemiresistors (i), a scanning electron microscopy image of chemiresistor (ii) and a gold nanoparticles film located between two adjacent electrodes (iii), and a transmission electron micrograph (TEM) of the monolayer-capped gold nanoparticles (iv). In these films, the metallic particles provide the electrical conductivity and the organic film component provides sites for the sorption of analyte molecules. b) Testing the exhaled breath and simulated breath using the array of gold nanoparticle sensors. c) Principal component analysis (PCA) of the dataset of real and simulated breath. Reprinted with permission from ref. 273. (B) Schematic illustration of human-olfactory mimetic bioelectronic nose for the detection of lung cancer biomarker from human blood. a) An artificial olfactory cell contains essential proteins for the olfactory signal transduction. b) The binding of specific odorants to ORs triggers the olfactory signalling and finally calcium ions flow into the cells. c) Olfactory nanovesicles with all components for the olfactory signalling were produced from the artificial olfactory cells by a treatment of cytochalasin B. d) Fabrication of bioelectronic nose sensor by immobilization of nanovesicles on single-walled carbon nanotubes (SWNT)-field-effect transistors (FETs). e) Real-time measurements of conductance changes generated by the addition of heptanal at concentrations ranging from  $1 \times 10^{-15}$  to  $1 \times 10^{-9}$  M. f) Real-time recognition of heptanal. Reprinted with permission from ref. 275.

non-invasive diagnostic tools for the widespread screening of cancers via breath analysis.

The array-based sensing method used in above sensor fabrication is analogous to mammalian olfaction, thus also called “chemical nose” strategy, providing an alternative to lock-and-key approaches that use specific recognition. A distinct pattern of response produced from a set of sensors in the array provides fingerprint that allows classification and identification of cancer biomarkers. However, this method is available for qualitative analysis but hard to realize quantitative

analysis, which degrades the accuracy of the diagnostic information. Alternatively, Park and coworkers presented a different type of human nose-mimetic diagnostic system that could sensitively and selectively distinguish the odor of a lung cancer biomarker, heptanal, from human blood (Fig. 16B).<sup>275</sup> Cell-derived nanovesicles, possessing the membrane proteins and cytosolic components needed for the olfactory signal transduction, were produced from the artificial olfactory cells and used to functionalize SWNT-FETs. The specific human olfactory receptors (hORs) on nanovesicles surface were served as the sensing ligands, which could selectively recognize the cancer biomarker heptanal and activate the olfactory signalling to generate the measurable electronic signal. The fabricated bioelectronics nose could selectively detect heptanal at a concentration as low as  $1 \times 10^{-14}$  M in real-time. This sensitivity and selectivity facilitated the detection of extremely small increase in the amount of chemical biomarkers from human blood plasma without the need for any pretreatment processes.

The above mentioned VOC biomarkers in exhaled breath samples are mainly used for lung cancer diagnosis. Early stage detection of other certain cancer, such as aggressive prostate cancer has also been linked to the presence of small biomarkers in urine. Biavardi *et al.* developed a hybrid silicon active surface by the covalent anchoring on Si substrates of a tetraphosphonate cavitand as supermolecular receptor for the specific recognition of sarcosine from its nonmethylated precursor, glycine, in water and urine.<sup>276</sup> The presence of sarcosine in water or urine was monitored via exchange reaction between amino acids and the Br-marked Tiii-Si•1 complex or fluorescence dye displacement. Once treated with sarcosine samples, the Br-marked guest or fluorescence guest were displaced, generating a decreased XPS or fluorescent signal. The use of Tiii cavitands can be further extended to the detection of biologically relevant compounds presenting N-CH<sub>3</sub> groups, such as drugs, neurotransmitters, painkillers, antidepressants, etc. Hamachi *et al.* fabricated a fluorocolorimetric sensor for the detection of important cancer biomarker spermine and spermidine in artificial urine.<sup>277</sup> The naturally abundant anionic layered material montmorillonite (MMT) was served as the host in supramolecular hydrogel to facilitate the aggregation of the cationic fluorescent probe. The adsorbed cationic probe illustrated a weak greenish, excimer emission, which converted to an intensified blue, monomer emission through its release via the cation-exchange with spermine or spermidine and the subsequent translocation to the supramolecular fibers. The fabricated hybrid fluorescent sensor was sensitive to spermine and spermidine in the range of 20–100  $\mu$ M with EC<sub>50</sub> of  $29 \pm 1.4$  and  $55 \pm 4.8$   $\mu$ M for spermine and spermidine, respectively, whereas was tolerant of biological fluids and substances. Furthermore, the potential practical utility of the hybrid sensor by conducting fluorocolorimetric imaging of spermine and spermidine in artificial urine demonstrated that changes in the fluorescence colours were clearly distinguished from green to blue for

spermidine and spermine in the concentration range relative to the criteria for cancer diagnosis.

## 2.5 Direct analysis of cancer cells

Cancer cells can produce on their surface or within the cell an abnormal quantity of proteins, receptors or specific enzymes. These overexpressed components can be detected and bound in order to detect, isolate, quantify and destroy tumour cells. Early and accurate detection of carcinoma cells is important for clinical diagnosis, effective toxicity monitoring and ultimately successful treatment of cancers. It is urgent to develop new diagnosis tools for rapid, selective and sensitive identification and detection of cancer cells at an early stage. Especially, being considered a “liquid biopsy”, circulating tumour cell (CTC) quantification is of great interest for evaluating cancer dissemination, predicting patient prognosis, and also for the evaluation of therapeutic treatments, representing a reliable potential alternative to invasive biopsies and subsequent proteomic and functional genetic analysis.

### 2.5.1 Isolation of CTCs

CTCs are cells that have shed into the vasculature from a primary tumour and circulate in the bloodstream, constituting seeds for subsequent growth of additional tumours (metastasis) in vital distant organs, triggering a mechanism that is responsible for the vast majority of cancer-related deaths.<sup>178, 278</sup> CTCs are pivotal to understanding the biology of metastasis and promise potential as a biomarker to noninvasively evaluate tumour progression and response to treatment.<sup>279</sup> However, isolation and characterization of CTCs represent a major technological challenge, since CTCs make up a minute number of the total cells in circulating blood, 1–10 CTCs per mL of whole blood compared to a few million white blood cells and a billion red blood cells.<sup>280</sup> Traditional isolation strategies are mainly focused on cell size, density, and specific molecules, lacking of specificity and efficiency. For example, the commercial FDA-approved screening system (CellSearch) is based on the use of iron nanoparticles coated with a polymer layer carrying antibodies anti-EpCAM for capturing CTCs and on the use of an analyzer to take images of isolated cells with multiplexed immunocytochemistry. This technology, however, is constrained by its low capture efficiency and variable detection rates caused by the limited blood volume used for CTC analysis.<sup>281</sup> In addition, it also has limited ability for post-capture molecular analysis. Recently, some magnetic nanoparticle-based multifunctional nanohybrids have been synthesized to improve the efficiency of immunomagnetic assay.<sup>282–284</sup> Gao *et al.* developed a photoacoustic imaging assay based on magneto-optical coupled nanoprobe, which streamlined the photoacoustic imaging process by combining magnetic enrichment and digital readout into a single step.<sup>285</sup> This method solved the low throughput problem of optical imaging and offered significantly improved sensitivity for CTCs quantitation with the detection limit at single cell/mL level. By combining the specific molecule recognition with the topographical interactions between cell surface structures and

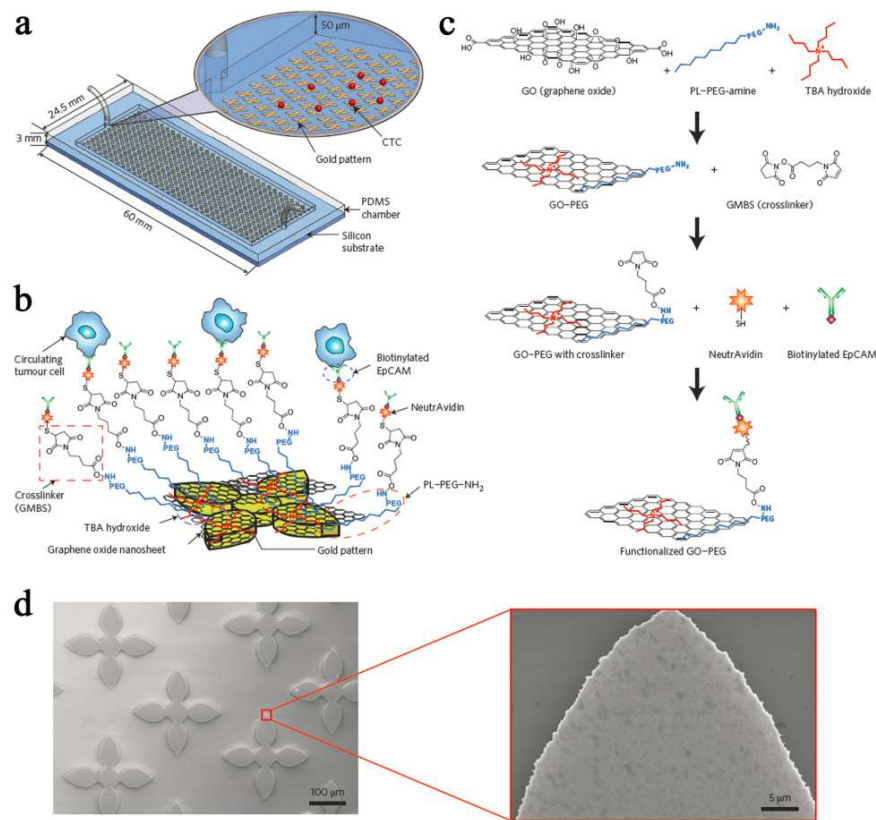


Fig. 17 Schematic representation of the graphene oxide chip (a), the conjugation chemistry between functionalized graphene oxide nanosheets and EpCAM antibodies (b), and preparation procedures for the functionalized graphene oxide (c). (d) Typical and magnified SEM images of adsorbed graphene oxide nanosheets on gold patterns. Reprinted with permission from ref. 296.

substrate structures, three-dimensional nano-biointerfaces have been designed for CTCs capture and isolation from whole blood.<sup>286-289</sup> Tseng's group worked on designing three-dimensional nanostructured substrates and using them to capture and isolate circulating tumour cells.<sup>290-292</sup> For example, they fabricated a three-dimensionally nanostructured silicon-nanopillar (SiNP) array and coated its surface with epithelial-cell adhesion-molecule antibody (anti-EpCAM), which allowed for enhanced local topographic interactions between the SiNP substrates and nanoscale components of the cellular surface (eg. microvilli and filopodia) and resulted in vastly improved CTCs-capture affinity.<sup>290</sup> EpCAM is a transmembrane glycoprotein that is frequently overexpressed in a variety of solid tumour cells and is absent from hematologic cells.<sup>293</sup> Further integrating the 3D-cell capture substrate with a serpentine chaotic mixing channel, the efficiency of CTC capture were improved by the synergistic effects of enhanced cell-substrate contact frequency as well as affinity.<sup>291</sup> Moreover, when combined with laser scanning cytometry

technique, the nanowire-substrate could also realize the large-area, automated quantitation of captured cells and rapid evaluation of functional cellular parameters (e.g., size, shape, and signalling protein) at the single-cell level.<sup>294</sup> Although promising, these three-dimensional structures are very rigid, which limits further characterization and expansion of cells on the substrate.

Extracellular matrix suitable for cell contact and survival is formed from soft materials with specific molecules and nanostructures. Inspired by this, Jiang's group developed soft polystyrene (PS) nanotube substrates that successfully achieved rapid and highly efficient breast cancer-cell capture from whole-blood samples with high cell viability by integrating the soft nature of PS polymer with specific capture agents and surface structures.<sup>295</sup> In addition, Nagrath and coworkers used functionalized graphene oxide nanosheets on a patterned gold surface to perform the isolation of CTCs from blood samples of pancreatic, breast and lung cancer patients (Fig. 17).<sup>296</sup> Taking

advantage of graphene oxide nanomaterial, CTCs were captured with high sensitivity at a low concentration of target

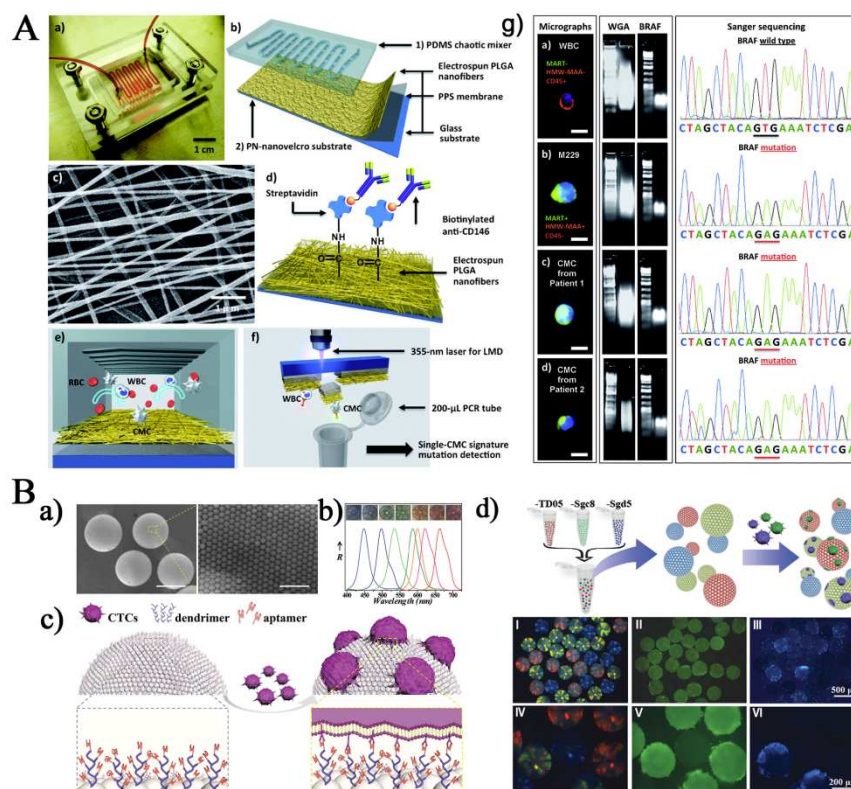


Fig. 18 (A) Polymer nanofiber (PN)-embedded microchips for detection, isolation, and molecular analysis of single circulating melanoma cells (CMCs). a) Photograph of PN-nanovelcro chip. b) Diagram of the composition of PN-nanovelcro chip: an overlaid PDMS chaotic mixer and a transparent PN-nanovelcro substrate. c) SEM images of electrospun PLGA nanofibers on PN-nanovelcro substrate. d) Schematic illustration of the conjugation of melanoma-specific antibody anti-CD146 to substrate. e) Schematic representation of the mechanism of the PN-nanovelcro CMC chip. f) Method of laser microdissection-based single-CMC isolation. g) Analysis of isolated single-CMC. Reprinted with permission from ref. 307. (B) Barcode assay for the capture and detection of multiple types of CTCs. a) Typical and magnified SEM images of the barcode particles. b) Microscopy images and reflection spectra of seven different types of barcode nanoparticles. c) Schematic of the barcode particles used for enhanced CTCs capture; the surface of the barcode particle is decorated with dendrimer and DNA aptamer. d) Application of the barcode particles for capturing multiple types of CTCs. Reprinted with permission from ref. 23.

cells ( $73 \pm 32.4\%$  at 3-5 cells per mL blood) by using functionalized graphene oxide nanosheets on a flat substrate.

The presently developed antibody-based capture assays for CTCs detection and isolation mostly rely on one common biomarker-EpCAM-expression on disseminated tumour cells. However, due to tumour heterogeneity and epithelial to mesenchymal transition, subpopulations of metastatic tumour cells often do not express this specific epithelial surface antigen or express it at very low levels, the value of EpCAM-based assays for CTCs detection is limited.<sup>280</sup> A microfluidic channel based on antibody-conjugated magnetic/plasmonic hybrid nanocarriers was developed to address this problem by separating cancer cells from normal blood cells with magnetic force in a microfluidic chamber.<sup>297</sup> Multivalent DNA aptamer was also employed in cell-capture microfluidic devices as the alternative of antibody to enhance the capture efficiency of CTCs.<sup>298, 299</sup> Furthermore, taking the advantage of the

differential adhesion preference of cancer cells to nanorough surfaces when compared to normal blood cells, Fu *et al.* also realized the isolation of CTCs in a simple yet effective manner without using any capture antibody.<sup>300</sup> Although the capturing and enumeration of CTCs provides preliminary diagnostic-relevant information, it is conceivable that the CTC-derived molecular signatures and functional readouts provide more valuable and significant insight into tumour biology during the critical window where therapeutic intervention could make a significant difference. In order to conduct molecular and functional analyses of CTCs, developing a new CTC assay that can not only capture CTCs with high efficiency, but also release CTCs with minimum contamination of the surrounding white blood cells and negligible disruption to viability and functions of the CTCs is an urgent need. Recently, significant progress has been made in fabricating nanomaterials-based smart platform for cell-affinity assay that is capable of not only

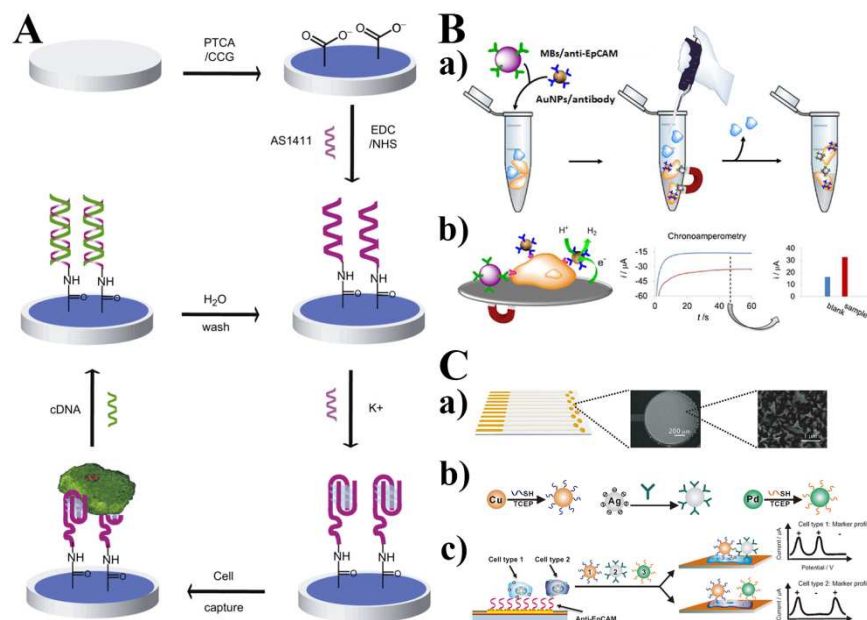


Fig. 19 (A) Schematic illustration of the reusable aptamer/graphene-based cytosensor. Reprinted with permission from ref. 309. (B) Schematic diagram of nanoparticle-based electrochemical sensor for cancer cell monitoring. a) Caco2 cells captured by MBs-anti-EpCAM and simultaneous labeling with AuNPs/specific antibodies in the presence of control cells. b) Electrochemical detection of labeled Caco2 cells through the hydrogen evolution reaction (HER) electrocatalyzed by the AuNPs labels. Reprinted with permission from ref. 314. (C) Multi-nanoparticle approach to specific cancer cell detection. a) Chip layout and SEM image of an electrode after plating. b) Metal nanoparticles (MNPs)-based electrochemical labels are made specific for cell surface markers with DNA aptamers attached using a thiol/metal bond to Cu or Pd nanoparticles or antibodies attached to Ag nanoparticles by electrostatic binding. c) Cancer cells are first captured on electrode surface. A mixture of modified MNPs is introduced and an electrochemical profile is generated using linear-sweep voltammetry. Reprinted with permission from ref. 313.

capturing CTCs with high efficiency, but also releasing the conjugated CTCs upon the application of an external stimulus, including temperature change,<sup>301</sup> electrical stimulation,<sup>302-304</sup> enzymatic treatment,<sup>305, 306</sup> etc. However, these technologies usually perform the simple function of cell capture or release while cannot effectively distinguish between different CTCs, thus constrains their application for the diagnosis of specific cancers. Therefore, the development of a new platform that can capture, detect and release multiple types of CTCs would dramatically increase the use of CTCs in diagnostics and prognostics. Tseng *et al.* replaced the non-transparent SiNP substrate in their earlier nanovelcro chip<sup>291, 305</sup> with a transparent PN-nanovelcro substrate by depositing electrospun poly(lactic-co-glycolic acid) (PLGA)-nanofibers onto a commercial laser microdissection (LMD) slide, and realized the identification and isolation of the single circulating melanoma cells (CMCs) using a highly accurate LMD technique (Fig. 18A).<sup>307</sup> The harvested single CMCs could be used for subsequent Sanger sequence analysis (Fig. 18A-g). This promising platform also showed excellent performance for single-CMC isolation and genotyping in peripheral blood samples collected from two stage-IV melanoma patients. The

modified nanovelcro chip was also feasible for enrichment and isolation of CTCs from patients with prostate cancer and studying the complex tumour heterogeneity of prostate cancer with whole exome sequencing.<sup>308</sup> Overall, the PN-Nanovelcro-LMD platform may enable a means to the potential of resolving questions of clonal evolution and drug resistant mechanisms upon disease progression at a single cell level with the prospect of improving personalized medicine. Recently, Gu and coworkers presented a new type of barcode particle and demonstrated its ability to capture, detect and release multiple types of CTCs.<sup>23</sup> As illustrated in Fig. 18B, the particles were spherical colloidal crystal clusters decorated with dendrimer-amplified aptamer probes, whose size were adjusted to suit cell dimensions by the microfluidic-droplet templates. The characteristic reflection peaks originating from the photonic bandgap structure of the colloidal crystals were very stable, which were considered as the encoding information in the particles. The decoration of highly branched dendrimer-amplified aptamer probes on barcode particle surface severely improved the sensitivity, reliability and specificity of cell capture. The barcode particle also facilitated the accurate and controlled release of the captured CTCs with high viability.

## 2.5.2 Measurement of cancer cells

### 2.5.2.1 Electrochemical methods

Electrochemical biosensors represent a particularly attractive solution to cancer cell analysis as they have previously been proved to feature clinically relevant sensitivity and specificity, simplicity, rapid response, the capacity for miniaturization, and low cost in related applications. Our group fabricated a label-free and reusable electrochemical cytosensor based on the first clinical trial II used aptamer AS1411 and functionalized graphene.<sup>309</sup> As shown in Fig. 19A, 3,4,9,10-perlene tetra-carboxylic acid (PTCA) was used to avoid graphene aggregation and introduced more negatively charged -COOH groups on graphene surface without destroying the conductivity property of graphene. Subsequently, NH<sub>2</sub>-modified aptamer strand was linked to above nanocomposite and the resulting aptamer-PTCA nanocomposite was then used as electrode materials to effectively capture cancer cells on electrode surface via the specific binding between cell surface nucleolin and the aptamer AS1411. The conjugation of cancer cells on electrode surface severely prevented the redox probe [Fe(CN)<sub>6</sub>]<sup>3-/4-</sup> close to the electrode surface, generating increased electrochemical impedance signal. This electrochemical aptasensor demonstrated high sensitivity toward cancer cells with the detection limit as low as one thousand cells and could also distinguish cancer cells and normal cells. Recently, Schmidt *et al.* presented a three-dimensional tubular impedimetric microsensors with rolled-up nanotechnology integrated into microfluidic chips, which had the potential to directly detect suspended cancer cells in flowing PBS down to single cell resolution in a real-time manner.<sup>310</sup> Apart from the direct monitoring of impedance to report the presence of cancer cells based on their dielectric property, the most employed strategy is the sandwich-type electrochemical cytosensor by using nanoparticles as the nanocarrier for electroactive molecules<sup>303, 311</sup> or as the electrochemical probes themselves<sup>312, 313</sup>. For instance, a new strategy for simple and fast detection of cancer circulating cells was developed based on the capturing capability of anti-EpCAM functionalized magnetic beads and the specific labelling through antibody-modified gold nanoparticles, with the sensitivity of the AuNPs-electrocatalyzed hydrogen evolution reaction detection technique (Fig. 19B).<sup>314</sup> The electrochemical results demonstrated that this method was selective for cancer cells without the interference caused by the presence of other circulating cells. In this view, for electrochemical biosensing, the detection sensitivity can be significantly improved through the designing of special electrocatalysts for signal amplification. Since the natural enzymes are easily subject to proteolytic degradation and their native conformations are sensitive to environment, their catalytic activities is unstable. Robust nonenzymatic nanoelectrocatalysts with high catalytic efficiencies, as gold nanoparticles used in previous work, have been chosen as the alternative candidate for electrochemical biosensor fabrication. Wang *et al.* discovered that the magnetic Fe<sub>3</sub>O<sub>4</sub> nanoparticles

exhibited an intrinsic catalytic activity toward the electrochemical reduction of small dye molecules, which could be further enhanced by metallic nanocages.<sup>315</sup> Therefore, they synthesized Fe<sub>3</sub>O<sub>4</sub>@nanocage core-satellite hybrid nanoelectrocatalysts as signal amplifying nanoprobes for the development of ultrasensitive electrochemical cytosensor. The electrochemical readout of several biomarkers simultaneously requires redox-active probes with well-separated potentials. Metal nanoparticles (MNPs) would serve as the best candidate as electrochemical scanning allows measurement of the direct oxidation of the MNPs and the redox chemistry of each nanoparticle could be resolved. Using a family of metal nanoparticles including Cu, Ag, and Pd to report the presence of target, Kelley and coworkers developed a novel electrochemical strategy for cancer cell identification and multi-marker analysis (Fig. 19C).<sup>313</sup> A novel microfabricated chip with multiple gold sensors was constructed to capture cells based on an epithelial marker, and then metal nanoparticles modified with antibodies or aptamers for the specific recognition of different biomarkers on cancer cell surface were introduced to produce electrochemical signal. The fabricated cytosensor enabled the detection and collection of surface marker profiles on as few as two cancer cells per sensor, the simultaneous analysis of three different surface biomarkers, and the discrimination of cancer cells even in the presence of an abundance of white cells typically found in patient samples.

### 2.5.2.2 Optical methods

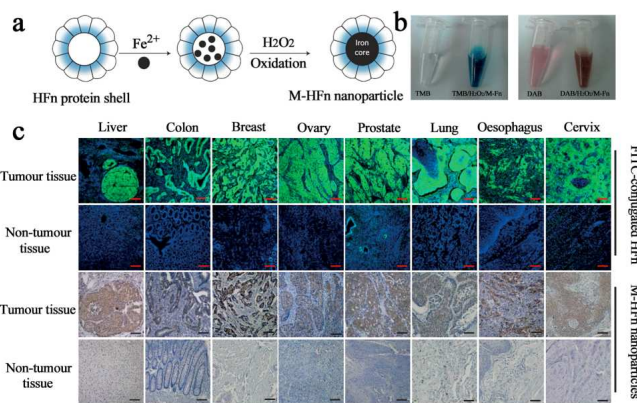


Fig. 20 a) Schematic diagram of the preparation of M-HFn nanoparticles and their structure. b) Characterization of peroxidase activity of M-HFn nanoparticles with peroxidase substrates TMB and DAB. c) Cancer diagnosis in clinical specimens using M-HFn nanoparticles. Reprinted with permission from ref. 319.

At present, the development of a highly sensitive and simply eye-detectable indicator is one of the most important subjects in the field of cancer identification. Carboxyl-modified graphene oxide (GO-COOH) is shown to possess intrinsic peroxidase-like activity that can catalyse the reaction of peroxidase substrate 3,3',5,5'-tetramethylbenzidine (TMB) in the presence of H<sub>2</sub>O<sub>2</sub> to produce a blue colour product.<sup>316</sup> This unique property firstly discovered by our group provides new insight into application of these nanomaterials to medical diagnosis and biosensing. Using folic acid (FA) conjugated

graphene-hemin composite (GFH)<sup>317</sup> or graphene oxide-gold nanoclusters (AuNCs) hybrid (GFA),<sup>318</sup> we realized the colorimetric detection of cancer cells based on the colour reaction catalysed by GFH or GFA synergetic peroxidase-like activity. Folic acid can specifically target folate receptors, which are overexpressed on the surface of different types of cancer cells. Because of the specificity and high affinity of folic acid, GFH and GFA could selectively bind to the surface of human cervical cancer cells (HeLa) and human breast cancer cells (MCF-7) by targeting folate receptors, which could not only be visualized under bright field microscopy but also be quantitatively determined by a colourimetric method. Since nanoparticles developed for cancer cell detection are typically modified with targeting ligands, such as antibodies, peptides, or small molecules using complicated processes and expensive reagents, the excess ligands on nanoparticle surface might cause nonspecific binding or aggregation of nanoparticles, which crippled the detection performance. Magnetoferritin nanoparticles (M-HFn) were synthesized for this purpose to directly target and visualize tumour tissues without the use of any targeting ligands or contrast agents (Fig. 20).<sup>319</sup> Ferritin is an iron storage protein composed of 24 subunits made up of the heavy-chain ferritin (HFn) and the light-chain ferritin, with an outer diameter of 12 nm and interior cavity diameter of 8 nm. Their cavity can be used as a reaction chamber to synthesize highly crystalline and monodisperse nanoparticles through biomimetic mineralization within the protein shell. In this design, iron oxide nanoparticles were encapsulated inside the recombinant human HFn protein shell, which could bind to tumour cells that overexpressed transferrin receptor 1 (TfR1). The iron oxide core had the peroxidase-like activity,<sup>320</sup> which catalyzed the oxidation of peroxidase substrates in the presence of hydrogen peroxide to produce a colour reaction for visualized sensing of tumour tissues. It was verified that these nanoparticles could distinguish cancerous cells from normal cells with a sensitivity of 98% and specificity of 95% by examining 474 clinical specimens from patients with nine types of cancer. Over all, this promising method based on one-step tumour targeting and visualization with low-cost and mass-produced M-HFn nanoparticles has high sensitivity and specificity, as well as high accuracy, credibility and repeatability for convenient monitoring and analysis of tumour cells in tissue specimens. Due to its high specificity toward TfR<sup>+</sup> cancer cells, transferrin was also employed as a bio-ligand in magneto-dendritic nanosystem for the isolation and detection of CTCs.<sup>321</sup>

Labelling and imaging of target cancer cells using fluorescent probes has become increasingly important in prognosis and treatment of cancer at the early stage. Conventional biolabels used in cell imaging studies, including organic dyes and fluorescent proteins, are often suffered from a high photobleaching or vulnerable to chemical and metabolic degradation, limiting the long-term cell tracking experiments. Although semiconductor quantum dots (QDs) have overcome the shortcomings with high brightness and good photostability,<sup>322, 323</sup> the heavy metal components of QDs

undergo oxidative degradation to release heavy metal ions that are highly toxic to the live biosubstrate. Recently, a series of novel fluorescent probes with low cytotoxicity, high fluorescence, and flexible surface functionalization have been explored and widely used for targeted cancer cell detection, including conjugated polymer nanoparticles,<sup>324, 325</sup> lanthanide-doped nanoprobes,<sup>326-328</sup> dye-doped silica nanoparticles,<sup>329</sup> and fluorescent carbon materials,<sup>330, 331</sup> etc. However, most of these labeling methods rely on the use of direct nanoparticle-ligand conjugates, wherein affinity ligands (e.g. antibodies, peptides) are covalently attached to the surface of nanoparticles. Such a conjugation strategy often requires time-consuming optimization processes to maximize the affinity, the ligand-to-nanoparticle ratio, and the colloidal stability of each new construct. To overcome these issues, Weissleder *et al.* fabricated a novel nanoparticle targeting platform based on bioorthogonal chemistry using a rapid, catalyst-free cycloaddition as the coupling mechanism.<sup>332</sup> In their design, antibodies against biomarkers of interest were modified with *trans*-cyclooctene and used as scaffolds to couple tetrazine-modified nanoparticles onto live cells (Fig. 21A). The bioorthogonal nanoparticle detection platform is general and can be extended in diverse nanoparticle targeting applications, including alternative bioorthogonal small-molecule chemistries, affinity molecule scaffolds (proteins, peptides, aptamers, natural products, engineered hybrids) and nanoparticle sensors such as carbon nanomaterials, metal nanoparticles and polymer matrices or vesicles. Host-guest interactions represented another promising strategy used for cellular labelling with nanoparticles due to their fast kinetics, specificity, stability, and bioorthogonal nature.<sup>333</sup> Apart from antibody-mediated cellular labelling, aptamers have also emerged as promising molecular probes for *in vivo* cancer imaging. To improve the sensing accuracy and avoid the high background and limited contrast remaining in “always-on” aptamer probes, an activatable aptamer probe was developed to target membrane proteins of living cancer cells and achieved contrast-enhanced cancer visualization inside mice.<sup>334</sup> Combining the special structure-switching properties of DNA aptamers with toehold-mediated strand displacement reactions, Tan *et al.* designed a DNA-based device, named “Nano-Claw”, to perform autonomous logic-based programmable analysis of multiple cancer-surface markers and in response, producing a diagnostic signal and targeted photodynamic therapy.<sup>335</sup>

Most presented methods for cancer cells detection are based on specific recognition of intracellular or extracellular biomarkers, requiring the previous knowledge of specific mutations in DNA/RNA, changes in the regulation of protein expression inside the cells or biomarkers on cells surfaces. However, there is no single marker or a combination of biomarkers that has efficient sensitivity and specificity to differentiate between normal, cancerous and metastatic cell types. Rotello's group put forward a different concept for cancer cell detection, called “chemical nose”, which was based on selective non-covalent interactions between cell surface components and nanoparticle-based sensor elements without

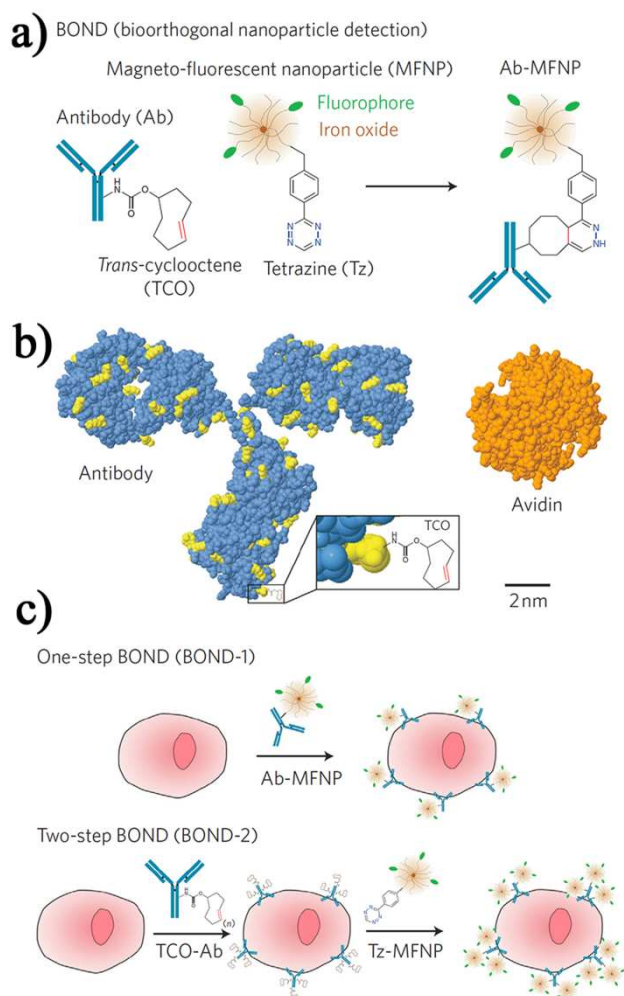


Fig. 21 Bioorthogonal nanoparticle detection (BOND) method for cell identification. a) Schematic illustration of conjugate chemistry between antibody and nanoparticle. b) Comparative sizes of a representative mouse IgG<sub>2a</sub> antibody, a trans-cyclooctene modification and an avidin protein for comparison. c) Application of BOND for one-step (direct) and two-step targeting of nanoparticles to cells. Reprinted with permission from ref. 332.

requiring of any previous knowledge of intracellular or extracellular biomarkers.<sup>21, 25, 336, 337</sup> The cell membrane surface consists primarily of a thin layer of amphipathic phospholipids, carbohydrates and many integral membrane proteins. The proportions of proteins, lipids and carbohydrates in the cell membrane vary with cell type according to the function of cells. The distinct cell membrane composition in different cell types suggests that there will be physicochemical (i.e. charge, hydrophobicity etc.) differences between cell types. Such physicochemical differences could potentially be detected by an array-based “chemical nose” approach that relies on selective interactions between multiple reporter elements and the target cell. A distinct pattern of responses produced from a set of sensors in the array provided a fingerprint that allowed classification and identification of the cell types. The constructed detection system was based on conjugates between an array of structurally related modified gold nanoparticles and the fluorescent polymer or protein. The interactions between

nanoparticles and polymer or protein were non-covalent, and predominantly electrostatic. When mammalian cells were incubated with these nanoparticle-polymer or nanoparticle-protein complexes, there was a competitive binding between nanoparticle-polymer or nanoparticle-protein complexes and cell types, enabled the displacement of the fluorophore polymer or protein from the nanoparticle-polymer or nanoparticle-protein complexes, generating a fluorescence response. Based on subtle variations in glycosylation patterns, Lavigne *et al.* also developed a “chemical nose” sensor using boronic acid functionalized synthetic lectins in an array format for the differentiation of structurally similar cancer associated glycans and cancer cell lines.<sup>338</sup> In addition, an array of magnetic glycol-nanoparticle bearing carbohydrates as the ligands was designed by Huang’s group to differentiate cancer cells and quantitatively profile their carbohydrate binding abilities by magnetic resonance imaging.<sup>339</sup> As the interactions between glycoconjugates and endogenous lectins present on cancer cell surface are crucial for cancer development and metastasis, the ability to characterize and unlock the glyco-code of individual cell lines can facilitate both the understanding of the roles of carbohydrates as well as the expansion of diagnostic and therapeutic tools for cancer.

Surface-enhanced Raman scattering (SERS) has recently emerged as an alternative to fluorescence-based spectroscopy in bioimaging for cancer diagnostics, as it can minimize photobleaching, peak overlapping, and low signal-to-noise ratio in complex biological systems and has higher multiplexing capability, ultra sensitivity even up to single molecule detection.<sup>340</sup> The Raman signals of molecules on colloidal gold or silver nanoparticles can be enhanced by several orders of magnitude (typically  $10^6$  to  $10^{14}$ ) as a result of the strong surface plasmon resonance of the nanostructured surface.<sup>341</sup> It is well established that SERS signals can be intensified via assembly of the plasmonic NPs into dimers/small clusters or co-encapsulation of nanoparticles and the SERS reporter molecules.<sup>342</sup> For example, Irudayaraj *et al.* fabricated DNA-assembled nanoparticle network structure on specific cell surface sites with excellent interparticle distance control and used them in SERS and SPR dual-mode sensing for multiplexed detection of cell surface markers for single cell phenotyping.<sup>343</sup> In their design, pointer particles functionalized with either anti-CD44 or anti-CD24 and ssDNA with different lengths and bases were selectively hybridized with two types of pointer particles, which were modified with respective Raman labels and complementary ssDNA. The obtained size of the nanoparticle network structure was proportional to the SERS intensity. The development of highly sensitive Raman reporters is another key point for improving the sensing performance of SERS assay. Olivo *et al.* used gold nanoparticles to enhance the inherently weak Raman signal of the metal carbonyl CO stretching vibrations of organometallic osmium carbonyl cluster  $\text{Os}_3(\text{CO})_{10}(\mu\text{-H})_2$  for live-cell imaging.<sup>344</sup> The clear advantage of transition-metal carbonyl compounds was that the CO stretching vibration signal was well-separated from other molecular vibrational modes of the cell in live-cell imaging.

Since most of the commonly used Raman signature molecules are active in the UV/Vis range, their potential for in vivo imaging has been severely restricted. The adequacy of the near-infrared (NIR) region for in vivo studies has raised the interest in NIR SERS-active molecules. A lipoic acid-containing NIR-active tricabocyanine library was applied to the preparation of ultrasensitive SERS probes for in vivo cancer imaging, which displayed high SERS intensity and selectivity towards specific cancer cells under both Raman and dark-field microscopes.<sup>12</sup> Further, the SERS probes also showed good performance for in vivo application in HER2-positive and -negative xenograft models. The high sensitivity and tumour specificity of the hybrid nano-tags proved their excellent potential as non-invasive diagnostic tools and opened up a new window for the development of SERS probes for cancer bioimaging.

### 3. Conclusion and future perspectives

The concept of early detection-finding tumours early, before they spread and become incurable-has tantalized cancer-control researchers for many years. This review provides an overview of the recent efforts to construct various chemical tools for sensitive detection of cancer biomarkers, including proteins, enzymes, nucleic acids, small molecules and cancer cells. We introduced several representative examples for each biomarker and showed that the multidisciplinary technology based cancer diagnostics are becoming an increasingly relevant alternative to traditional techniques. With respect to current and future technologies for cancer diagnostics in general, and cancer biomarker detection in particular, comprehensive work still need to be carried out. The exploration of new technologies and new biomarkers for basic and advanced cancer diagnostics is constantly gaining momentum. Since the analytical methods and molecular methods currently used in well-equipped clinical and professional laboratories are highly sophisticated, the future goal is to achieve fast, portable, cost-efficient and user-friendly personalized point-of-care diagnostics that could be introduced to home disease monitoring.

Although, tremendous progress has been made over the past few decades creating assays for detecting cancer biomarkers, most of these developments are merely proof-of-concept demonstrations and their practicability are only achievable under highly optimized conditions in a lab. Some outstanding challenges remain obstacles to translate these sensing platforms from clean buffered solutions of a research environment to more practical settings and real world clinical samples in hospital or other medical situations, such as cell lysate, blood serum, and urine. Firstly, the outstanding performance of a biosensor depends on its sensitivity, selectivity, detection range, temporal resolution, reproducibility, response time, cost, etc. An ability to sensitively transduce recognition events to readout signal is the basic requirement in cancer diagnostics. Although ELISA and PCR remain to be the gold standards for protein and nucleic acids assays in clinical diagnosis, each of them still has the shortages for advanced diagnostic applications. Hence,

continuous efforts have been devoted to further optimize these standard methods or find new and better techniques for the measurement of cancer biomarkers. Aside from this point of view, a means to reliably and robustly amplify the signal is essential for the application of these technologies to the detection of trace cancer biomarkers at the clinical level. With the rapid emergence of nanotechnology and nanoscience, hybrid bio/nano-structures-based signal amplification hold great promise in realizing high sensitivity and selectivity for in situ or online detection of biomolecules, which can not only produce a synergic effect among catalytic activity, conductivity and biocompatibility to accelerate the signal transduction, but also provide amplified recognition events by high loading of signal tags. Although promising, nanomaterials based methods also bring about problems such as low recognition efficiency, slow binding kinetics caused by the presence of heterogeneous interfaces, non-specific binding for detection in complex biological matrix, operation complexity, and also a lack of generality. Parameters of nanomaterials should undoubtedly undergo further improvements and refinements in the future to meet the requirement of clinically diagnostic applications. Secondly, the naturally occurring biomarkers are frequently found in low concentrations and most of them cannot be “amplified” as nucleic acids since they cannot replicate themselves and exponentially increase their concentration for the purpose of detection. The translation of specific ligand-target recognition process into DNA detection events or other encoded information recognition for the rapid, convenient, sensitive and accurate evaluation of non-nucleic acids cancer biomarkers would be a “game changer” in cancer monitoring. Thirdly, since the simultaneous analysis is required in practice to improve the diagnostic accuracy and provide more efficient biological information, it is of key important for the development of high-throughput techniques for the parallel analysis of numerous components in samples in a single test. Fourthly, since physiological fluidic samples have emerged as a non-invasive liquid biopsy in tumour diagnostics that is easily accessible for patient and physician, greater demands are placed on the sensing methods by their complex components. Microfluidic chips allow considerable throughput portability and the capacity for a high level of integration and thus fulfill the requirements of fluidic sample based point-of-care diagnostics as sample preparation and advanced technologies and biotechnologies can be introduced in a single monolithic disposable device. However, future optimizations of these technologies remain to be required before commercialization becomes feasible. Therefore, with the demand in life sciences and clinical diagnostics, the future perspectives in cancer biomarker detection lie in developing efficient detection platform with high sensitivity and selectivity, miniaturization, versatility, high-throughput and identification of new biomarkers specifying for early diagnosis. New progress and improvements are expected to be achieved by the cooperation and endeavour from different communities of chemists, physicists, biologists, clinicians, material-scientists, engineering and technical researchers, etc.

## Acknowledgements

This work was supported by 973 Project (2011CB936004, 2012CB720602), and NSFC (21210002, 21431007, 91413111).

## Notes and references

1. J. Ferlay, I. Soerjomataram, M. Ervik, R. Dikshit, S. Eser, C. Mathers, M. Rebelo, D. M. Parkin, D. Forman and F. Bray, *GLOBOCAN 2012 Cancer Incidence and Mortality Worldwide: IARC CancerBase No. 11. Lyon, France: International Agency for Research on Cancer*, 2013, available from <http://globocan.iarc.fr>.
2. O. Golubnitschaja and J. Flammer, *Surv. Ophthalmol.*, 2007, **52**, S155-161.
3. C. L. Sawyers, *Nature*, 2008, **452**, 548-552.
4. C. Pfitzner, I. Schroeder, C. Scheungraber, A. Dogan, I. B. Runnebaum, M. Duerst and N. Haefner, *Sci. Rep.*, 2014, **4**, 3970.
5. S. A. Kazane, D. Sok, E. H. Cho, M. L. Uson, P. Kuhn, P. G. Schultz and V. V. Smider, *Proc. Natl. Acad. Sci. USA*, 2012, **109**, 3731-3736.
6. R. de la Rica and M. M. Stevens, *Nat. Nanotechnol.*, 2012, **7**, 821-824.
7. D. Alberti, M. v. t. Erve, R. Stefania, M. R. Ruggiero, M. Tapparo, S. Geninatti Crich and S. Aime, *Angew. Chem. Int. Ed.*, 2014, **53**, 3488-3491.
8. G. Garcia-Schwarz and J. G. Santiago, *Angew. Chem. Int. Ed.*, 2013, **52**, 11534-11537.
9. H. Lee, J.-E. Park and J.-M. Nam, *Nat. Commun.*, 2014, **5**, 3367.
10. W.-C. Law, K.-T. Yong, A. Baev and P. N. Prasad, *ACS Nano*, 2011, **5**, 4858-4864.
11. S. Krishnan, V. Mani, D. Wasalathanthri, C. V. Kumar and J. F. Rusling, *Angew. Chem. Int. Ed.*, 2011, **50**, 1175-1178.
12. A. Samanta, K. K. Maiti, K.-S. Soh, X. Liao, M. Vendrell, U. S. Dinish, S.-W. Yun, R. Bhuvaneshwari, H. Kim, S. Rautela, J. Chung, M. Olivo and Y.-T. Chang, *Angew. Chem. Int. Ed.*, 2011, **50**, 6089-6092.
13. S. R. Panikkanvalappil, M. A. Mackey and M. A. El-Sayed, *J. Am. Chem. Soc.*, 2013, **135**, 4815-4821.
14. M. Li, S. K. Cushing, J. Zhang, S. Suri, R. Evans, W. P. Petros, L. F. Gibson, D. Ma, Y. Liu and N. Wu, *ACS Nano*, 2013, **7**, 4967-4976.
15. G. H. Wu, R. H. Datar, K. M. Hansen, T. Thundat, R. J. Cote and A. Majumdar, *Nat. Biotechnol.*, 2001, **19**, 856-860.
16. L. Loo, J. A. Capobianco, W. Wu, X. Gao, W. Y. Shih, W. H. Shih, K. Pourrezaei, M. K. Robinson and G. P. Adams, *Anal. Chem.*, 2011, **83**, 3392-3397.
17. J. Wang, L. Wu, J. Ren and X. Qu, *Small*, 2012, **8**, 259-264.
18. Y. Song, W. Wei and X. Qu, *Adv. Mater.*, 2011, **23**, 4215-4236.
19. M. Labib, N. Khan, S. M. Ghobadloo, J. Cheng, J. P. Pezacki and M. V. Berezovski, *J. Am. Chem. Soc.*, 2013, **135**, 3027-3038.
20. B. V. Chikkaveeraiah, A. A. Bhirde, N. Y. Morgan, H. S. Eden and X. Chen, *ACS Nano*, 2012, **6**, 6546-6561.
21. S. Rana, A. K. Singla, A. Bajaj, S. G. Elci, O. R. Miranda, R. Mout, B. Yan, F. R. Jirik and V. M. Rotello, *ACS Nano*, 2012, **6**, 8233-8240.
22. K. Mizusawa, Y. Takaoka and I. Hamachi, *J. Am. Chem. Soc.*, 2012, **134**, 13386-13395.
23. F. Zheng, Y. Cheng, J. Wang, J. Lu, B. Zhang, Y. Zhao and Z. Gu, *Adv. Mater.*, 2014, **26**, 7333-7338.
24. S. S. Agasti, M. Liong, V. M. Peterson, H. Lee and R. Weissleder, *J. Am. Chem. Soc.*, 2012, **134**, 18499-18502.
25. A. Bajaj, O. R. Miranda, I.-B. Kim, R. L. Phillips, D. J. Jerry, U. H. F. Bunz and V. M. Rotello, *Proc. Natl. Acad. Sci. USA*, 2009, **106**, 10912-10916.
26. H. Pei, J. Li, M. Lv, J. Wang, J. Gao, J. Lu, Y. Li, Q. Huang, J. Hu and C. Fan, *J. Am. Chem. Soc.*, 2012, **134**, 13843-13849.
27. K. J. Martin, M. V. Fournier, G. P. V. Reddy and A. B. Pardee, *Cancer Res.*, 2010, **70**, 5203-5206.
28. D. Cai, L. Ren, H. Zhao, C. Xu, L. Zhang, Y. Yu, H. Wang, Y. Lan, M. F. Roberts, J. H. Chuang, M. J. Naughton, Z. Ren and T. C. Chiles, *Nat. Nanotechnol.*, 2010, **5**, 597-601.
29. K. Mohan, K. C. Donovan, J. A. Arter, R. M. Penner and G. A. Weiss, *J. Am. Chem. Soc.*, 2013, **135**, 7761-7767.
30. J.-J. Xu, W.-W. Zhao, S. Song, C. Fan and H.-Y. Chen, *Chem. Soc. Rev.*, 2014, **43**, 1601-1611.
31. M. Perfezou, A. Turner and A. Merkoci, *Chem. Soc. Rev.*, 2012, **41**, 2606-2622.
32. J. F. Rusling, C. V. Kumar, J. S. Gutkind and V. Patel, *Analyst*, 2010, **135**, 2496-2511.
33. J. Li, S. Li and C. F. Yang, *Electroanalysis*, 2012, **24**, 2213-2229.
34. X. Luo and J. J. Davis, *Chem. Soc. Rev.*, 2013, **42**, 5944-5962.
35. M. Swierczewska, G. Liu, S. Lee and X. Chen, *Chem. Soc. Rev.*, 2012, **41**, 2641-2655.
36. S. K. Keesee, J. V. Briggman, G. Thill and Y. K. Wu, *Crit. Rev. Eukar. Gene*, 1996, **6**, 189-214.
37. G. Tarro, A. Perna and C. Esposito, *J. Cell. Physiol.*, 2005, **203**, 1-5.
38. S. M. Hanash, S. J. Pitteri and V. M. Faca, *Nature*, 2008, **452**, 571-579.
39. P. J. Morin, *Cancer Res.*, 2005, **65**, 9603-9606.
40. J. D. Wulfschlegel, L. A. Liotta and E. F. Petricoin, *Nat. Rev. Cancer*, 2003, **3**, 267-275.
41. M. F. Clark and A. N. Adams, *J. Gen. Virol.*, 1977, **34**, 475-483.
42. E. Engvall and P. Perlmann, *Immunochemistry*, 1971, **8**, 871-874.
43. D. J. Reen, *Methods Mol. Biol.*, 1994, **32**, 461-466.
44. J. E. Oesterling, *J. Urol.*, 1991, **145**, 907-923.
45. S. J. Freedland, E. B. Humphreys, L. A. Mangold, M. Eisenberger, F. J. Dorey, P. C. Walsh and A. W. Partin, *JAMA-J. Am. Med. Assoc.*, 2005, **294**, 433-439.
46. Z. Gao, L. Hou, M. Xu and D. Tang, *Sci. Rep.*, 2014, **4**, 3966.
47. M. I. Kim, Y. Ye, M.-A. Woo, J. Lee and H. G. Park, *Adv. Healthcare Mater.*, 2014, **3**, 36-41.
48. Y. Lin, J. Ren and X. Qu, *Acc. Chem. Res.*, 2014, **47**, 1097-1105.
49. D. Liu, X. Huang, Z. Wang, A. Jin, X. Sun, L. Zhu, F. Wang, Y. Ma, G. Niu, A. R. H. Walker and X. Chen, *ACS Nano*, 2013, **7**, 5568-5576.
50. J.-u. Shim, R. T. Ransinghe, C. A. Smith, S. M. Ibrahim, F. Hollfelder, W. T. S. Huck, D. Klenerman and C. Abell, *ACS Nano*, 2013, **7**, 5955-5964.
51. R. S. Gaster, D. A. Hall, C. H. Nielsen, S. J. Osterfeld, H. Yu, K. E. Mach, R. J. Wilson, B. Murmann, J. C. Liao, S. S. Gambhir and S. X. Wang, *Nat. Med.*, 2009, **15**, 1327-1332.
52. Y. Song, Y. Zhang, P. E. Bernard, J. M. Reuben, N. T. Ueno, R. B. Arlinghaus, Y. Zu and L. Qin, *Nat. Commun.*, 2012, **3**, 1283.
53. L. A. Cole, *Reprod. Biol. Endocrin.*, 2009, **7**, 8.
54. Y. Song, X. Xia, X. Wu, P. Wang and L. Qin, *Angew. Chem. Int. Ed.*, 2014, **53**, 12451-12455.
55. S.-J. Park, T. A. Taton and C. A. Mirkin, *Science*, 2002, **295**, 1503-1506.
56. G. Zheng, F. Patolsky, Y. Cui, W. U. Wang and C. M. Lieber, *Nat. Biotechnol.*, 2005, **23**, 1294-1301.
57. T. G. Drummond, M. G. Hill and J. K. Barton, *Nat. Biotechnol.*, 2003, **21**,

- 1192-1199.
58. J. M. Thomas, B. Chakraborty, D. Sen and H.-Z. Yu, *J. Am. Chem. Soc.*, 2012, **134**, 13823-13833.
59. J. Peng, L.-N. Feng, Z.-J. Ren, L.-P. Jiang and J.-J. Zhu, *Small*, 2011, **7**, 2921-2928.
60. Z.-H. Yang, Y. Zhuo, Y.-Q. Chai and R. Yuan, *Sci. Rep.*, 2014, **4**, 4747.
61. H.-W. Yang, C.-W. Lin, M.-Y. Hua, S.-S. Liao, Y.-T. Chen, H.-C. Chen, W.-H. Weng, C.-K. Chuang, S.-T. Pang and C.-C. M. Ma, *Adv. Mater.*, 2014, **26**, 3662-3666.
62. G. Lai, J. Wu, H. Ju and F. Yan, *Adv. Funct. Mater.*, 2011, **21**, 2938-2943.
63. B. S. Munge, A. L. Coffey, J. M. Doucette, B. K. Somba, R. Malhotra, V. Patel, J. S. Gutkind and J. F. Rusling, *Angew. Chem. Int. Ed.*, 2011, **50**, 7915-7918.
64. E. Prats-Alfonso, X. Sisqueira, N. Zine, G. Gabriel, A. Guimera, F. Javier del Campo, R. Villa, A. H. Eisenberg, M. Mrksich, A. Errachid, J. Aguilo and F. Albericio, *Small*, 2012, **8**, 2106-2115.
65. F.-N. Xiao, M. Wang, F.-B. Wang and X.-H. Xia, *Small*, 2014, **10**, 706-716.
66. S. Myung, A. Solanki, C. Kim, J. Park, K. S. Kim and K.-B. Lee, *Adv. Mater.*, 2011, **23**, 2221-2225.
67. L. Wang, Y. Wang, J. I. Wong, T. Palacios, J. Kong and H. Y. Yang, *Small*, 2014, **10**, 1101-1105.
68. A. de la Escosura-Muniz and A. Merkoci, *Small*, 2011, **7**, 675-682.
69. S. Wang, F. Haque, P. G. Rychahou, B. M. Evers and P. Guo, *ACS Nano*, 2013, **7**, 9814-9822.
70. J. S. Daniels and N. Pourmand, *Electroanalysis*, 2007, **19**, 1239-1257.
71. F. Lisdat and D. Schäfer, *Anal. Bioanal. Chem.*, 2008, **391**, 1555-1567.
72. B.-Y. Chang and S.-M. Park, *Ann. Rev. Anal. Chem.*, 2010, **3**, 207-229.
73. R. Singh and I. I. Suni, *J. Electrochem. Soc.*, 2010, **157**, J334-J337.
74. L. Feng, L. Wu, J. Wang, J. Ren, D. Miyoshi, N. Sugimoto and X. Qu, *Adv. Mater.*, 2012, **24**, 125-131.
75. C. J. Sherr, *Science*, 1996, **274**, 1672-1677.
76. M. Pagano, R. Pepperkok, F. Verde, W. Ansorge and G. Draetta, *Embo J.*, 1992, **11**, 961-971.
77. K. Handa, M. Yamakawa, H. Takeda, S. Kimura and T. Takahashi, *Int. J. Cancer*, 1999, **84**, 225-233.
78. P. Paterlini, A. M. Suberville, F. Zindy, J. Melle, M. Sonnier, J. P. Marie, F. Dreyfus and C. Bréchet, *Cancer Res.*, 1993, **53**, 235-238.
79. J. Mrena, J. P. Wiksten, A. Kokkola, S. Nordling, C. Haglund and A. Ristimäki, *Int. J. Cancer*, 2006, **119**, 1897-1901.
80. M. Lotayef, G. D. Wilson, F. M. Daley, H. K. Awwad and T. Shouman, *Brit. J. Cancer*, 2000, **83**, 30-34.
81. N. Canela, M. Orzaez, R. Fucho, F. Mateo, R. Gutierrez, A. Pineda-Lucena, O. Bachs and E. Perez-Paya, *J. Biol. Chem.*, 2006, **281**, 35942-35953.
82. X. Wang, L. Wu, J. Ren, D. Miyoshi, N. Sugimoto and X. Qu, *Biosens. Bioelectron.*, 2011, **26**, 4804-4809.
83. G. P. Smith, *Science*, 1985, **228**, 1315-1317.
84. J. W. Kehoe and B. K. Kay, *Chem. Rev.*, 2005, **105**, 4056-4072.
85. M. M. Richter, *Chem. Rev.*, 2004, **104**, 3003-3036.
86. W. Miao, *Chem. Rev.*, 2008, **108**, 2506-2553.
87. L. Wu, J. Wang, M. Yin, J. Ren, D. Miyoshi, N. Sugimoto and X. Qu, *Small*, 2013, **10**, 330-336.
88. M.-S. Wu, D.-J. Yuan, J.-J. Xu and H.-Y. Chen, *Chem. Sci.*, 2013, **4**, 1182-1188.
89. B. L. Allen, P. D. Kichambare and A. Star, *Adv. Mater.*, 2007, **19**, 1439-1451.
90. D. R. Kauffman and A. Star, *Chem. Soc. Rev.*, 2008, **37**, 1197-1206.
91. M. B. Lerner, J. D'Souza, T. Pazina, J. Dailey, B. R. Goldsmith, M. K. Robinson and A. T. C. Johnson, *ACS Nano*, 2012, **6**, 5143-5149.
92. H.-K. Chang, F. N. Ishikawa, R. Zhang, R. Datar, R. J. Cote, M. E. Thompson and C. Zhou, *ACS Nano*, 2011, **5**, 9883-9891.
93. B. S. Ferguson, S. F. Buchsbaum, T.-T. Wu, K. Hsieh, Y. Xiao, R. Sun and H. T. Soh, *J. Am. Chem. Soc.*, 2011, **133**, 9129-9135.
94. L. Y. Yeo, H.-C. Chang, P. P. Y. Chan and J. R. Friend, *Small*, 2011, **7**, 12-48.
95. S. Choi, M. Goryll, L. Sin, P. Wong and J. Chae, *Microfluid. Nanofluid.*, 2011, **10**, 231-247.
96. A. M. Foudeh, T. Fatanat Didar, T. Veres and M. Tabrizian, *Lab Chip*, 2012, **12**, 3249-3266.
97. E. Stern, A. Vacic, N. K. Rajan, J. M. Criscione, J. Park, B. R. Ilic, D. J. Mooney, M. A. Reed and T. M. Fahmy, *Nat. Nanotechnol.*, 2010, **5**, 138-142.
98. J. Mok, M. N. Mindrinos, R. W. Davis and M. Javanmard, *Proc. Natl. Acad. Sci. USA*, 2014, **111**, 2110-2115.
99. L. Gervais, N. de Rooij and E. Delamar, *Adv. Mater.*, 2011, **23**, H151-H176.
100. J. Sun, Y. Xianyu and X. Jiang, *Chem. Soc. Rev.*, 2014.
101. A. K. Yetisen, M. S. Akram and C. R. Lowe, *Lab Chip*, 2013, **13**, 2210-2251.
102. C. Parolo and A. Merkoci, *Chem. Soc. Rev.*, 2013, **42**, 450-457.
103. L. Ge, J. Yan, X. Song, M. Yan, S. Ge and J. Yu, *Biomaterials*, 2012, **33**, 1024-1031.
104. X. Wang, C. Wang, K. Qu, Y. Song, J. Ren, D. Miyoshi, N. Sugimoto and X. Qu, *Adv. Funct. Mater.*, 2010, **20**, 3967-3971.
105. J.-L. Chabard, C. Krishnamurthy, W. Yi, D. F. Smith and L. C. Hsieh-Wilson, *J. Am. Chem. Soc.*, 2012, **134**, 4489-4492.
106. P. D. Howes, S. Rana and M. M. Stevens, *Chem. Soc. Rev.*, 2014, **43**, 3835-3853.
107. B. Zhao, J. Yan, D. Wang, Z. Ge, S. He, D. He, S. Song and C. Fan, *Small*, 2013, **9**, 2595-2601.
108. G. Tavoosidana, G. Ronquist, S. Darmanis, J. Yan, L. Carlsson, D. Wu, T. Conze, P. Ek, A. Semjonow, E. Eltze, A. Larsson, U. D. Landegren and M. Kamali-Moghaddam, *Proc. Natl. Acad. Sci. USA*, 2011, **108**, 8809-8814.
109. S. Fredriksson, M. Gullberg, J. Jarvius, C. Olsson, K. Pietras, S. M. Gustafsdottir, A. Ostman and U. Landegren, *Nat. Biotechnol.*, 2002, **20**, 473-477.
110. A. Csordas, A. E. Gerdon, J. D. Adams, J. Qian, S. S. Oh, Y. Xiao and H. T. Soh, *Angew. Chem. Int. Ed.*, 2010, **49**, 355-358.
111. T. Konry, I. Smolina, J. M. Yarmush, D. Irimia and M. L. Yarmush, *Small*, 2011, **7**, 395-400.
112. C. Shad Thaxton, R. Elghanian, A. D. Thomas, S. I. Stoeva, J.-S. Lee, N. D. Smith, A. J. Schaeffer, H. Klocker, W. Horninger, G. Bartsch and C. A. Mirkin, *Proc. Natl. Acad. Sci. USA*, 2009, **106**, 18437-18442.
113. J.-M. Nam, C. S. Thaxton and C. A. Mirkin, *Science*, 2003, **301**, 1884-1886.
114. D. G. Georganopoulou, L. Chang, J.-M. Nam, C. S. Thaxton, E. J. Mufson, W. L. Klein and C. A. Mirkin, *Proc. Natl. Acad. Sci. USA*, 2005, **102**, 2273-2276.
115. D. Geissler, S. Stuffer, H.-G. Loehmannsroeben and N. Hildebrandt, *J. Am. Chem. Soc.*, 2013, **135**, 1102-1109.

116. T. Y. Rakovich, O. K. Mahfoud, B. M. Mohamed, A. Prina-Mello, K. Crosbie-Staunton, T. Van den Broeck, L. De Kimpe, A. Sukhanova, D. Baty, A. Rakovich, S. A. Maier, P. F. Alves, F. Nauwelaers, I. Nabiev, P. Chames and Y. Volkov, *ACS Nano*, 2014, **8**, 5682-5695.
117. M. P. Hwang, J.-W. Lee, K. E. Lee and K. H. Lee, *ACS Nano*, 2013, **7**, 8167-8174.
118. B.-Y. Wu, H.-F. Wang, J.-T. Chen and X.-P. Yan, *J. Am. Chem. Soc.*, 2011, **133**, 686-688.
119. J. Park, Y. Park and S. Kim, *ACS Nano*, 2013, **7**, 9416-9427.
120. H. Shi, J. Liu, J. Geng, B. Z. Tang and B. Liu, *J. Am. Chem. Soc.*, 2012, **134**, 9569-9572.
121. J. Homola, *Chem. Rev.*, 2008, **108**, 462-493.
122. E. Hutter and J. H. Fendler, *Adv. Mater.*, 2004, **16**, 1685-1706.
123. C. Cao, J. Zhang, X. Wen, S. L. Dodson, D. Nguyen Thuan, L. M. Wong, S. Wang, S. Li, P. Anh Tuan and Q. Xiong, *ACS Nano*, 2013, **7**, 7583-7591.
124. V. R. Dantham, S. Holler, C. Barbre, D. Keng, V. Kolchenko and S. Arnold, *Nano Lett.*, 2013, **13**, 3347-3351.
125. H. Cho, E.-C. Yeh, R. Sinha, T. A. Laurence, J. P. Bearinger and L. P. Lee, *ACS Nano*, 2012, **6**, 7607-7614.
126. S. M. Tabakman, L. Lau, J. T. Robinson, J. Price, S. P. Sherlock, H. Wang, B. Zhang, Z. Chen, S. Tangsombatvisit, J. A. Jarrell, P. J. Utz and H. Dai, *Nat. Commun.*, 2011, **2**, 466.
127. R. J. Simpson, J. W. E. Lim, R. L. Moritz and S. Mathivanan, *Expert Rev. Proteomic.*, 2009, **6**, 267-283.
128. D. D. Taylor and C. Gerceel-Taylor, *Gynecol. Oncol.*, 2008, **110**, 13-21.
129. J. Nilsson, J. Skog, A. Nordstrand, V. Baranov, L. Mincheva-Nilsson, X. O. Breakefield and A. Widmark, *Brit. J. Cancer*, 2009, **100**, 1603-1607.
130. H. Im, H. Shao, Y. I. Park, V. M. Peterson, C. M. Castro, R. Weissleder and H. Lee, *Nat. Biotechnol.*, 2014, **32**, 490-495.
131. X. Wu, L. Xu, L. Liu, W. Ma, H. Yin, H. Kuang, L. Wang, C. Xu and N. A. Kotov, *J. Am. Chem. Soc.*, 2013, **135**, 18629-18636.
132. A. H. Zhang, H. Sun, P. Wang, Y. Han and X. J. Wang, *Analyst*, 2012, **137**, 293-300.
133. T. V. Pham, S. R. Piersma, G. Oudgenoeg and C. R. Jimenez, *Expert Rev. Mol. Diagn.*, 2012, **12**, 343-359.
134. C. Simó, C. Ibáñez, Á. Gómez-Martínez, J. A. Ferragut and A. Cifuentes, *Electrophoresis* 2011, **32**, 1765-1777.
135. J. Peng, Y.-T. Chen, C.-L. Chen and L. Li, *Anal. Chem.*, 2014, **86**, 6540-6547.
136. T. Shi, T. L. Fillmore, X. Sun, R. Zhao, A. A. Schepmoes, M. Hossain, F. Xie, S. Wu, J.-S. Kim, N. Jones, R. J. Moore, L. Pasa-Tolic, J. Kagan, K. D. Rodland, T. Liu, K. Tang, D. G. Camp, II, R. D. Smith and W.-J. Qian, *Proc. Natl. Acad. Sci. USA*, 2012, **109**, 15395-15400.
137. J. Tan, W.-J. Zhao, J.-K. Yu, S. Ma, M. J. Sailor and J.-M. Wu, *Adv. Healthcare Mater.*, 2012, **1**, 742-750.
138. R. S. Gaster, L. Xu, S.-J. Han, R. J. Wilson, D. A. Hall, S. J. Osterfeld, H. Yu and S. X. Wang, *Nat. Nanotechnol.*, 2011, **6**, 314-320.
139. J. Joo, D. Kwon, C. Yim and S. Jeon, *ACS Nano*, 2012, **6**, 4375-4381.
140. I. K. Kwon, M. S. Song, S. H. Won, S. P. Choi, M. Kim and S. J. Sim, *Small*, 2012, **8**, 209-213.
141. A. Ranzoni, G. Sabatte, L. J. van Ijzendoorn and M. W. J. Prins, *ACS Nano*, 2012, **6**, 3134-3141.
142. E. H. Blackburn, *Nature*, 1991, **350**, 569-573.
143. N. Kim, M. Piatyszek, K. Prowse, C. Harley, M. West, P. Ho, G. Coviello, W. Wright, S. Weinrich and J. Shay, *Science*, 1994, **266**, 2011-2015.
144. J. W. Shay and S. Bacchetti, *Eur. J. Cancer*, 1997, **33**, 787-791.
145. Y. Hirano, K. Fujita, K. Suzuki, T. Ushiyama, Y. Ohtawara and F. Tsuda, *Cancer*, 1998, **83**, 772-776.
146. K.-i. Yoshida, S.-i. Sakamoto, S. Sumi, Y. Higashi and S. Kitahara, *Cancer*, 1998, **83**, 760-766.
147. X. Zhou and D. Xing, *Chem. Soc. Rev.*, 2012, **41**, 4643-4656.
148. A. De Cian, G. Cristofari, P. Reichenbach, E. De Lemos, D. Monchaud, M.-P. Teulade-Fichou, K. Shin-ya, L. Lacroix, J. Lingner and J.-L. Mergny, *Proc. Natl. Acad. Sci. USA*, 2007, **104**, 17347-17352.
149. G. Krupp, K. Kühne, S. Tamm, W. Klapper, K. Heidorn, A. Rott and R. Parwaresch, *Nucleic Acids Res.*, 1997, **25**, 919-921.
150. E. Sharon, E. Golub, A. Niazov-Elkan, D. Balogh and I. Willner, *Anal. Chem.*, 2014, **86**, 3153-3158.
151. H.-R. Zhang, M.-S. Wu, J.-J. Xu and H.-Y. Chen, *Anal. Chem.*, 2014, **86**, 3834-3840.
152. Z. Yi, H.-B. Wang, K. Chen, Q. Gao, H. Tang, R.-Q. Yu and X. Chu, *Biosens. Bioelectron.*, 2014, **53**, 310-315.
153. J. Liu, C.-Y. Lu, H. Zhou, J.-J. Xu, Z. Wang and H.-Y. Chen, *Chem. Commun.*, 2013, **49**, 6602-6604.
154. Z. Zhang, E. Sharon, R. Freeman, X. Liu and I. Willner, *Anal. Chem.*, 2012, **84**, 4789-4797.
155. B. H. Chung, J. Jung, Q. H. Quach and H. Kim, *Chem. Commun.*, 2013, **49**, 6596-6598.
156. H. Wang, S. Wu, X. Chu and R.-q. Yu, *Chem. Commun.*, 2012, **48**, 5916-5918.
157. Y. Zhang, L.-j. Wang and C.-y. Zhang, *Chem. Commun.*, 2013, **50**, 1909-1911.
158. H. Wang, M. J. Donovan, L. Meng, Z. Zhao, Y. Kim, M. Ye and W. Tan, *Chem. Eur. J.*, 2013, **19**, 4633-4639.
159. K. Woo Kim, Y. Shin, A. Promoda Perera, Q. Liu, J. Sheng Kee, K. Han, Y.-J. Yoon and M. Kyoung Park, *Biosens. Bioelectron.*, 2013, **45**, 152-157.
160. X. Zhu, H. Xu, R. Lin, G. Yang, Z. Lin and G. Chen, *Chem. Commun.*, 2014, **50**, 7897-7899.
161. H. Hwang, P. Opreko and S. Myong, *Sci. Rep.*, 2014, **4**, 6391.
162. L. Tian and Y. Weizmann, *J. Am. Chem. Soc.*, 2013, **135**, 1661-1664.
163. L. Tian, T. Cronin and Y. Weizmann, *Chem. Sci.*, 2014, **5**, 4153-4162.
164. J. Wang, L. Wu, J. Ren and X. Qu, *Nanoscale*, 2013, **6**, 1661-1666.
165. S. Zong, Z. Wang, H. Chen and Y. Cui, *Small*, 2013, **9**, 4215-4220.
166. J. Lei and H. Ju, *Chem. Soc. Rev.*, 2012, **41**, 2122-2134.
167. L. Wu, J. Wang, L. Feng, J. Ren, W. Wei and X. Qu, *Adv. Mater.*, 2012, **24**, 2447-2452.
168. L. Wu, J. Wang, H. Sun, J. Ren and X. Qu, *Adv. Healthcare Mater.*, 2013, **3**, 588-595.
169. L. Wu, J. Wang, J. Ren and X. Qu, *Adv. Funct. Mater.*, 2014, **24**, 2727-2733.
170. Z. Zhang, L. Wu, J. Wang, J. Ren and X. Qu, *Chem. Commun.*, 2013, **49**, 9986-9988.
171. J. Wang, *Biosens. Bioelectron.*, 2006, **21**, 1887-1892.
172. D. Grieshaber, R. MacKenzie, J. Voerres and E. Reimhult, *Sensors*, 2008, **8**, 1400-1458.
173. D. Chen, L. Tang and J. Li, *Chem. Soc. Rev.*, 2010, **39**, 3157-3180.
174. M. Pumera, *Chem. Soc. Rev.*, 2010, **39**, 4146-4157.
175. Y. Liu, X. Dong and P. Chen, *Chem. Soc. Rev.*, 2012, **41**, 2283-2307.
176. C. G. Pheaney, L. F. Guerra and J. K. Barton, *Proc. Natl. Acad. Sci. USA*,

- 2012, **109**, 11528-11533.
177. C. Zhao, L. Wu, J. Ren and X. Qu, *Chem. Commun.*, 2011, **47**, 5461-5463.
178. S. C. P. Williams, *Proc. Natl. Acad. Sci. USA*, 2013, **110**, 4861.
179. C. Alix-Panabières and K. Pantel, *Clin. Chem.*, 2013, **59**, 110-118.
180. R. Qian, L. Ding, L. Yan, M. Lin and H. Ju, *Anal. Chem.*, 2014, **86**, 8642-8648.
181. R. Qian, L. Ding and H. Ju, *J. Am. Chem. Soc.*, 2013, **135**, 13282-13285.
182. R. Qian, L. Ding, L. Yan, M. Lin and H. Ju, *J. Am. Chem. Soc.*, 2014, **136**, 8205-8208.
183. S. Tyagi and F. R. Kramer, *Nat. Biotechnol.*, 1996, **14**, 303-308.
184. M. J. Duffy, *Clin. Cancer Res.*, 1996, **2**, 613-618.
185. M. Stefanini, *Cancer*, 1985, **55**, 1931-1936.
186. H. Zhang, J. Fan, J. Wang, S. Zhang, B. Dou and X. Peng, *J. Am. Chem. Soc.*, 2013, **135**, 11663-11669.
187. P. C. A. Kam and A. U. L. See, *Anaesthesia*, 2000, **55**, 442-449.
188. D. L. Simmons, R. M. Botting and T. Hla, *Pharmacol. Rev.*, 2004, **56**, 387-437.
189. M. Katori and M. Majima, *Inflamm. Res.*, 2000, **49**, 367-392.
190. H. Zhang, J. Fan, J. Wang, B. Dou, F. Zhou, J. Cao, J. Qu, Z. Cao, W. Zhao and X. Peng, *J. Am. Chem. Soc.*, 2013, **135**, 17469-17475.
191. W. C. Silvers, B. Prasai, D. H. Burk, M. L. Brown and R. L. McCarley, *J. Am. Chem. Soc.*, 2013, **135**, 309-314.
192. J. Zhang, A. Shibata, M. Ito, S. Shuto, Y. Ito, B. Mannervik, H. Abe and R. Morgenstern, *J. Am. Chem. Soc.*, 2011, **133**, 14109-14119.
193. L. E. Edgington, M. Verdoes, A. Ortega, N. P. Withana, J. Lee, S. Syed, M. H. Bachmann, G. Blum and M. Bogoyo, *J. Am. Chem. Soc.*, 2013, **135**, 174-182.
194. Y.-J. Chen, S.-C. Wu, C.-Y. Chen, S.-C. Tzou, T.-L. Cheng, Y.-F. Huang, S.-S. Yuan and Y.-M. Wang, *Biomaterials*, 2014, **35**, 304-315.
195. Y. Wang, Y. Jiang, M. Zhang, J. Tan, J. Liang, H. Wang, Y. Li, H. He, V. C. Yang and Y. Huang, *Adv. Funct. Mater.*, 2014, **24**, 5443-5453.
196. S. B. Lowe, J. A. G. Dick, B. E. Cohen and M. M. Stevens, *ACS Nano*, 2011, **6**, 851-857.
197. J. Park, J. Yang, E.-K. Lim, E. Kim, J. Choi, J. K. Ryu, N. H. Kim, J.-S. Suh, J. I. Yook, Y.-M. Huh and S. Haam, *Angew. Chem. Int. Ed.*, 2012, **51**, 945-948.
198. M. Fischbach, U. Resch-Genger and O. Seitz, *Angew. Chem. Int. Ed.*, 2014, **53**, 11955-11959.
199. S.-Y. Kwak, J.-K. Yang, S.-J. Jeon, H.-I. Kim, J. Yim, H. Kang, S. Kyeong, Y.-S. Lee and J.-H. Kim, *Adv. Funct. Mater.*, 2014, **24**, 5119-5128.
200. Z. Yue, P. Lv, H. Yue, Y. Gao, D. Ma, W. Wei and G.-H. Ma, *Chem. Commun.*, 2013, **49**, 3902-3904.
201. G. Lee, K. Eom, J. Park, J. Yang, S. Haam, Y.-M. Huh, J. K. Ryu, N. H. Kim, J. I. Yook, S. W. Lee, D. S. Yoon and T. Kwon, *Angew. Chem. Int. Ed.*, 2012, **51**, 5837-5841.
202. C. Sun, K.-H. Su, J. Valentine, Y. T. Rosa-Bauza, J. A. Ellman, O. Elboudwarej, B. Mukherjee, C. S. Craik, M. A. Shuman, F. F. Chen and X. Zhang, *ACS Nano*, 2010, **4**, 978-984.
203. A. D. Warren, S. T. Gaylord, K. C. Ngan, M. Dumont Milutinovic, G. A. Kwong, S. N. Bhatia and D. R. Walt, *J. Am. Chem. Soc.*, 2014, **136**, 13709-13714.
204. A. D. Warren, G. A. Kwong, D. K. Wood, K. Y. Lin and S. N. Bhatia, *Proc. Natl. Acad. Sci. USA*, 2014, **111**, 3671-3676.
205. G. A. Kwong, G. von Maltzahn, G. Murugappan, O. Abudayyeh, S. Mo, I. A. Papayannopoulos, D. Y. Sverdlov, S. B. Liu, A. D. Warren, Y. Popov, D. Schuppan and S. N. Bhatia, *Nat. Biotechnol.*, 2013, **31**, 63-70.
206. P. Anker, H. Mulcahy, X. Qi Chen and M. Stroun, *Cancer Metast. Rev.*, 1999, **18**, 65-73.
207. G. Sozzi, D. Conte, M. Leon, R. Cirincione, L. Roz, C. Ratcliffe, E. Roz, N. Cirenei, M. Bellomi, G. Pelosi, M. A. Pierotti and U. Pastorino, *J. Clin. Oncol.*, 2003, **21**, 3902-3908.
208. G. Sozzi, D. Conte, L. Mariani, S. Lo Vullo, L. Roz, C. Lombardo, M. A. Pierotti and L. Tavecchio, *Cancer Res.*, 2001, **61**, 4675-4678.
209. F. Diehl, K. Schmidt, M. A. Choti, K. Romans, S. Goodman, M. Li, K. Thornton, N. Agrawal, L. Sokoll, S. A. Szabo, K. W. Kinzler, B. Vogelstein and L. A. Diaz, *Nat. Med.*, 2008, **14**, 985-990.
210. A. M. Newman, S. V. Bratman, J. To, J. F. Wynne, N. C. W. Eclow, L. A. Modlin, C. L. Liu, J. W. Neal, H. A. Wakelee, R. E. Merritt, J. B. Shrager, B. W. Loo, Jr., A. A. Alizadeh and M. Diehn, *Nat. Med.*, 2014, **20**, 548-554.
211. M. W. Schmitt, S. R. Kennedy, J. J. Salk, E. J. Fox, J. B. Hiatt and L. A. Loeb, *Proc. Natl. Acad. Sci. USA*, 2012, **109**, 14508-14513.
212. P. Martinez, N. McGranahan, N. J. Birkbak, M. Gerlinger and C. Swanton, *Sci. Rep.*, 2013, **3**, 3309.
213. R. Novak, Y. Zeng, J. Shuga, G. Venugopalan, D. A. Fletcher, M. T. Smith and R. A. Mathies, *Angew. Chem. Int. Ed.*, 2011, **50**, 390-395.
214. K. D. Robertson, *Oncogene*, 2001, **20**, 3139-3155.
215. P. M. Das and R. Singal, *J. Clin. Oncol.*, 2004, **22**, 4632-4642.
216. K. C. A. Chan, P. Jiang, C. W. M. Chan, K. Sun, J. Wong, E. P. Hui, S. L. Chan, W. C. Chan, D. S. C. Hui, S. S. M. Ng, H. L. Y. Chan, C. S. C. Wong, B. B. Y. Ma, A. T. C. Chan, P. B. S. Lai, H. Sun, R. W. K. Chiu and Y. M. D. Lo, *Proc. Natl. Acad. Sci. USA*, 2013, **110**, 18761-18768.
217. P. W. Laird and R. Jaenisch, *Hum. Mol. Genet.*, 1994, **3**, 1487-1495.
218. X. Duan, L. Liu, F. Feng and S. Wang, *Acc. Chem. Res.*, 2010, **43**, 260-270.
219. M. S. Fliss, H. Usadel, O. L. Cabellero, L. Wu, M. R. Buta, S. M. Eleff, J. Jen and D. Sidransky, *Science*, 2000, **287**, 2017-2019.
220. B. R. Cipriany, P. J. Murphy, J. A. Hagarman, A. Cerf, D. Latulippe, S. L. Levy, J. J. Benitez, C. P. Tan, J. Topolancik, P. D. Soloway and H. G. Craighead, *Proc. Natl. Acad. Sci. USA*, 2012, **109**, 8477-8482.
221. Q. Yang, Y. Dong, W. Wu, C. Zhu, H. Chong, J. Lu, D. Yu, L. Liu, F. Lv and S. Wang, *Nat. Commun.*, 2012, **3**, 1206.
222. J. Shim, G. I. Humphreys, B. M. Venkatesan, J. M. Munz, X. Zou, C. Sathe, K. Schulten, F. Kosari, A. M. Nardulli, G. Vasmatzis and R. Bashir, *Sci. Rep.*, 2013, **3**, 1389.
223. I. Kang, Y. Wang, C. Reagan, Y. Fu, M. X. Wang and L.-Q. Gu, *Sci. Rep.*, 2013, **3**, 2381.
224. A. H. Laszlo, I. M. Derrington, H. Brinkerhoff, K. W. Langford, I. C. Nova, J. M. Samson, J. J. Bartlett, M. Pavlenok and J. H. Gundlach, *Proc. Natl. Acad. Sci. USA*, 2013, **110**, 18904-18909.
225. N. B. Muren and J. K. Barton, *J. Am. Chem. Soc.*, 2013, **135**, 16632-16640.
226. N. Siddiqui and K. L. B. Borden, *Wiley Interdiscip. Rev.-RNA*, 2012, **3**, 13-25.
227. P. P. Pandolfi, *Oncogene*, 2004, **23**, 3134-3137.
228. A. Bhattacharjee, W. G. Richards, J. Staunton, C. Li, S. Monti, P. Vasa, C. Ladd, J. Beheshti, R. Bueno, M. Gillette, M. Loda, G. Weber, E. J. Mark, E. S. Lander, W. Wong, B. E. Johnson, T. R. Golub, D. J. Sugarbaker and M. Meyerson, *Proc. Natl. Acad. Sci. USA*, 2001, **98**, 13790-13795.
229. K. Cuschieri and N. Wentzensen, *Cancer Epidem. Biomar.*, 2008, **17**,

- 2536-2545.
230. Y. Li, D. Elashoff, M. Oh, U. Sinha, M. A. R. St John, X. F. Zhou, E. Abemayor and D. T. Wong, *J. Clin. Oncol.*, 2006, **24**, 1754-1760.
231. J. Lu, G. Getz, E. A. Miska, E. Alvarez-Saavedra, J. Lamb, D. Peck, A. Sweet-Cordero, B. L. Ebt, R. H. Mak, A. A. Ferrando, J. R. Downing, T. Jacks, H. R. Horvitz and T. R. Golub, *Nature*, 2005, **435**, 834-838.
232. T. A. Farazi, J. I. Spitzer, P. Morozov and T. Tuschl, *J. Pathol.*, 2011, **223**, 102-115.
233. J. C. Brase, M. Johannes, T. Schlomm, M. Falth, A. Haese, T. Steuber, T. Beissbarth, R. Kuner and H. Sultmann, *Int. J. Cancer*, 2011, **128**, 608-616.
234. M. Boeri, C. Verri, D. Conte, L. Roz, P. Modena, F. Facchinetti, E. Calabro, C. M. Croce, U. Pastorino and G. Sozzi, *Proc. Natl. Acad. Sci. USA*, 2011, **108**, 3713-3718.
235. H. Zhao, J. Shen, L. Medico, D. Wang, C. B. Ambrosone and S. Liu, *PLoS One*, 2010, **5**, 12.
236. J. Li, S. Tan, R. Kooger, C. Zhang and Y. Zhang, *Chem. Soc. Rev.*, 2013, **43**, 506-517.
237. Z. Williams, I. Z. Ben-Dov, R. Elias, A. Mihailovic, M. Brown, Z. Rosenwaks and T. Tuschl, *Proc. Natl. Acad. Sci. USA*, 2013, **110**, 4255-4260.
238. J. Takamizawa, H. Konishi, K. Yanagisawa, S. Tomida, H. Osada, H. Endoh, T. Harano, Y. Yatabe, M. Nagino, Y. Nimura, T. Mitsudomi and T. Takahashi, *Cancer Res.*, 2004, **64**, 3753-3756.
239. G. Garcia-Schwarz, A. Rogacs, S. S. Bahga and J. G. Santiago, *J. Visualized Exp.*, 2012, **61**, e3890.
240. M. V. Iorio and C. M. Croce, *EMBO Mol. Med.*, 2012, **4**, 143-159.
241. D. W. Wegman and S. N. Krylov, *Angew. Chem. Int. Ed.*, 2011, **50**, 10335-10339.
242. L.-Q. Gu, M. Wanunu, M. X. Wang, L. McReynolds and Y. Wang, *Expert Rev. Mol. Diagn.*, 2012, **12**, 573-584.
243. S. Howorka, S. Cheley and H. Bayley, *Nat. Biotechnol.*, 2001, **19**, 636-639.
244. M. Wanunu, T. Dadosh, V. Ray, J. Jin, L. McReynolds and M. Drndic, *Nat. Nanotechnol.*, 2010, **5**, 807-814.
245. Y. Wang, D. Zheng, Q. Tan, M. X. Wang and L.-Q. Gu, *Nat. Nanotechnol.*, 2011, **6**, 668-674.
246. K. Tian, Z. He, Y. Wang, S.-J. Chen and L.-Q. Gu, *ACS Nano*, 2013, **7**, 3962-3969.
247. D. Silhavy, A. Molnar, A. Luciolli, G. Szittyta, C. Hornyik, M. Tavazza and J. Burgyan, *Embo J.*, 2002, **21**, 3070-3080.
248. S. Campuzano, R. M. Torrente-Rodríguez, E. López-Hernández, F. Conzuelo, R. Granados, J. M. Sánchez-Puelles and J. M. Pingarrón, *Angew. Chem. Int. Ed.*, 2014, **53**, 6168-6171.
249. E. Vasilyeva, B. Lam, Z. Fang, M. D. Minden, E. H. Sargent and S. O. Kelley, *Angew. Chem. Int. Ed.*, 2011, **50**, 4137-4141.
250. Y. Wen, H. Pei, Y. Shen, J. Xi, M. Lin, N. Lu, X. Shen, J. Li and C. Fan, *Sci. Rep.*, 2012, **2**, 867.
251. A. Markou, E. G. Tsaroucha, L. Kaklamanis, M. Fotinou, V. Georgoulas and E. S. Lianidou, *Clin. Chem.*, 2008, **54**, 1696-1704.
252. T. Mishima, Y. Mizuguchi, Y. Kawahigashi, T. Takizawa and T. Takizawa, *Brain Res.*, 2007, **1131**, 37-43.
253. B.-C. Yin, Y.-Q. Liu and B.-C. Ye, *J. Am. Chem. Soc.*, 2012, **134**, 5064-5067.
254. D. A. Shagin, D. V. Rebrikov, V. B. Kozhemyako, I. M. Altshuler, A. S. Sheglov, P. A. Zhulidov, E. A. Bogdanova, D. B. Staroverov, V. A. Rasskazov and S. Lukyanov, *Genome Res.*, 2002, **12**, 1935-1942.
255. R. Duan, X. Zuo, S. Wang, X. Quan, D. Chen, Z. Chen, L. Jiang, C. Fan and F. Xia, *J. Am. Chem. Soc.*, 2013, **135**, 4604-4607.
256. H. Dong, L. Ding, F. Yan, H. Ji and H. Ju, *Biomaterials*, 2011, **32**, 3875-3882.
257. N. Li, C. Chang, W. Pan and B. Tang, *Angew. Chem. Int. Ed.*, 2012, **51**, 7426-7430.
258. S.-R. Ryoo, J. Lee, J. Yeo, H.-K. Na, Y.-K. Kim, H. Jang, J. H. Lee, S. W. Han, Y. Lee, V. N. Kim and D.-H. Min, *ACS Nano*, 2013, **7**, 5882-5891.
259. L. Qiu, C. Wu, M. You, D. Han, T. Chen, G. Zhu, J. Jiang, R. Yu and W. Tan, *J. Am. Chem. Soc.*, 2013, **135**, 12952-12955.
260. S. Soundararajan, L. Wang, V. Sridharan, W. Chen, N. Courtenay-Luck, D. Jones, E. K. Spicer and D. J. Fernandes, *Mol. Pharmacol.*, 2009, **76**, 984-991.
261. P. Shah, A. Rørvig-Lund, S. B. Chaabane, P. W. Thulstrup, H. G. Kjaergaard, E. Fron, J. Hofkens, S. W. Yang and T. Vosch, *ACS Nano*, 2012, **6**, 8803-8814.
262. W. Wei, X. He and N. Ma, *Angew. Chem. Int. Ed.*, 2014, **53**, 5573-5577.
263. H. Dong, J. Lei, H. Ju, F. Zhi, H. Wang, W. Guo, Z. Zhu and F. Yan, *Angew. Chem. Int. Ed.*, 2012, **51**, 4607-4612.
264. E. Kim, J. Yang, J. Park, S. Kim, N. H. Kim, J. I. Yook, J.-S. Suh, S. Haam and Y.-M. Huh, *ACS Nano*, 2012, **6**, 8525-8535.
265. N. C. Seeman, *Nature*, 2003, **421**, 427-431.
266. Z. Ezziane, *Nanotechnology*, 2006, **17**, R27.
267. S. M. Douglas, I. Bachelet and G. M. Church, *Science*, 2012, **335**, 831-834.
268. M. Rudchenko, S. Taylor, P. Pallavi, A. Dechkovskaia, S. Khan, V. P. Butler Jr, S. Rudchenko and M. N. Stojanovic, *Nat. Nanotechnol.*, 2013, **8**, 580-586.
269. Z. Xie, L. Wroblewska, L. Prochazka, R. Weiss and B. Yaakov, *Science*, 2011, **333**, 1307-1311.
270. J. Hemphill and A. Deiters, *J. Am. Chem. Soc.*, 2013, **135**, 10512-10518.
271. H. Haick, Y. Y. Broza, P. Mochalski, V. Ruzsanyi and A. Amann, *Chem. Soc. Rev.*, 2014, **43**, 1423-1449.
272. G. Konvalina and H. Haick, *Acc. Chem. Res.*, 2014, **47**, 66-76.
273. G. Peng, U. Tisch, O. Adams, M. Hakim, N. Shehata, Y. Y. Broza, S. Billan, R. Abdah-Bortnyak, A. Kuten and H. Haick, *Nat. Nanotechnol.*, 2009, **4**, 669-673.
274. Y. Zilberman, U. Tisch, G. Shuster, W. Pisula, X. Feng, K. Muellen and H. Hoick, *Adv. Mater.*, 2010, **22**, 4317-4320.
275. J. H. Lim, J. Park, E. H. Oh, H. J. Ko, S. Hong and T. H. Park, *Adv. Healthcare Mater.*, 2014, **3**, 360-366.
276. E. Biavardi, C. Tudisco, F. Maffei, A. Motta, C. Massera, G. G. Condorelli and E. Dalcanale, *Proc. Natl. Acad. Sci. USA*, 2012, **109**, 2263-2268.
277. M. Ikeda, T. Yoshii, T. Matsui, T. Tanida, H. Komatsu and I. Hamachi, *J. Am. Chem. Soc.*, 2011, **133**, 1670-1673.
278. V. Plaks, C. D. Koopman and Z. Werb, *Science*, 2013, **341**, 1186-1188.
279. D. L. Adams, S. S. Martin, R. K. Alpaugh, M. Charpentier, S. Tsai, R. C. Bergan, I. M. Ogden, W. Catalona, S. Chumsri, C.-M. Tang and M. Cristofanilli, *Proc. Natl. Acad. Sci. USA*, 2014, **111**, 3514-3519.
280. S. A. Joosse and K. Pantel, *Cancer Res.*, 2013, **73**, 8-11.
281. J. C. Fischer, D. Niederacher, S. A. Topp, E. Honisch, S. Schumacher, N. Schmitz, L. Z. Foehrding, C. Vay, I. Hoffmann, N. S. Kasprovicz, P. G. Hepp, S. Mohrmann, U. Nitz, A. Stresemann, T. Krahn, T. Henze, E. Griebisch, K. Raba, J. M. Rox, F. Wenzel, C. Sproll, W. Janni, T. Fehm,

- C. A. Klein, W. T. Knoefel and N. H. Stoecklein, *Proc. Natl. Acad. Sci. USA*, 2013, **110**, 16580-16585.
282. C.-Y. Wen, L.-L. Wu, Z.-L. Zhang, Y.-L. Liu, S.-Z. Wei, J. Hu, M. Tang, E.-Z. Sun, Y.-P. Gong, J. Yu and D.-W. Pang, *ACS Nano*, 2014, **8**, 941-949.
283. E.-Q. Song, J. Hu, C.-Y. Wen, Z.-Q. Tian, X. Yu, Z.-L. Zhang, Y.-B. Shi and D.-W. Pang, *ACS Nano*, 2011, **5**, 761-770.
284. Y. Mi, K. Li, Y. Liu, K.-Y. Pu, B. Liu and S.-S. Feng, *Biomaterials*, 2011, **32**, 8226-8233.
285. X. Hu, C.-W. Wei, J. Xia, I. Pelivanov, M. O'Donnell and X. Gao, *Small*, 2013, **9**, 2046-2052.
286. J. Meng, H. Liu, X. Liu, G. Yang, P. Zhang, S. Wang and L. Jiang, *Small*, 2014, **10**, 3735-3741.
287. X. Liu and S. Wang, *Chem. Soc. Rev.*, 2014, **43**, 2385-2401.
288. G.-S. Park, H. Kwon, D. W. Kwak, S. Y. Park, M. Kim, J.-H. Lee, H. Han, S. Heo, X. S. Li, J. H. Lee, Y. H. Kim, J.-G. Lee, W. Yang, H. Y. Cho, S. K. Kim and K. Kim, *Nano Lett.*, 2012, **12**, 1638-1642.
289. N. Zhang, Y. Deng, Q. Tai, B. Cheng, L. Zhao, Q. Shen, R. He, L. Hong, W. Liu, S. Guo, K. Liu, H.-R. Tseng, B. Xiong and X.-Z. Zhao, *Adv. Mater.*, 2012, **24**, 2756-2760.
290. S. Wang, H. Wang, J. Jiao, K.-J. Chen, G. E. Owens, K.-i. Kamei, J. Sun, D. J. Sherman, C. P. Behrenbruch, H. Wu and H.-R. Tseng, *Angew. Chem. Int. Ed.*, 2009, **48**, 8970-8973.
291. S. Wang, K. Liu, J. Liu, Z. T. F. Yu, X. Xu, L. Zhao, T. Lee, E. K. Lee, J. Reiss, Y.-K. Lee, L. W. K. Chung, J. Huang, M. Rettig, D. Seligson, K. N. Duraiswamy, C. K. F. Shen and H.-R. Tseng, *Angew. Chem. Int. Ed.*, 2011, **50**, 3084-3088.
292. J. Sekine, S.-C. Luo, S. Wang, B. Zhu, H.-R. Tseng and H.-h. Yu, *Adv. Mater.*, 2011, **23**, 4788-4792.
293. P. T. Went, A. Lugli, S. Meier, M. Bundi, M. Mirlacher, G. Sauter and S. Dirnhofer, *Hum. Pathol.*, 2004, **35**, 122-128.
294. S.-K. Lee, G.-S. Kim, Y. Wu, D.-J. Kim, Y. Lu, M. Kwak, L. Han, J.-H. Hyung, J.-K. Seol, C. Sander, A. Gonzalez, J. Li and R. Fan, *Nano Lett.*, 2012, **12**, 2697-2704.
295. X. Liu, L. Chen, H. Liu, G. Yang, P. Zhang, D. Han, S. Wang and L. Jiang, *NPG Asia Mater.*, 2013, **5**, e63.
296. H. J. Yoon, T. H. Kim, Z. Zhang, E. Azizi, T. M. Pham, C. Paoletti, J. Lin, N. Rammath, M. S. Wicha, D. F. Hayes, D. M. Simeone and S. Nagrath, *Nat. Nanotechnol.*, 2013, **8**, 735-741.
297. C.-H. Wu, Y.-Y. Huang, P. Chen, K. Hoshino, H. Liu, E. P. Frenkel, J. X. J. Zhang and K. V. Sokolov, *ACS Nano*, 2013, **7**, 8816-8823.
298. W. Zhao, C. H. Cui, S. Bose, D. Guo, C. Shen, W. P. Wong, K. Halvorsen, O. C. Farokhzad, G. S. L. Teo, J. A. Phillips, D. M. Dorfman, R. Karnik and J. M. Karp, *Proc. Natl. Acad. Sci. USA*, 2012, **109**, 19626-19631.
299. W. Sheng, T. Chen, W. Tan and Z. H. Fan, *ACS Nano*, 2013, **7**, 7067-7076.
300. W. Chen, S. Weng, F. Zhang, S. Allen, X. Li, L. Bao, R. H. W. Lam, J. A. Macoska, S. D. Merajver and J. Fu, *ACS Nano*, 2012, **7**, 566-575.
301. S. Hou, H. Zhao, L. Zhao, Q. Shen, K. S. Wei, D. Y. Suh, A. Nakao, M. A. Garcia, M. Song, T. Lee, B. Xiong, S.-C. Luo, H.-R. Tseng and H.-h. Yu, *Adv. Mater.*, 2012, **25**, 1547-1551.
302. S. Jeon, J.-M. Moon, E. S. Lee, Y. H. Kim and Y. Cho, *Angew. Chem. Int. Ed.*, 2014, **53**, 4597-4602.
303. W. Y. Hong, S. H. Jeon, E. S. Lee and Y. Cho, *Biomaterials*, 2014, **35**, 9573-9580.
304. P. Zhang, L. Chen, T. Xu, H. Liu, X. Liu, J. Meng, G. Yang, L. Jiang and S. Wang, *Adv. Mater.*, 2013, **25**, 3566-3570.
305. Q. Shen, L. Xu, L. Zhao, D. Wu, Y. Fan, Y. Zhou, W.-H. OuYang, X. Xu, Z. Zhang, M. Song, T. Lee, M. A. Garcia, B. Xiong, S. Hou, H.-R. Tseng and X. Fang, *Adv. Mater.*, 2013, **25**, 2368-2373.
306. S. Li, N. Chen, Z. Zhang and Y. Wang, *Biomaterials*, 2013, **34**, 460-469.
307. S. Hou, L. Zhao, Q. Shen, J. Yu, C. Ng, X. Kong, D. Wu, M. Song, X. Shi, X. Xu, W.-H. OuYang, R. He, X.-Z. Zhao, T. Lee, F. C. Brunicaardi, M. A. Garcia, A. Ribas, R. S. Lo and H.-R. Tseng, *Angew. Chem. Int. Ed.*, 2013, **52**, 3379-3383.
308. L. Zhao, Y.-T. Lu, F. Li, K. Wu, S. Hou, J. Yu, Q. Shen, D. Wu, M. Song, W.-H. OuYang, Z. Luo, T. Lee, X. Fang, C. Shao, X. Xu, M. A. Garcia, L. W. K. Chung, M. Rettig, H.-R. Tseng and E. M. Posadas, *Adv. Mater.*, 2013, **25**, 2897-2902.
309. L. Feng, Y. Chen, J. Ren and X. Qu, *Biomaterials*, 2011, **32**, 2930-2937.
310. C. Martinez, S. Sanchez, W. Xi and O. G. Schmidt, *Nano Lett.*, 2014, **14**, 2219-2224.
311. X. Zhang, Y. Teng, Y. Fu, S. Zhang, T. Wang, C. Wang, L. Jin and W. Zhang, *Chem. Sci.*, 2011, **2**, 2353-2360.
312. L. Wu, J. Wang, J. Ren, W. Li and X. Qu, *Chem. Commun.*, 2013, **49**, 5675-5677.
313. Y. Wan, Y.-G. Zhou, M. Poudineh, T. S. Safaei, R. M. Mohamadi, E. H. Sargent and S. O. Kelley, *Angew. Chem. Int. Ed.*, 2014, **53**, 13145-13149.
314. M. Maltez-da Costa, A. de la Escosura-Muniz, C. Noguez, L. Barrios, E. Ibanez and A. Merckoci, *Nano Lett.*, 2012, **12**, 4164-4171.
315. T. Zheng, Q. Zhang, S. Feng, J.-J. Zhu, Q. Wang and H. Wang, *J. Am. Chem. Soc.*, 2014, **136**, 2288-2291.
316. Y. Song, K. Qu, C. Zhao, J. Ren and X. Qu, *Adv. Mater.*, 2010, **22**, 2206-2210.
317. Y. Song, Y. Chen, L. Feng, J. Ren and X. Qu, *Chem. Commun.*, 2011, **47**, 4436-4438.
318. Y. Tao, Y. Lin, Z. Huang, J. Ren and X. Qu, *Adv. Mater.*, 2013, **25**, 2594-2599.
319. K. Fan, C. Cao, Y. Pan, D. Lu, D. Yang, J. Feng, L. Song, M. Liang and X. Yan, *Nat. Nanotechnol.*, 2012, **7**, 459-464.
320. L. Gao, J. Zhuang, L. Nie, J. Zhang, Y. Zhang, N. Gu, T. Wang, J. Feng, D. Yang, S. Perrett and X. Yan, *Nat. Nanotechnol.*, 2007, **2**, 577-583.
321. S. S. Banerjee, A. Jalota-Badwar, S. D. Satavalekar, S. G. Bhansali, N. D. Aher, R. R. Mascarenhas, D. Paul, S. Sharma and J. J. Khandare, *Adv. Healthcare Mater.*, 2013, **2**, 800-805.
322. K. D. Wegner, S. Linden, Z. Jin, T. L. Jennings, R. el Khoulati, P. M. P. v. B. E. Henegouwen and N. Hildebrandt, *Small*, 2014, **10**, 734-740.
323. K.-T. Yong, H. Ding, I. Roy, W.-C. Law, E. J. Bergey, A. Maitra and P. N. Prasad, *ACS Nano*, 2009, **3**, 502-510.
324. K. Li, Y. Liu, K.-Y. Pu, S.-S. Feng, R. Zhan and B. Liu, *Adv. Funct. Mater.*, 2011, **21**, 287-294.
325. K. Li, D. Ding, D. Huo, K.-Y. Pu, T. Ngo Nguyen Phuong, Y. Hu, Z. Li and B. Liu, *Adv. Funct. Mater.*, 2012, **22**, 3107-3115.
326. P. Huang, W. Zheng, S. Zhou, D. Tu, Z. Chen, H. Zhu, R. Li, E. Ma, M. Huang and X. Chen, *Angew. Chem. Int. Ed.*, 2014, **53**, 1252-1257.
327. Y. Liu, S. Zhou, D. Tu, Z. Chen, M. Huang, H. Zhu, E. Ma and X. Chen, *J. Am. Chem. Soc.*, 2012, **134**, 15083-15090.
328. W. Zheng, S. Zhou, Z. Chen, P. Hu, Y. Liu, D. Tu, H. Zhu, R. Li, M. Huang and X. Chen, *Angew. Chem. Int. Ed.*, 2013, **52**, 6671-6676.
329. L. Cai, Z.-Z. Chen, M.-Y. Chen, H.-W. Tang and D.-W. Pang, *Biomaterials*, 2013, **34**, 371-381.

330. H. Sun, L. Wu, W. Wei and X. Qu, *Mater. Today*, 2013, **16**, 433-442.
331. S. Y. Lim, W. Shen and Z. Gao, *Chem. Soc. Rev.*, 2015, **44**, 362-381.
332. J. B. Haun, N. K. Devaraj, S. A. Hilderbrand, H. Lee and R. Weissleder, *Nat. Nanotechnol.*, 2010, **5**, 660-665.
333. S. S. Agasti, M. Liong, C. Tassa, H. J. Chung, S. Y. Shaw, H. Lee and R. Weissleder, *Angew. Chem. Int. Ed.*, 2011, **51**, 450-454.
334. H. Shi, X. He, K. Wang, X. Wu, X. Ye, Q. Guo, W. Tan, Z. Qing, X. Yang and B. Zhou, *Proc. Natl. Acad. Sci. USA*, 2011, **108**, 3900-3905.
335. A. Aigner, *J. Mol. Med.*, 2011, **89**, 445-457.
336. A. Bajaj, S. Rana, O. R. Miranda, J. C. Yawe, D. J. Jerry, U. H. F. Bunz and V. M. Rotello, *Chem. Sci.*, 2010, **1**, 134-138.
337. A. Bajaj, O. R. Miranda, R. Phillips, I.-B. Kim, D. J. Jerry, U. H. F. Bunz and V. M. Rotello, *J. Am. Chem. Soc.*, 2009, **132**, 1018-1022.
338. K. L. Bicker, J. Sun, M. Harrell, Y. Zhang, M. M. Pena, P. R. Thompson and J. J. Lavigne, *Chem. Sci.*, 2012, **3**, 1147-1156.
339. K. El-Boubbou, D. C. Zhu, C. Vasileiou, B. Borhan, D. Prosperi, W. Li and X. Huang, *J. Am. Chem. Soc.*, 2010, **132**, 4490-4499.
340. A. Champion and P. Kambhampati, *Chem. Soc. Rev.*, 1998, **27**, 241-250.
341. J. R. Lombardi and R. L. Birke, *Acc. Chem. Res.*, 2009, **42**, 734-742.
342. A. S. D. S. Indrasekara, B. J. Paladini, D. J. Naczynski, V. Starovoytov, P. V. Moghe and L. Fabris, *Adv. Healthcare Mater.*, 2013, **2**, 1370-1376.
343. K. Lee, V. P. Drachev and J. Irudayaraj, *ACS Nano*, 2011, **5**, 2109-2117.
344. K. V. Kong, Z. Lam, W. D. Goh, W. K. Leong and M. Olivo, *Angew. Chem. Int. Ed.*, 2012, **51**, 9796-9799.